Demand response in a market environment

Larsen, Emil Mahler; Pinson, Pierre; Ding, Yi; Østergaard, Jacob

Publication date:
2016

Document Version
Publisher's PDF, also known as Version of record

Ph.D. Thesis
Doctor of Philosophy

DTU Center for Electric Power and Energy
Department of Electrical Engineering

Demand response in a market environment

Emil Mahler Larsen

Denmark 2015

DTU CEE
Center for Electric Power and Energy
Technical University of Denmark

DTU Electrical Engineering
Center for Electric Power and Energy
Building 776
4000 Roskilde
Denmark
Phone +45 4525 3500
emlar@elektro.dtu.dk
www.cee.elektro.dtu.dk

Summary

This thesis addresses the design, deployment and benefits of demand response in a market environment. Demand response is consumption that can be controlled by an external stimulus in the power system. Flexible consumption is a useful tool for absorbing volatile power from renewable sources like wind power and photovoltaics, and dealing with decentralised activity like electric vehicle charging. Without flexible consumption or other new technologies like storage, there will be several occasions of surplus or deficit of generation to meet the demand of the future, sometimes expected and sometimes not, that will lead to power system failure.

The type of demand response investigated is consumption controlled by indirect means, like an electricity price. Initially, algorithms responding to real-time electricity prices are researched and benchmarked according to comfort and cost. After this simulation, real power system data from the Danish island of Bornholm is introduced and methods to quantify an aggregated load is developed. These methods can be used for real-time operation and to support investment decisions. More specifically, they can be used to forecast the response to electricity pricing and to classify different types of customers. The proposed models are then embedded into new five-minute electricity markets for system balancing and local congestion management. New market tools for exploiting and maintaining a degree of control over demand are developed, and the value of DR using indirect control is determined in terms of social welfare.

This thesis is written in the context of Danish and European power systems because the data used - and the data-driven models subsequently created - come from and were developed for the EcoGrid EU project. The demand forecasting models and electricity markets proposed in this thesis have been implemented on the Danish island of Bornholm in the EcoGrid EU project. The real-time balancing market ran from October 2014 until May 2015, the congestion market operated from January 2015 onwards, and the demand forecast module operated from February 2015 onwards.

EcoGrid EU is a large-scale smart grid demonstration with 1900 residential households and 100 industrial customers with a peak load above 5MW. Customers are equipped with smart meters and a range of distributed energy resources with automated controllers that receive a new electricity price every five minutes and optimize consumption levels accordingly. DR from these customers is bid into the electric-

ity market as balancing power and customer measurements are used in real-time to update the demand forecast.

Resumé

Denne afhandling behandler design, deployering af og fordelene ved demand response - fleksibelt forbrug - under markedsforhold. Demand response er forbrug, der kan styres ved stimuli, der virker ind på elsystemet udefra. Det resulterende fleksible forbrug er et nyttigt redskab til absorbering af volatil elektricitet, der produceres af vedvarende energikilder såsom vindkraft og solceller samt til at håndtere stigningen i decentrale aktiviteter såsom opladning af elektriske køretøjer. Uden fleksibelt forbrug eller andre, nye teknologier som oplagring vil der opstå en kløft mellem udbud og efterspørgsel i fremtiden, sommetider forventet, sommetider uventet, som vil medføre, at elsystemet går ned.

Den form for demand response, der har været genstand for undersøgelse, vedrører forbrug, der styres indirekte, eksempelvis via elprisen. Indledningsvis undersøges og benchmarkes styringsdesign ud fra komfort og omkostninger i lyset af realtidselpriser. Efter denne simulering introduceres reelle elsystemdata fra Bornholm, og der udvikles metoder til kvantificering af den samlede belastning. Metoderne kan bruges til realtidsdrift og til støtte for investeringsbeslutninger. Mere specifikt kan de bruges til at forudsige reaktionen på fastsættelse af elpriser og til klassificering af forskellige typer kunder. De foreslåede modeller indbygges så i nye fem-minutters elmarkeder med henblik på at skabe balance i systemet og undgå flaskehalse. Der udvikles markedsredskaber til udnyttelse og fastholdelse af en vis styring af efterspørgselen, og værdien af demand response ved indirekte styring bestemmes i form af sociale velfærd.

Denne afhandling tager nødvendigvis udgangspunkt i danske og europæiske elsystemer, fordi de anvendte data - og de datastyrede modeller, der efterfølgende er skabt - kommer fra og blev udviklet til EcoGrid EU-projektet. Modellerne til forudsigelse af efterspørgsel og de foreslåede elmarkeder i afhandlingen er blevet implementeret på Bornholm i EcoGrid EU-projektet. Regulærkraftmarkedet kørte fra oktober 2014 indtil maj 2015, flaskehals-markedet kørte fra januar 2015, og efterspørgselsprognosemodulet kørte fra februar 2015.

EcoGrid EU er et smart-grid demonstrationsprojekt i stor skala med 1900 husholdninger og 100 industrikunder med en belastning, der topper over 5MW. Kunderne får installeret smart-elmålere og en række distribuerede energiressourcer med automatisk styring, der modtager en ny elpris hvert femte minut og optimerer forbrugsniveauerne

tilsvarende. Demand responsen fra disse kunder bydes ind på elmarkedet som balanceeffekt, og der bruges kundemålinger til realtids-opdatering af efterspørgselsprognoserne.

Dissemination

Papers included in the Thesis

A E. Larsen, F. Leimgruber, P. Pinson, F. Judex; "From demand response evaluation to forecasting - Methods and results from the EcoGrid EU experiment", submitted to IEEE Transactions on Power Systems.

B G. le Ray, E. Larsen, P. Pinson; "Evaluating price-based demand response in practice - with application to the EcoGrid EU experiment", submitted to IEEE Transactions on Smart Grid.

C E. Larsen, P. Pinson, G. Giannopoulos, G. Le Ray, "Demonstration of market-based real-time electricity pricing on a congested feeder", presented at the 12th International Conference on the European Energy Market.

D E. Larsen, P. Pinson, J. Wang, Y. Ding, J. Østergaard; "The Cobweb effect in balancing markets with demand response", submitted to IEEE Transactions on Power Systems.

Other publications not included

E E. Larsen, Y. Ding, Y. Li, E. Zio; "Reliability evaluation of multi-performance multi-state k-out-of-n systems", submitted to IEEE Transactions on Power Systems.

F Y. Ding, S. Pineda, P. Nyeng, J. Østergaard, E. Larsen and Q. Wu; "Real-time market concept architecture for EcoGrid EU – A prototype for European smart grids", *IEEE Transactions on Smart Grid*, vol. 4, issue 4, pp. 2006-2016, 2013.

G A. Troi, B. N. Jørgensen, E. Larsen, F. Blaabjerg, G. L. Mikkelsen, H. P. Slente, H. Madsen, J. Østergaard, J. M. Entwistle, M. C. Nordentoft, P. Meibom, R. H. Jacobsen, S. Thorvildsen and U. Jørgensen; "The smart grid research network: Roadmap for Smart Grid research, development and demonstration up to 2020", The Smart Grid Network's Recommendations, *Danish Ministry of Climate, Energy and Building*, 2013.

H C. Latour, M. Norton, E. Larsen, H. Vandenbroucke, C. Dyke, S. Banares and V. V. Thong; "Demand side response - ENTSO-E policy paper", *ENTSO-E*, 2014.

I Y. Ding, E. Larsen, B. Mo, I. Petersen, Q. Wu, B. Bletterie, K. Kok, D. Gantenbein, B. Jansen, A. Arendt, H. Oschsenfeld, W. Ziel, M. Bendtsen, M. Mosehold, P. Nyeng; "Demonstration phase 2 and 3 specification", *EcoGrid EU project report*, 2014.

Datasets and software

J E. Larsen; "EcoGrid EU market code for real-time implementation", *https://github.com/emillarsen*, 2014.

K E. Larsen; "EcoGrid EU demand forecasting code for real-time implementation", *https://github.com/emillarsen*, 2015.

L E. Larsen; "EcoGrid EU demand dataset", *Internal*, 2014.

Acknowledgements

I would like to thank my supervisors, Pierre Pinson, Yi Ding and Jacob Østergaard, for their guidance and patience. Many other colleagues at the Center for Electric Power and Energy (CEE) also deserve credit for the many interesting research discussions and for teaching me new hard skills.

Thank you also to Salvador Pineda Morente from Copenhagen University, whose time and advice was fundamental to my understanding of electricity markets, and Preben Nyeng from Siemens for his frequent clarifications regarding TSO matters. I would also like to thank all EcoGrid EU partners for their feedback and corroboration through weekly telephone conferences and monthly workshops. Bernhard Jansen and Stephen Hall from IBM were particularly supporting with implementation of server-side code.

I am also grateful to Jianhui Wang for accommodating me at Argonne National Laboratory and giving me the freedom to do interesting work in a new field.

Finally, this work would not have been possible without the patience and support of my wife, immediate and extended family, who helped with a wide range of issues including, but not limited to, operations research and proof reading.

Nomenclature

Frequently used variables and parameters are defined here. The nomenclature of the thesis differs in parts to that of the individual papers.

Table 1: Device, house and controller modelling nomenclature

$n \in N$	Set of time steps	5 min intervals
T^i	Temperature of light mass in house	°C
T^a	Ambient (outside) temperature	°C
T^e	Building envelope temperature	°C
Φ^e	Energy flux into heat pump	W/m^2
Φ^h	Energy flux from heat pump	W/m^2
Φ^s	Energy flux from global solar irradiation	W/m^2
A^w	Effective window area	m^2
C^i	Heat capacity of the house interior	J/°C
C^e	Heat capacity of the building envelope	J/°C
R^{i-a}	Ventilation resistance between interior/ambient	W
R^{i-e}	Thermal resistance between interior/envelope	W
R^{e-a}	Thermal resistance between envelope/ambient	W
λ	Real-time price	€/MWh
μ^λ	Median historical price	€/MWh
T	Temperature set-point	€/MWh
$T^{\min\,/\,\max}$	Min/max customer comfort level	°C
x	Binary heat-pump on/off decision	{0, 1}
v_n/w_n	Heat pump on/off start	{0, 1}
$z^{\text{on/off}}$	Minimum on/off time	5 min intervals
$m^{\text{on/off}}$	On/off countdown	5 min intervals
$\bar{T}^i$	Mean indoor temperature over all historical values	°C

Table 2: Aggregated demand modelling nomenclature

$t \in T$	Set of time steps	5 min intervals
λ_t	Electricity price	5 min intervals
z_t	External variable	-

χ_t	Interaction variable	-
θ_t	Parameters for price	kWh^2/€
θ_z	Parameters for external variables	-
θ_χ	Parameters for interactions	-
ϵ_t	Model residuals	kWh
c_t	Observed consumption	kWh
c'_t	Model of consumption	kWh
η	Tuning parameter	-
A_t	DR range	kWh
B_t	DR shape parameter	kWh

Table 3: Market nomenclature

$t \in T$	Set of time steps	5 min intervals
$g \in G$	Set of generators	-
$l \in L$	Set of loads	-
α^{DA}	Day-ahead demand price elasticity	€/MWh^2
ΔC_t^{DA}	Day-ahead demand response	MWh
$P_{g,t}^{DA}$	Day-ahead generation	MWh
$\lambda_{g,t}$	Day-ahead generator bid price	€/MWh
$Q_{g,t}^{\max}$	Maximum generator bid quantity	MWh
W_t^{DA}	Day-ahead wind power forecast	MWh
λ_t^{DA}	Day-ahead price	€/MWh
α	Real-time demand price elasticity	€/MWh^2
ΔC_t	Real-time demand response	MWh
$\Delta C^{\min\,/\,\max}$	Maximum/minimum DR	MWh
λ_t^{RT}	Real-time price	€/MWh
C_t^{DA}	Day-ahead load	MWh
$\lambda_{g,t}^{\uparrow/\downarrow}$	Generator bid price (up/down regulation)	€/MWh
$Q_{g,t}^{\uparrow/\downarrow}$	Generator bid quantity (up/down regulation)	MWh
$P_{g,t}^{\uparrow/\downarrow}$	Generator regulation (up/down)	MWh
λ^{spill}	Price wind spillage (curtailment)	€/MWh
λ^{shed}	Price for load shedding	€/MWh
W_t^{spill}	Wind spillage (curtailment)	MWh
C_t^{shed}	Load shedding	MWh
B_t	Imbalance	MWh
$C_{l,t}^{\min\,/\,\max}$	Minimum/maximum feeder consumption	MW

Contents

Summary i

Resumé iii

Dissemination v

Acknowledgements vii

Nomenclature viii

Contents x

1 Introduction 1
- 1.1 Motivation . . . 1
- 1.2 Electricity markets . . . 2
- 1.3 Demand response . . . 5
- 1.4 Objectives and contributions . . . 8
- 1.5 Structure of thesis . . . 9

2 Characterising price-based DR 11
- 2.1 Introduction . . . 11
- 2.2 Experimental observations . . . 12
- 2.3 Simulation Method . . . 13
- 2.4 Results . . . 21
- 2.5 Household benefit conclusions . . . 28

3 Aggregated response evaluation 30
- 3.1 Introduction . . . 30
- 3.2 The basics of indirect control . . . 31
- 3.3 Flexibility estimation and demand forecasting . . . 31
- 3.4 Linear model verification . . . 34
- 3.5 Evidence for a non-linear response . . . 36
- 3.6 Clustering approach for identifying households delivering DR . . . 39
- 3.7 Consequences for the forecast responsible party . . . 44

4 Electricity market design 45

4.1 Introduction 45
4.2 Definitions of price and cross-price elasticity 46
4.3 Price discovery in a market environment 47
4.4 General market constraints 50
4.5 Specifics of the EcoGrid EU market 59
4.6 Empirical results and discussion 62
4.7 Market conclusions 67

5 Conclusion **69**
5.1 Discussion of key results and contributions 69
5.2 Future work 71
5.3 Opportunities for DR growth 73

Bibliography **75**

A Paper A: From demand response evaluation to forecasting - Methods and results from the EcoGrid EU experiment **84**

B Paper B: Evaluating price-based demand response in practice - with application to the EcoGrid EU experiment **93**

C Paper C: Demonstration of market-based real-time electricity pricing on a congested feeder **102**

D Paper D: The Cobweb effect in balancing markets with demand response **108**

CHAPTER 1

Introduction

1.1 Motivation

Energy use has grown astronomically since the beginning of the industrial age. This is unsurprising, since increased energy consumption leads to increased economic growth [1, 2]. Living standards have risen greatly, but there is academic consensus that increasing consumption of fossil fuels is unsustainable. The new reality presents a stark choice: we can change the way we produce and use energy, or do nothing and allow living standards to fall as climate change makes its impact.

Not until 2014 did renewable energy sources (RES) surpass oil and coal as the fastest growing primary energy sources in absolute terms [3]. However, fossil fuels still dominate to such an extent that RES, even with the robust projected growth, will still comprise only 7% of worldwide primary energy sources by 2035 [4]. These predictions all but guarantee a 2.6°C temperature rise by 2100 [5].

In spite of these miserable projections, in OECD countries we can see a glimmer of hope for changing our energy-behaviour. Denmark in particular is a leading light in renewable energy. Political will, windy shores, and collaborative neighbours give Denmark every chance of achieving 50% electricity consumption from wind power in 2020, and 100% of total energy consumption from renewable energy in 2050 [6]. Wind and sun can be difficult to predict, however, and even their expected patterns will involve periods of over- and under-production. New technologies are needed to fill in the gaps, and traditional demand at home and in the office can be a part of the solution.

Controlled flexibility on the demand side, so called demand response (DR), can complement uncertain and discontinuous RES supply: when the wind blows most, demand can consume most, when there is little wind, demand is reduced. Increasing DR prevalence is not just about counteracting RES in the power system; by strengthening the consumer's ability to reject the highest prices, it will create a needed check on the market power of the energy providers, thereby helping to counteract post-deregulation market trends such as rising prices and insufficient promotion of renewables. The increase in decentralised activity - production and consumption from electric vehicles (EVs), heat pumps, and photovoltaics (PV) - requires an unprecedented and unforeseen level of flexibility in the power system. In today's fast changing power system, the idea of controlling large centralised generators to meet a fixed demand seems

quaint, and it is almost folly to distinguish between a generation-side and a demand-side.

Claiming that DR is the best solution to our future electricity woes is, however, short sighted. Introducing demand charges for residential customers is a compelling solution to limit the impact of increasing distributed activity [7]. France, Italy and Spain already charge customers for the capacity of the connected load: in Italy for example, a household pays a higher distribution charge if its peak consumption is above 3kW. Such an approach tends to alter household usage patterns and may be well suited to compelling smart-charging of EVs and self-consumption of PV generation.

Increasing interconnection capacity is claimed to be better than DR for balancing wind power, ensuring the value of wind when it is windy, and ensuring sufficient capacity when wind levels are low [8]. Integration with the transport and heating systems may also be preferable to DR in Denmark's future power system. Denmark is lucky to have such options. In a small country with a well developed district heating infrastructure, cross-sector energy transfer should be easy and relatively cheap to implement, while interconnection capacity is almost sufficient for Denmark to have enough external capacity to meet its needs on a zero-wind day. This current capacity gap is a small fraction of that faced by larger nations like the UK and Spain [9]. Thus relying on trade with neighbouring countries is clearly not enough if much of Europe attempts to go for renewable energy. From an international perspective then, we will need every technology we have developed so far, and many that are still being researched, to maintain a stable power system at a reasonable cost.

The need for DR is compelling, and so the primary questions involve how to do it. Which concepts, technologies, customers and markets to use? And when? As soon as possible, or in 20 or 40 years time? The answers depend upon the ultimate cost/benefit to the power system and to individual customers.

1.2 Electricity markets

Growing production from RES has coincided with deregulation of power systems and an increase in demand-side management (DSM) programs - although these three developments have often progressed for unrelated reasons.

Deregulation in power systems kicked off in the 1980s when Chile privatised its electric utilities to fund public projects. Governments privatise their power generation, transmission and distribution in order to increase efficiency (e.g. bill collection) and service quality (e.g. through competition), or simply to sell assets to raise funds for other public projects such as healthcare and education. Large industrial and commercial customers, unhappy with high electricity bills, have supported deregulation out of a hope that new competition would pressure costs downwards [10]. Organisations

without a commercial interest have also favoured deregulation out of a belief that energy choice would let them support greener energy sources.

In fact, there is widespread evidence that deregulation has increased electricity bills, and there remains no evidence that it has promoted green sources of energy. In the USA, electricity prices in states with deregulated power systems are 10-48% higher than in states with price regulation [11, 12]. In general, when considering whether or not the privatisation of public utilities is beneficial for society, there appears only to be one significant and measurable variable: competition [13]. In any given sector, competition is key to efficient operation. It's therefore highly likely that deregulation failed to bring down costs due to insufficient competition.

In addition to an increase in prices, deregulation has also been blamed for the decline of DSM from 1993 to 2007. DSM programs, which comprise DR and other activities like energy efficiency (e.g. building insulation) and voltage regulation, were first enacted following the oil embargo and world-wide energy shortages of the 1970s as a way of increasing efficiency and blunting the impact of future energy blockades. Spending on DSM and energy efficiency programs peaked at $2.28bn (2015$) in 1993 in the USA [14], followed by a dark period where spending dropped, only finally reaching similar levels in 2007, from which spending exploded to $7.12bn in 2013 [15] and may increase to $16.8bn by 2025 [16].

Utilities operating pre-deregulation had to meet energy needs by producing it themselves with existing means and, when that wasn't enough, by building expensive new plants or encouraging customers to use less electricity. Wholly public utilities, not driven by profit, often decided to both build new plants and implement public DSM programs. Such an approach entailed less risk for (often elected) public bodies and could also easily be presented as good for society. Post-deregulation, utilities feared new competitive threats and often reacted with cost-cutting, including the dumping of costly DSM schemes with payback times of several years [14].

Today's renewed interest in DSM is not necessarily driven by a desire to lower costs, but rather by a desire to facilitate consumption from RES. A deregulated, market-oriented system, whatever its merits and disadvantages, is the framework within which this goal must be achieved. Figure 1.1 illustrates the challenge and goal of DSM programs in Denmark today. In a power system with a large share of generation from RES, supply can exceed demand. RES also has the attribute of being uncertain, so that the forecasted output may not be realised. DR, an important part of DSM, can shift load from periods of low generation to high, such as when supply exceeds demand, and can potentially react to unforeseen generation, such as when the production forecast was wrong.

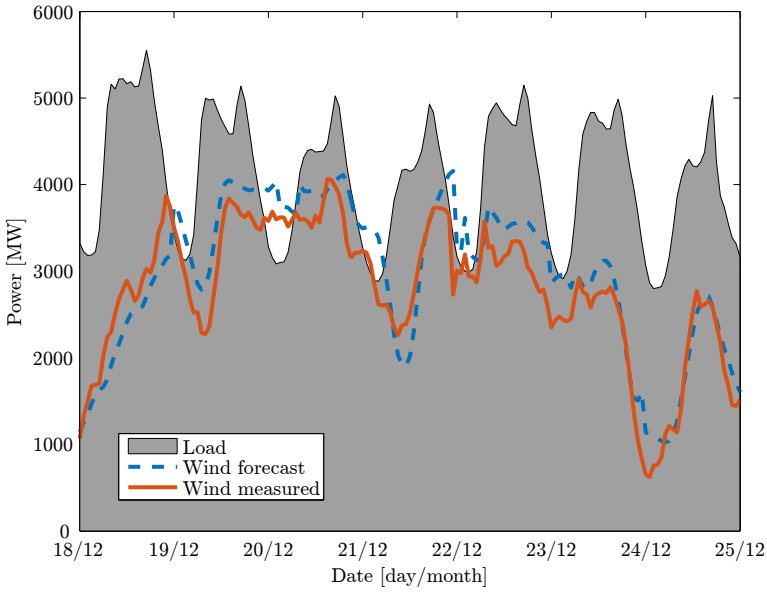

Figure 1.1: Load and wind power generation during the 2014 Christmas week in Denmark

EU-wide actions like the Third Energy Package and TSO policy [17] support a market-based trigger for DR. The U.S. Federal Energy Regulatory Commission has also proposed to pay the locational marginal price for all types of DR [18], which is supported by the Department of Energy's funding of dynamic pricing [19]. The preference for market activation is driven by security of supply concerns, which are primarily due to the large volumes being traded in electricity markets today, the risk posed by increased decentralised activity, and the desire to improve market efficiency. Once again, competition is the key to efficient operation of a utility. More specifically, markets where demand is a price-taker are inefficient, since generators exhibiting market power have amplified influence, leading to higher prices for consumers than in a market where consumers can reject high prices.

This thesis focuses on power pools, where bids from buyers and sellers are matched quickly and the commodity is delivered in the coming minutes, hours or days. While forward contracts are also widely used, it is through power pools that the largest volumes of energy move in deregulated power systems today. Figure 1.2 shows the existing supply and demand curves from the Nord Pool day-ahead market (blue and red curves respectively) and demand function estimates for the real-time EcoGrid EU load. Notably, in 2014 there was no DR in the Danish regulating market, which would equate to a straight, vertical red line.

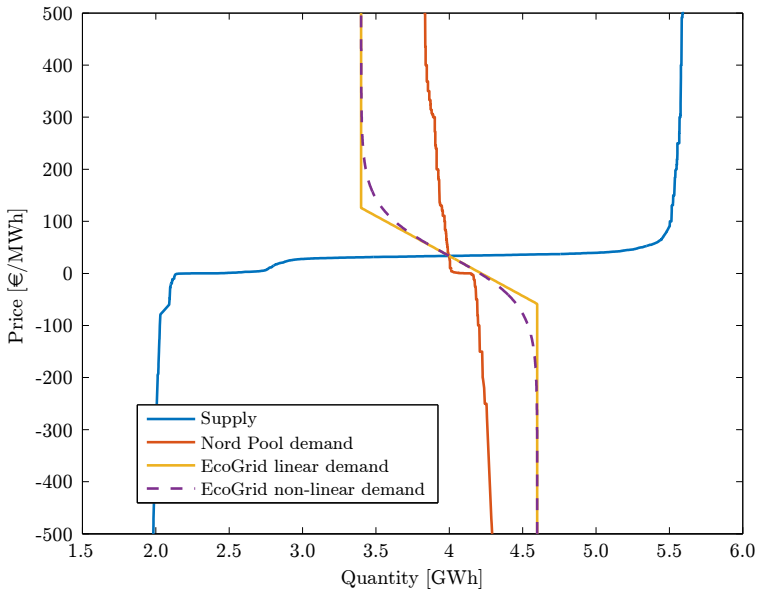

Figure 1.2: Supply and demand curves from the existing day ahead Nord Pool market and linear and non-linear approximations of EcoGrid EU demand curves.

The challenges of making the demand more elastic are not as trivial as this figure might suggest. The volume of energy shifted is far larger in a real-time market than in a day-ahead market due to more regular (e.g. 5 minute) activations. The resulting price discovery and system dynamics are complex.

1.3 Demand response

1.3.1 Resource of interest

While previous DSM programs have been branded variously as disappointing [20] and successful [14], the changing types of DR make learning from past experiences difficult. Earlier DR programs were focussed on time-of-use (TOU), volume-capping and critical peak pricing (CPP) schemes, often reducing peak load and shifting energy systematically based on regular patterns. Now, power system operators face increased decentralised activity and large-scale wind power installations. These make power systems more volatile, less predictable, and topologically different.

In Denmark, these changes are particularly startling. Wind power accounted for 40% of consumption in 2014, and current plans call for 35% of final energy consumption to come from RES by 2020. A big target here is household heating, since it represents

25% of Denmark's final energy consumption; yet today, 70% of heating comes from fossil fuel sources [6]. In light of these ambitions and the high present-day cost of electric heating compared with district heating, Denmark is currently offering tax reductions worth 15% of the cost of electricity for electric heat customers [21]. In addition, green laws prohibit new house construction with fossil-fuel based heating, meaning heat pump installations are expected to double by 2035 [22].

Using heating to solve the problems caused by decentralised activity and RES integration is a high priority, especially given the refusal of industrial loads to participate in the Danish regulating market today. Thankfully, electric heating offers a degree of controllability, since a house can act as a temporary heat storage. Heating can be turned on and off for short periods using a control signal without upsetting the comfort of the user. Its power delivery and energy shift capabilities exceed other residential devices and comes close to EVs [23]. As such, electric heating is the main focus of this thesis.

Previous DSM schemes are not well suited to controlling electric heating or meeting the fast changing needs of RES. Instead, DSM schemes involving direct control (system operators giving on/off requests to customers through a bilateral contract) and indirect control (system operators using incentive signals to influence load) have been identified as more appropriate in today's power system [24].

1.3.2 Previous research

Several contract types can activate DR and incentivise the customer. Flexible electricity tariffs have been discussed for over a century; they can be traced all the way back to 1892 when John Hopkinson, inventor of the three phase power system, noted similarities between the railway and electricity systems, and posited that railway tickets should cost more in peak hours, since peak-costs are genuinely higher [25]. Ultimately, however, Hopkinson did not advocate time of use (TOU) contracts for electricity consumption, but rather a contract based on the peak-capacity and overall consumption of the customer. In all, five generic contract types for customer settlement and activation have been identified [26]:

1. Volume-based static contracts (e.g. fixed load capping);
2. Volume-based dynamic contracts (e.g. dynamic load capping and interruptible contracts);
3. Control-based contracts (e.g. direct control);
4. Price-based static contracts (i.e. TOU); and
5. Price-based dynamic contracts (e.g. real-time pricing).

Each contract has its pros and cons and is suited to different types of markets and DR goals. Static volume-based contracts are generally reserved for large industrial

loads, e.g. 200kW or greater [27], where capacity is an issue. Dynamic volume-based contracts are somewhat more common, as in [28] where critical peak pricing (CPP) customers receive period text, email or phone notifications of high price periods up to six hours long, during which customers exceeding certain volumes will incur premium pricing of up to five times the normal standard. With these contract types, however, defining a fair limit for customers to stay under can prove difficult, especially since a truly fair value may vary by customer and be liable to manipulation.

Static price-based contracts, or TOU contracts, are the most common way of varying electricity prices for end consumers. TOU contracts seek to shift some day-time peak consumption to the night-time lull, thereby increasing the feasibility of conventional generation with long minimum on and off times (such as nuclear), while reducing the need for expensive peaking generators. The consumer receives a fixed tariff for a longer period of time, typically several months or a year, where prices change two or three times a day.

A seminal 1957 paper proposed the first mathematical proof for twice-daily discriminatory pricing in order to reduce peak demand [29]. Since then, TOU contracts - also called TOD (time of day) contracts - have been shown in Connecticut to successfully shift the morning peak consumption by plus or minus two hours and to reduce the evening peak consumption significantly [30]. Hourly TOD pricing also reduced overall demand by 5% in this experiment, possibly because of increased consumer cost awareness. A separate study of 1500 German consumers showed that two daily TOD periods reduced peak consumption by 6-7%, but without any corresponding rise in off-peak consumption [31]. Clearly the effect of TOU contracts depends heavily on consumer type. Simply reducing consumption - which in a worst case scenario implies a reduction in economic output - may not by itself lead to an increase in social welfare. The benefits of static price-based contracts include easy customer understanding and easy implementation with mature, affordable metering technology. The resulting decreases in peak-consumption lower overall costs for consumers.

But the results from one demonstration of TOU contracts have not always proven repeatable elsewhere. Additionally, TOU contracts are not unlocking the full potential of the DR resource. In Europe, that potential is 60GW DR, with at least 12GW already activated [32]. A large part of this comes from households with TOU contracts. Exact figures are hard to come by, although in the UK it is about 20% of households, and in Italy it is 90%. Europe-wide, the level is probably somewhere in-between. Despite such a large installation of TOU contracts, total energy utilization hovers at around only 10% of flexible demand potential [17]. In a power system dominated by stochastic production, like wind and solar, TOU pricing is less effective in meeting the needs of the system. While an underlying shift of day-time to night-time consumption may still be desirable, the biggest problems of integrating renewables into the power system - variable and uncertain production – simply is not something existing TOU contracts can accommodate.

Control-based contracts have reduced demand by 15% for two hours a day in Australia, using air-conditioning units and paying customers a flat fee of $100AUS per year. In Denmark, control-based contracts have also been gaining traction through commercial partnerships like one between DONG and the now bust Better Place, through which DONG helped Better Place strategically charge their EV fleet using direct control, considering local congestion and the market price [33]. The benefit of direct control is its predictability. The downsides are that it requires extensive control and communication equipment (thus lending itself to larger loads), and it does not necessarily make efficient use of the resource if it is only being used rarely. In addition, direct-control is synonymous with distribution system operators (DSO) like DONG, who operate natural monopolies, which does not advance regulators' desire to increase market efficiency.

Finally, dynamic price-based contracts are a fashionable topic in power system engineering. Before this form of control could ever become a reliable reserve, however, proponents would need to prove the ability to forecast responses and exploit them in spite of their stochastic nature. The societal value of dynamic price-based contracts is potentially easier to quantify though, since customers are rewarded and penalised for their electricity consumption choices with a real market price that reflects the true state of the power system.

One of the most prominent research projects demonstrating control-by-price and control-by-frequency was the GridWise initiative [34, 35], which compared real-time pricing favourably to TOU contracts. More recently, real-time pricing for small consumers was tried in Chicago, where 590 customers with air-conditioning received an hourly price [36]. These households reduced their annual electricity bills by 1-2%, or an average of 50W to 100W during the highest price period each day. In a follow-up study of the impact of real-time pricing in the PJM area in the Eastern USA, simulations showed increased social welfare of $21 per year for each customer moving to real-time pricing, thanks to reduced generation capacity costs and lower market clearing prices [37]. This evidence is a useful starting point, but questions of scalability and stability remain [38].

1.4 Objectives and contributions

This thesis aims to study and develop the tools needed to activate small-scale DR in a market setting, considering the limitations of the power system, DERs, balancing constraints and operational procedures in Scandinavia today. More specifically, the contributions of this work are:

- For the financial benefits for heat pump owners responding to real-time prices, evaluation of smart control algorithms with explicit modelling of minimum on- and off-times and comfort and wear and tear analyses. Annual savings as little

as €2 per customer are identified, which contrasts heavily with previous studies and assumptions that thermostatically controlled load (TCL) automation is significantly rewarding;

- For the quantity of DR available, statistical models to estimate flexibility based on empirical data from residential loads. Models describe DR ramping, time to peak response, peak response and duration of response;
- For the overall electricity market, simulations with binary variables on the supply-side and an extensive expression of DR characterised by the statistical models on the demand-side - a more complete combination that has not previously been investigated to our knowledge;
- For volatility in the power system, an effective measuring tool that provides a more intuitive understanding of volatility caused by DR; and
- For demand forecasting and market clearing, applied research permitting delivery of prices to households in an experimental setup.

1.5 Structure of thesis

The thesis is organised in three self-contained chapters and four attached papers. Some of the chapters rely on the findings of the attached papers and these will be identified where necessary.

The closed loop nature of the power system means that research could start either with individual consumers, aggregation strategies, or with markets that trade energy, as shown in Figure 1.3. Ultimately, a bottom-up approach was taken here, and the individual control algorithms for the heating devices that consumers own were investigated first. As such, Chapter 2 investigates smart controllers that respond to real-time prices and price forecasts through model-based and hysteresis-based algorithms. Empirical results from the demonstration and presented and used to guide new simulations. The consumer benefit of a heat pump responding to prices and the impact of comfort settings is estimated by simulating an average Danish house for 2014.

Chapter 3 investigates how the individual devices presented in Chapter 2 can be aggregated and system-level flexibility estimated. An intuitive linear model with non-linear price terms quantifies the DR potential of different groups of houses. These results are a unique estimate of the flexibility of a large population of houses with heat pumps, resistive heating, controllable PV, and water boilers. The chapter also explores the ramifications of customer classification through clustering - an important tool for aggregators to identify and exploit customer flexibility.

Chapter 4 presents a market concept that aims to schedule supply and demand optimally, reducing wind power curtailment and use of conventional generation. This

thesis further develops a balancing market, using novel constraints and structural changes to ensure feasibility and scalability in the existing power system. Financial benefits to the market are estimated and operational problems are identified. The troublesome issue of volatility is analysed, and potential solutions are presented. The market concept is also extended to perform centralised congestion management on low-voltage feeders.

Two of the main contributions of this thesis, DR forecasting using the model developed in Chapter 3 and real-time implementation of the EcoGrid EU market developed in Chapter 4, were used to create prices every five minutes in 2014/2015 on Bornholm. The market sends real-time prices to 1900 houses every five minutes and uses feedback from demand to update forecasts. A summary of this field-test, with an analysis of the controllability of the load, is given in this thesis.

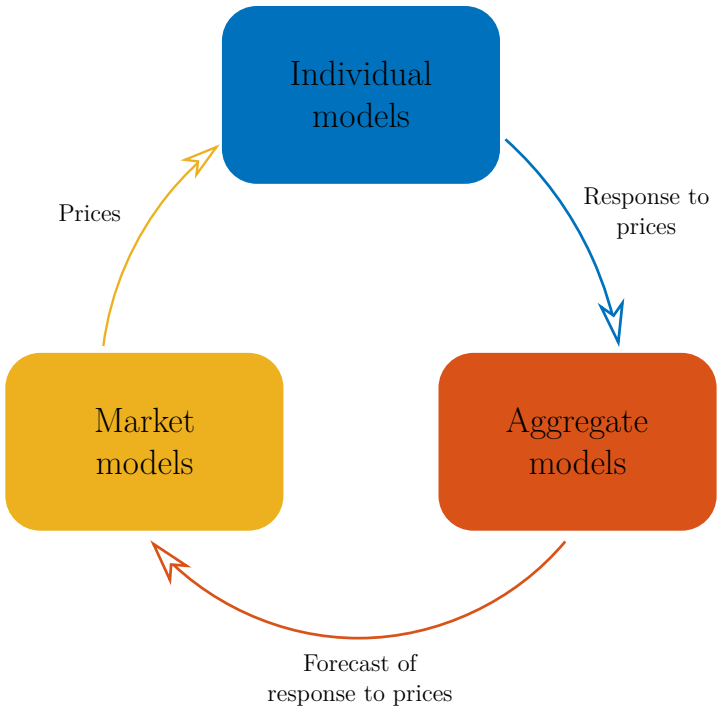

Figure 1.3: How different chapters and the models they contain relate to each other

CHAPTER 2

Characterising price-based DR

Price-based DR programmes may assume that price volatility is incentive enough for participants to invest in the necessary hardware. This chapter investigates whether this is the case considering controller design for thermostatically controlled loads under real-time pricing. Different algorithms are combined with data collected and constraints learnt from experimental work to simulate the customer benefits of residential heat pumps participating in an electricity market. Heat pumps are expected to be the largest and easiest-to-exploit residential DR resources in Denmark.

2.1 Introduction

Thermostatically-controlled loads (TCL) in conjunction with a building can effectively deliver demand response (DR) because such a load only needs to turn on sporadically to maintain a minimum level of user comfort. Modelling thermostatic loads, primarily for forecasting and subsequently for control, was initially proposed 35 years ago [39, 40], spawning numerous research projects analysing different types of TCLs, delivering different services, with different modelling approaches and from single and aggregated perspectives.

Indirect control requires just one-way communication, making it cheap and naturally suited to a large number of smaller loads, such as residential houses with TCLs. Activating DR via a price signal (one form of indirect control) was the main scope of this PhD project. Five minute intervals were first proposed as the threshold for pricing 35 years ago [41]. Below five minutes, non-price signals may be a more effective and less complex approach. For example, power system frequency deviations in Eastern Denmark change sign every 2.7 minutes (on average), which is one option for activation below five minutes. The most advanced heat pumps have minimum on- and off-times of at least 5 minutes (inverter based compressor) and 15 minutes (fixed speed compressor), making them less suited to system-frequency activation.

Previous relevant research of smart TCLs are the hysteresis control algorithms that

base a decision only on historical prices [34], [42], while model predictive control (MPC) algorithms for heating buildings have been discussed [43], [44], also considering stochastic approaches [45]. Hysteresis and MPC approaches have been compared in a five day experiment [46], but how this relates to annual customer savings using real-time pricing and imperfect weather and price forecasts has not been studied.

Simulations using hourly pricing have suggested annual savings of €25-40, €63-71, $27.20 and a 7.7% cost reduction respectively [47, 48, 49, 50]. However, constraints on heat pump usability like minimum on/off-times and customer comfort bounds were either missing or unrealistic. The economic perspective of residential DR with many appliances has also been investigated, with speculative investment recovery times of 6 years [51], far lower than investment recovery rates for residential PV.

The EcoGrid EU demonstration used equipment costing over €350 per customer to enable automated price-responsive control. Other costs include a half to a full day's labour to install the equipment and communication, maintenance, smart meter and server costs. Assuming that real-time price volatility is the only incentive, this chapter asks whether such investment can be justified for a customer or aggregator. Previous studies regularly overlook the on/off nature of heat pumps or consider unrealistic comfort limitations, thereby overstating the flexibility TCLs offer and the cost savings possible. Our objective was to remedy this issue using the experiences learnt and observations obtained in the EcoGrid EU experiment to simulate realistic annual savings for a heat pump customer responding to real-time pricing.

This chapter is structured as follows: Section 2.2 presents summary statistics from the EcoGrid EU experiment that shape subsequent simulations. Section 2.3 presents the method for simulating a house with different controller designs that optimise heating systems economically and comfortably. The cost, wear and tear, and comfort results under real-time pricing are presented in Section 2.4, also with experimental cost savings observed from 285 heat pump customers in the demonstration. Section 2.5 concludes.

2.2 Experimental observations

This section presents statistics from the EcoGrid EU demonstration to form the basis of follow-up simulations. The EcoGrid EU demonstration has 1900 houses fitted with smart meters and a range of distributed energy resources (DERs) that react to electricity prices sent every five minutes. Smart meter data is collected in real-time to update the demand forecast (described in Chapter 3), which is subsequently traded in a real-time balancing market (described in Chapter 4). The market then generates new pricing for customers. DERs include hot water boilers, controllable PV and, most significantly, a mix of heat pumps and resistive-electric heating devices.

To simulate a house with TCLs, assumptions must be made about the temperature bounds that customers find comfortable. We base these assumptions on empirical data from houses that measure indoor temperature throughout the experiment. Absolute thermostat bounds are not logged, so some preprocessing must be performed; To remove outliers in temperature that could be caused by external factors like leaving a window open, the extreme 5% percent of values are removed. The top plot in Figure 2.1 shows the 5th and 95th percentiles through the winter months. The mean temperature range considering these percentiles is 5°C. When considering a slightly narrower range, the 10th to 90th percentiles, a mean temperature range of 4°C is observed. The mean temperature was 21.1°C in both cases. The second plot in Figure 2.1 shows the median temperature range is 3°C, which translates to a heat pump control objective of 21°C ± 1.5°C.

Plots 3 and 4 in Figure 2.1 show the size of the heated area for homes with heat pumps and the nominal power (electrical) of the heat pumps in the EcoGrid EU demonstration. The average house size is 163m^2, larger than the average Danish house of 133m^2, while the average heat pump size is 5kW (this is a combined figure for the houses with multiple heat pumps). These statistics were used for simulation.

2.3 Simulation Method

This section defines a thermal model of a house with a heat pump and presents different control algorithms to steer the heat pump. Air-source heat pumps make up 64% of the heat pumps used by the EcoGrid EU participants. This figure, combined with the continued growth and publicity surrounding heat pumps, means they were modelled instead of resistive-electric heating.

Two control approaches are presented: hysteresis and economic model predictive control (EMPC). Hysteresis controllers take a decision based upon the current electricity price with respect to historical and forecast prices. Hysteresis controllers are robust against modelling errors and computationally lightweight, but may lead to unsatisfactory indoor comfort and suboptimal economic performance. EMPC algorithms take control decisions based upon weather and price forecasts that lead to an optimal comfort and economic outcome in a system without uncertainty. The EMPC approach is, however, computationally heavy and requires far more input data as well as an accurate model of the area being heated.

2.3.1 Thermal model of a house

The heat flows in and out of a house, also considering the contribution from the heat pump, were modelled with differential equations. A grey-box approach can be used to find the parameters for such a model, by combining the properties of a physical model

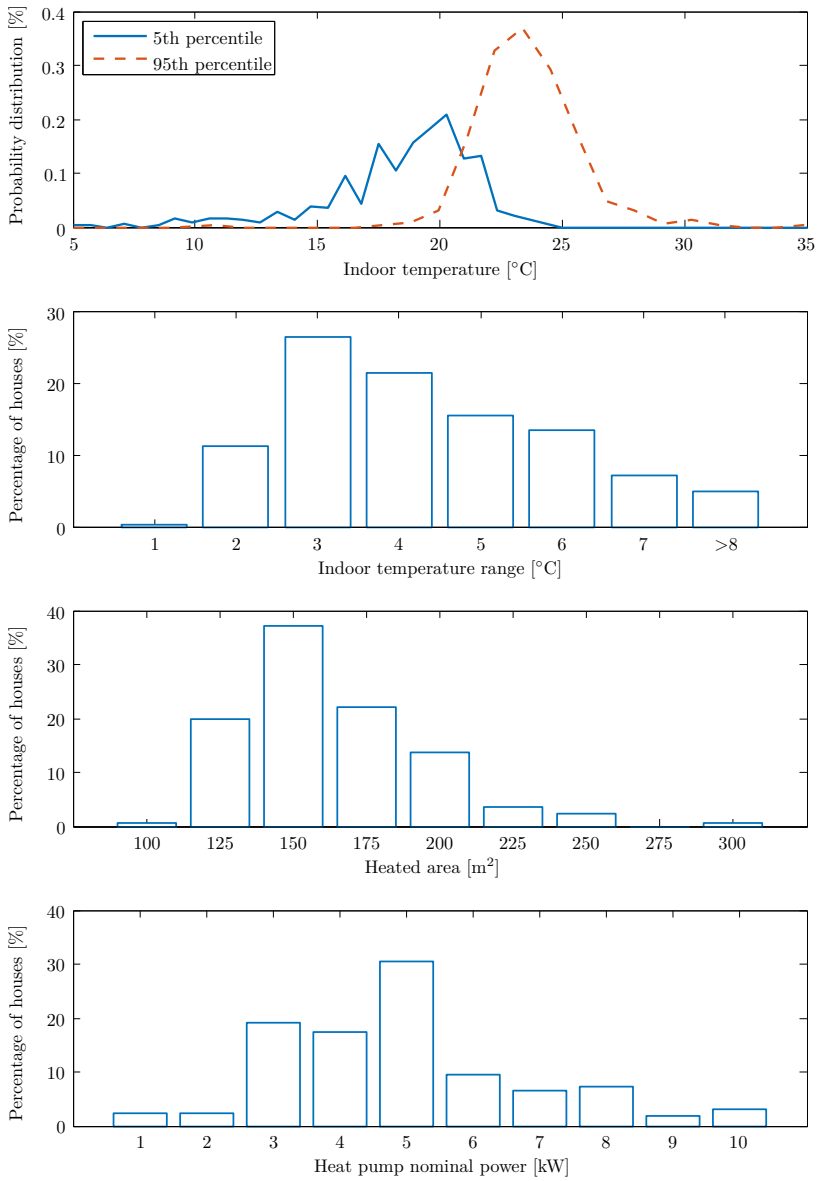

Figure 2.1: Percentiles of temperature bounds experienced by customers in the EcoGrid EU experiment, histogram of temperature ranges showing a 3°C range is most common, histogram of heated area and histogram of heat pump nominal power.

that accurately describes a real system with a black-box model where the underlying process is not well understood [52]. The set of differential equations that describe the first order dynamics of how heat transfers throughout the house are

$$dT^i = \frac{1}{R^{i-e}C^i}\left(T^e - T^i\right)dn + \frac{1}{R^{i-a}C^i}\left(T^a - T^i\right)dn + \frac{1}{C^i}\Phi^h dn + \frac{1}{C^i}A^w\Phi^s dn \quad (2.1)$$

$$dT^e = \frac{1}{R^{i-e}C^e}\left(T^i - T^e\right)dn + \frac{1}{R^{e-a}C^e}\left(T^a - T^e\right)dn \quad (2.2)$$

where n is the time, R^{i-e}, R^{i-a} and R^{e-a} are the thermal resistances between the interior and the building envelope, the interior and the ambient, and the building envelope and ambient respectively. C^i and C^e are the heat capacities of the interior (light mass) and building envelope (heavy mass) respectively. T^e, T^i and T^a are the temperatures of the building envelope, interior and ambient respectively. Φ^h and Φ^s are the energy flux from the heat pump and sun respectively. A^w is the effective window area.

The parameters for this model are based upon experimentally found results in Denmark [52, 53] and are shown in Table 2.1. These equations can be represented as an RC-circuit, as in Figure 2.2. The dotted dividing lines in this figure show different heat contributions to the house which, going from left to right, are the interior of the house, the heat pump, solar irradiance, the building envelope (i.e. the walls) and the outdoors.

Table 2.1: House thermal model parameters

Parameter	Unit	Value
C^i	$\frac{J}{^\circ C}$	1467
C^e	$\frac{J}{^\circ C}$	16300
A^w	m^2	8
R^{i-e}	W	3489
R^{e-a}	W	262
R^{i-a}	W	69

The coefficient of performance (COP) describes the efficiency of a heat pump. Based upon a range of heat pump specification manuals [54, 55] and assuming a fixed indoor temperature of 21°C, the COP can be approximated as

$$\Phi^h = \Phi^e \cdot (0.0606 \cdot T^a + 2.612) \quad (2.3)$$

This relationship means that, at 0°C, the heat pump produces 2.6 times more (thermal) energy than the (electrical) energy it consumes, thus highlighting the benefit of a heat pump.

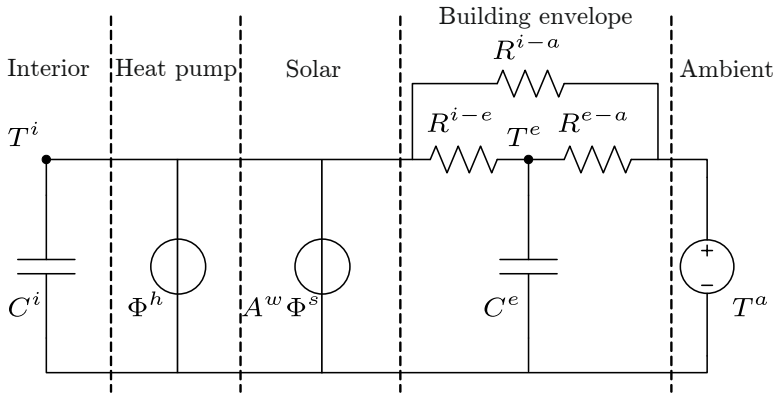

Figure 2.2: RC-circuit representation of differential equations describing the transfer of heat in a house.

2.3.2 Basic thermostatic control

To compare the benefit of smart control algorithms, a non-smart thermostat can be defined. This basic thermostat also sets the boundaries for smart control, i.e. it is used for all subsequent controller designs. The heat pump is turned on at the minimum temperature comfort limit and turns off at the maximum temperature limit, i.e.

if $x_n = 1$ and $x_{n-1} = 0$ **then**
  $m^{\text{on}} = z^{\text{on}}$
else if $x_n = 0$ and $x_{n-1} = 1$ **then**
  $m^{\text{off}} = z^{\text{off}}$
else $m^{\text{on}} = m^{\text{on}} - 1$
$m^{\text{off}} = m^{\text{off}} - 1$
end if
if $m^{\text{on}} \leq 0$ and $m^{\text{off}} \leq 0$ **then**
  if $T_n^i < T^{\min}$ **then**
    $x_n = 1$
  else if $T_n^i > T^{\max}$ **then**
    $x_n = 0$
  else Do smart control
  end if
end if

Figure 2.3: Basic thermostat algorithm with a further option for smart control statments.

where x is a binary variable that turns heating on or off. The integer variables m^{on}

and m^{off} control minimum on- and off-times by counting down from the minimum on- and off-times, z^{on} and z^{off} respectively, every time the device is turned on or off. The smart control statement is called upon for the hysteresis and EMPC cases.

2.3.3 Hysteresis control

A hysteresis controller adjusts the temperature set-point according to the current price relative to median price over the recent history and near future, optimising consumption for the next five minutes only. The temperature set-point is governed by T, such that

$$T_n = T^{\text{offset}} - \frac{\lambda_n - \mu_n^{\lambda}}{k} + T_n^{\text{tracking}} \tag{2.4}$$

where $\lambda - \mu^{\lambda}$ is the relative price, given current price λ and the median of recent and forecast prices μ^{λ}. k governs the sensitivity to prices and is found by testing the controller on one month of data and ensuring that the full range of temperatures are activated considering the range of relative prices activated in the test month. T^{offset} is defined as

$$T^{\text{offset}} = \frac{\left(T^{\max} - T^{\min}\right)}{2} \tag{2.5}$$

To ensure that a minimum mean temperature is observed during the experiment, and allowing comparison to other controllers, a tracking temperature variable, T^{tracking}, is added to the set-point. It is calculated in short recursive process, i.e.,

$$T_n^{\text{tracking}} = T_{n-1}^{\text{tracking}} + T^{\text{offset}} - \bar{T^i} \tag{2.6}$$

where $\bar{T^i}$ is the mean of all historical indoor temperatures. Changes in the tracking variable decrease as time goes on, since $\bar{T^i}$ becomes less influenced by new values as the set $\bar{T^i}$ averages over increases in size. T is the temperature set-point that is subsequently used in the algorithm in Figure 2.4.

if $T_n > T_n^i$ **then**
  $x_n = 1$
else if $T_n < T_n^i$ **then**
  $x_n = 0$
end if

Figure 2.4: Smart control algorithm for hysteresis controllers.

Hysteresis controllers regularly overshoot the upper and lower temperature comfort bounds, especially in milder ambient temperatures when heating occurs rapidly. This is because the hysteresis controller has no expectation of how indoor temperature will develop. In essence, this means that a hysteresis controller without reinforcement

learning is not viable. Therefore, basic rules in Figure 2.5 are performed at the start of every time interval to avoid heating over- and undershoots. The algorithm is

if Heating ended and $T_n > T^{\max}$ **then**
  In future, do not heat above $T_{\text{start}}^{\text{initial}}$
else if Heating ended and $T_n < T^{\max}$ **then**
  $T_{\text{start}}^{\text{initial}} = T_{\text{start}}^{\text{initial}} - \beta$
else if Heating started and $T_n < T^{\min}$ **then**
  In future, do heat below $T_{\text{end}}^{\text{initial}}$
else if Heating started and $T_n > T^{\min}$ **then**
  $T_{\text{end}}^{\text{initial}} = T_{\text{end}}^{\text{initial}} + \beta$
end if

Figure 2.5: Rules for avoiding overshoot for hysteresis controllers.

where $T_{\text{start}}^{\text{initial}}$ and $T_{\text{end}}^{\text{initial}}$ are the indoor temperatures when the temperature was last outside of comfort limits when heating started and ended respectively. Every time heating and cooling ends and comfort limits are not breached, these limits are relaxed by β, so that the breached temperature values tend towards the absolute comfort limits, i.e. $T_{\text{end}}^{\text{initial}} \to T^{\min}$ and $T_{\text{start}}^{\text{initial}} \to T^{\max}$. β was found experimentally as 0.2°C, at which point the limits relax sufficiently fast so that the full range of temperatures are activated as the ambient and building envelope temperatures develop to new, previously unseen states.

2.3.4 Economic Model Predictive Control (EMPC)

Hysteresis controllers are simple and require no information beyond a price. The downside to such simplicity is that, when more information is available, then poor decisions may be taken. An EMPC-based controller can, however, use all available information, like weather forecasts and heating and cooling time expectations, to schedule the heat pump's activity in the best way to meet comfort goals at optimal cost.

Previous EMPC approaches use a relaxed formulation (without integer decision variables) that disregards the on/off nature of the heat pump to reduce computational complexity [44]. However, this appears outdated considering the performance of modern mixed integer solvers. The approach here is therefore to explicitly model binary variables in a mathematical program with equilibrium constraints (MPEC) rather than a state space model. Deviations from a desired mean temperature are penalised, making the problem formulation quadratic. The EMPC optimisation is called upon in the smart control section of the basic thermostat algorithm in Figure 2.3. The overall problem reads

$$\min_{\Theta} \sum_{n} \lambda_n \Phi_n^e x_n + \alpha \left(T_n^i - T^{\text{ref}}\right)^2 + \gamma T_n^{\text{soft}} \tag{2.7}$$

subject to

$$Q_n^{i-a} = R^{i-a}\left(T_{n-1}^i - T_n^a\right) \qquad \forall n \tag{2.8}$$
$$Q_n^{i-e} = R^{i-e}\left(T_{n-1}^i - T_{n-1}^e\right) \qquad \forall n \tag{2.9}$$
$$Q_n^{e-a} = R^{e-a}\left(T_{n-1}^e - T_n^a\right) \qquad \forall n \tag{2.10}$$
$$T_n^i = T_{n-1}^i + \frac{\Phi_n^h x_n + A^w \Phi_n^s - Q_n^{i-a} - Q_n^{i-e}}{C^i} \qquad \forall n \tag{2.11}$$
$$T_n^e = T_{n-1}^e + \frac{Q_n^{i-a} - Q_n^{i-e}}{C^e} \qquad \forall n \tag{2.12}$$
$$T^{\min} - T_n^{\text{soft}} < T_n^i < T^{\max} + T_n^{\text{soft}} \qquad \forall n \tag{2.13}$$
$$v_n \geq x_n - x_{n-1} \qquad \forall n \tag{2.14}$$
$$w_n \geq x_{n-1} - x_n \qquad \forall n \tag{2.15}$$
$$\sum_{n' \geq n}^{n' < (n + z^{\text{on}})} x_{n'} \geq v_n z^{\text{on}} \qquad \forall n \tag{2.16}$$
$$\sum_{n' \geq n}^{n' < \left(n + z^{\text{off}}\right)} 1 - x_{n'} \geq w_n z^{\text{off}} \qquad \forall n \tag{2.17}$$

where the set of decision variables includes the transfer of heat from the interior to the ambient, the interior to the building envelope and the building envelope to the ambient, and the light house and heavy house masses, the start-on and -off variables and the on/off status variable, i.e., $\Theta = \left\{Q^{i-a}, Q^{i-e}, Q^{e-a}, T^i, T^e, T^{\text{soft}}, v, w, x\right\}$.

The first term in the objective function minimises cost over the forecast horizon. The second term penalises deviations from the reference temperature. The third term adds an additional penalty for exceeding the comfort bounds. The tracking temperature, T_n^{ref}, is a temperature that ensures that a mean indoor temperature is reached over a long enough period. Similar to the hysteresis tracking variable, it is defined in a recursive manner, but unlike the hysteresis tracking, it is only defined every day, i.e.

if New day started and $\bar{T}^i < T^{\text{offset}}$ **then**
  $T^{\text{ref}} = T^{\text{ref}} + \eta^{\uparrow}$
else if New day started and $\bar{T}^i > T^{\text{offset}}$ **then**
  $T^{\text{ref}} = T^{\text{ref}} - \eta^{\downarrow}$
end if

Figure 2.6: Rules for EMPC temperature tracking.

where $\eta^{\uparrow}$ and $\eta^{\downarrow}$ are found experimentally so that the EMPC algorithm produces a mean temperature that is comparable with the hysteresis mean temperature and the EMPC does not exhibit any obvious oscillating behaviour due to periodic changes in temperature tracking. Values of 0.01°C and 0.001°C were found to be appropriate for $\eta^{\uparrow}$ and $\eta^{\downarrow}$.

Constraints (2.8), (2.9) and (2.10) describe the transfer of heat from the interior to the ambient, the interior to the building envelope and the building envelope to the ambient respectively. Constraint (2.11) describes the evolution of the interior temperature, considering thermal heat from the heat pump and solar irradiance, and the heat capacity of the interior. Constraint (2.12) describes the building envelope temperature considering the heat capacity of the envelope. Constraint (2.13) defines comfort boundaries that should not be breached. These boundaries are made soft by the slack variable T_n^{soft}, which is multiplied by the arbitrarily high parameter γ in the objective function. Soft comfort bounds ensure that a feasible solution can always be found. Constraints (2.14) and (2.15) contain binary variables v and w that track when heating started and stopped respectively. Constraints (2.16) and (2.17) enforce minimum on- and off-times respectively.

The problem is a mixed integer quadratically constrained problem (MIQCP) solved using the CPLEX solver. Solutions considering the binary nature of a heat pump are typically found in around one second when the dynamics are considered with five minute intervals and a four hour forecast horizon is used.

2.3.5 Data sources with uncertainty

Controllers were simulated with 2014 price and weather data. Prices have a five-minute resolution and come from the balancing market framework presented in Chapter 4. Prices are generated by a market that co-optimises DR and conventional generation to remedy the imbalance caused by wind power. Wind power represents a larger share than is the case today, with a wind power forecast error double that of the current Danish national imbalance from wind. These prices therefore capture the level of volatility that might be expected in the coming decades, should DR participation increase significantly and wind power become the largest source of generation. Real-time prices are closely correlated with the 2014 day-ahead prices, i.e. the day-ahead price is the observed spot price from 2014, plus or minus an offset to activate balancing power. Figure 2.7 shows an example day of spot and real-time prices. New real-time price forecasts are created every five minutes but, for clarity, only forecasts created at midnight, 08:00 and 16:00 are shown in Figure 2.7.

Uncertainty in weather forecasts is also taken into account. EMPC algorithms receive weather forecasts from the Danish Meteorological Institute (DMI) four times per day with an hourly resolution, which are subsequently used in the optimisation problem in Equations (2.7)-(2.17). These forecasts differ from the observations that are used

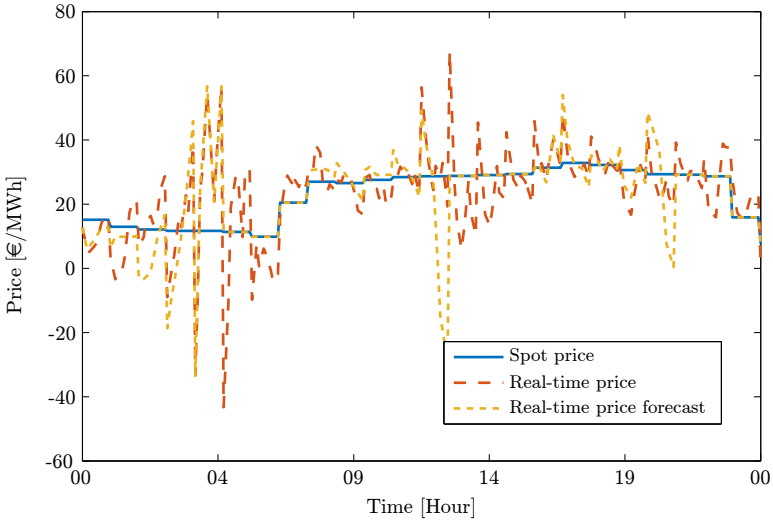

Figure 2.7: A single day of electricity prices, showing that real-time prices are far more volatile that day-ahead prices, and that there can be a significant error in the price forecasts.

in the thermal model of a house in Equations (2.1) and (2.2).

2.4 Results

Simulations were performed for a range of comfort settings ($T^{\min}$ and $T^{\max}$), which are the minimum and maximum interior temperature that the user will accept. The bigger the gap between $T^{\min}$ and $T^{\max}$, the less desirable the comfort is from a user perspective. Minimum on- and off-times of 20 minutes were used.

A half day of simulations are shown in Figure 2.8. The first plot shows the real-time price, which ranges from 25 to 55€/MWh. The second plot shows the ambient temperature, which drops from 3°C to 0°C as the day wears on. The third plot shows the global solar irradiation, which starts at the noon peak and falls to zero at 17:00 UTC. The fourth plot shows the heat pump state (on or off). The basic thermostat activates the heat pump far less than the smart control algorithms, since its target temperature simply oscillates between the upper and lower comfort bounds. All thermostats exhibit longer on-periods during colder conditions, due to higher heat loss to the ambient. The final plot shows the indoor temperature for each controller, and comfort bounds, which are 19.5°C and 22.5°C in this example. Both hysteresis and EMPC algorithms turn the heat pump off for part of the high-price period (17:00

- 19:00). The basic thermostat also, coincidentally, is turned off for much of the last high-price hour. Both smart controllers successfully prepare for the high pricing period by activating the heat pump so that the indoor temperature reaches the upper comfort bound in the low-price period that occurs during the preceding hours.

2.4.1 Cost and comfort results

The main results for comfort and cost are shown in Figure 2.9. The plots show the indoor temperature standard deviation, the mean indoor temperature and the annual cost for electricity (excluding taxes and tariffs) for different comfort bounds. The indoor temperature standard deviation increases for all controllers as the comfort bounds are widened, especially for the basic thermostat. This highlights that flexibility is only extracted in return for a less stable indoor temperature. The mean temperature is highest for the 1°C comfort bound, caused by frequent temperature overshoots and suggesting that a 5kW heat pump may be oversized for a 1°C comfort bound and a house with the thermal characteristics simulated. An alternative explanation is that the first-order dynamics in Equations (2.1) and (2.2), which assume even temperature distributions for the light- and heavy-masses of the houses, are overly simplistic.

The mean temperature for the hysteresis and EMPC algorithms stays close to the desired temperature, 21°C, for all other comfort bounds, validating temperature tracking functions. The basic thermostat has no temperature tracking, which leads to lower mean temperatures as the comfort bound increases. Non-linear thermal dynamics dictate this behaviour as the indoor temperature cools slower than it heats when below the mean temperature, causing many observations at temperatures near the lower comfort bound. This effect can also be seen in the probability distribution of temperatures shown in Figure 2.10.

The basic annual cost for a heat pump with a 2°C comfort range is €293. At this comfort level, the hysteresis and EMPC algorithms deliver annual savings of €1 compared to the basic thermostat. At a 3°C comfort range, which is the median comfort range assumed to be used by EcoGrid EU customers, both smart algorithms lead to annual costs of €284, a €9 saving compared with the basic thermostat and a 2°C comfort range. The annual costs are €274 for the smart algorithms under a 4°C comfort range, leading to savings of €19 per year. Only with a 7°C comfort range is the EMPC able to outclass the hysteresis algorithm with savings of €31 versus €27. It should be noted that these cost savings come about by increased temperature variations. The temperature standard deviation increases by 14%-61% for the 3-7°C comfort bounds compared with the 1-2°C comfort bounds.

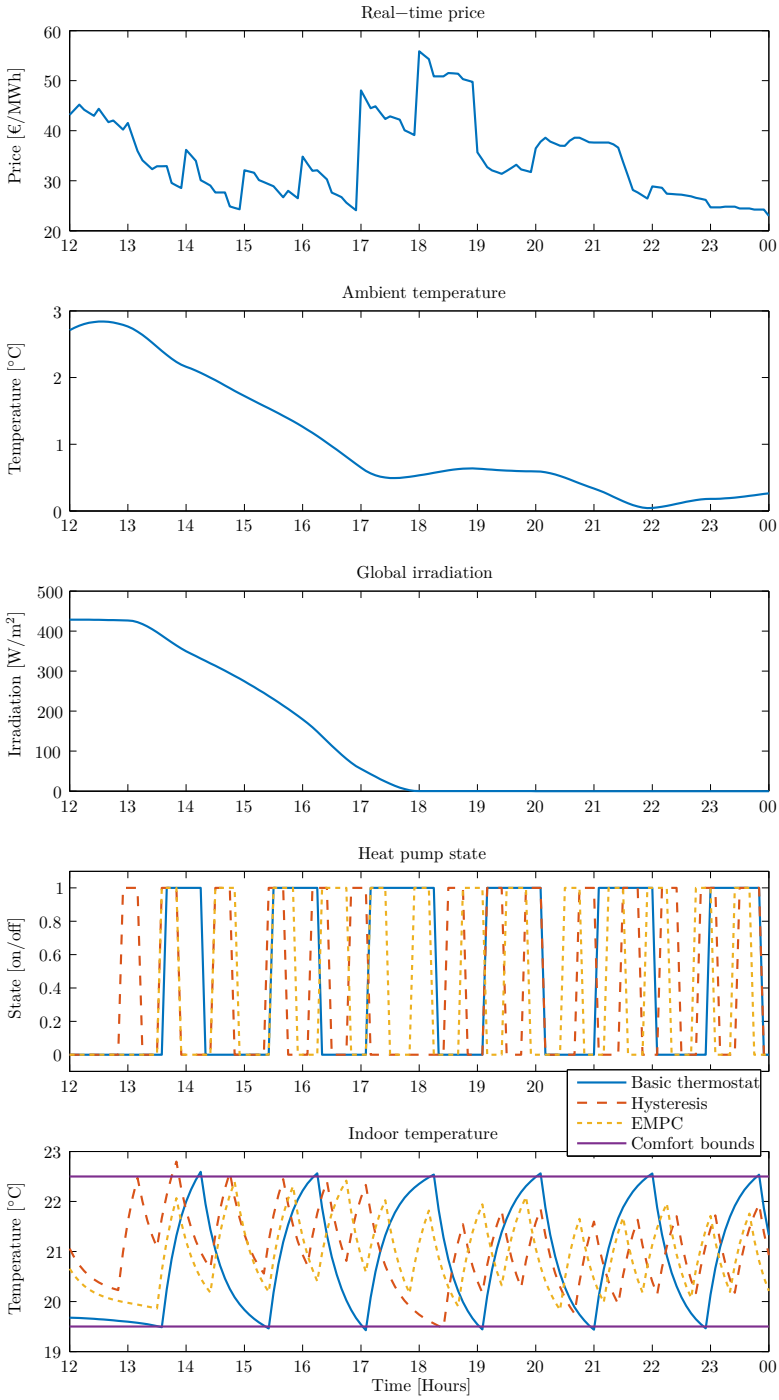

Figure 2.8: A half day example of the simulation.

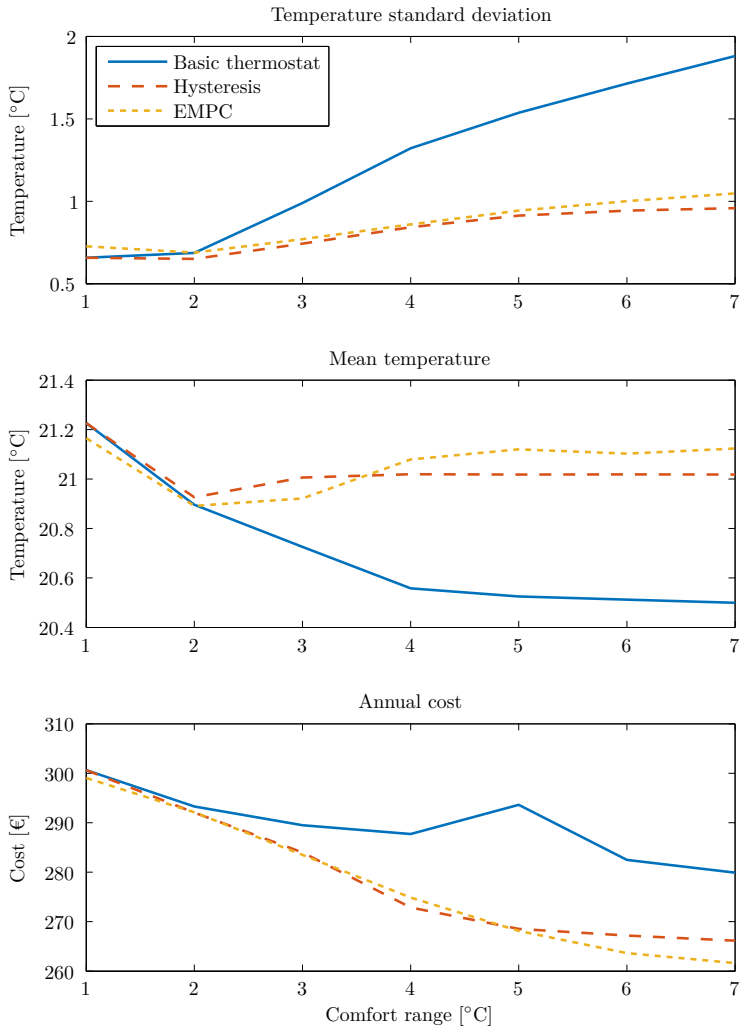

Figure 2.9: Temperature and cost results for different comfort bounds.

Further evidence of why the financial savings are so low can by found by seeing how often heat pumps were activated during the cheapest and most expensive periods of the year. For a 3°C comfort bound and looking at the cheapest and dearest 20 hours, the percentage of time activated are shown in Table 2.2. Here, it can be seen that activation is only increased by an additional 6.8% compared with a non-smart controller during high-price periods. Activations are reduced by up to 5.4% during the lowest price periods. Clearly, comfort bounds, minimum on/off times and price and weather forecast uncertainty limit the heat pump's ability to deliver flexibility

during extreme price periods.

Table 2.2: Percentage of time activated during extreme price periods

	Basic thermostat	Hysteresis	EMPC
Activation in cheapest 20 hours	33.6%	40.4%	40.1%
Activation in dearest 20 hours	21.7%	16.3%	18.7%

Figure 2.10 shows the probability distribution of indoor temperatures for a 4°C comfort bound. Temperature tracking for the hysteresis algorithm and deviation penalisation for the EMPC algorithm ensure that a desirable distribution is reached for the smart controllers, spending little time at extreme temperature ranges.

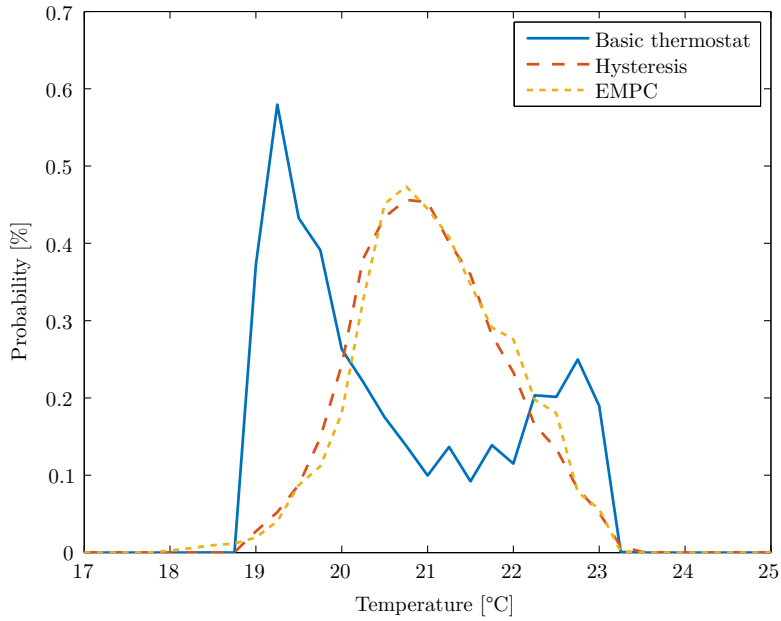

Figure 2.10: Temperature distribution for a 4°C comfort bound.

2.4.2 On/off cycling rates

Heat pumps have a lifetime of 15-20 years, but several moving parts mean that frequent on/off cycling of a heat pump reduces the lifetime of the device [56]. The impact

a cost- and comfort-driven control algorithm has on the number of heat pump activations is therefore of interest. Daily activations are shown in Table 2.3. Activation rates stay fairly constant for smart algorithms as the comfort bounds are widened, but drop dramatically for the basic thermostat. Compared to the base case thermostat with a 1°C comfort bound, the hysteresis and EMPC algorithms increase activations by 15% and 19% respectively. In the worst case, activations are 20 times higher than a basic thermostat. While we cannot conclusively state the detrimental impact of increased activations, it is clear that the smart algorithms developed do not have desirable characteristics for reducing wear and tear.

Table 2.3: Daily heat pump activations during heating season

	1°C	2°C	3°C	4°C	5°C	6°C	7°C
Basic thermostat	24.1	29.0	5.4	12.7	1.6	2.5	1.2
Hysteresis	27.6	29.1	27.0	27.6	26.2	26.5	26.1
EMPC	28.6	29.4	26.6	27.4	25.4	26.0	25.0

2.4.3 Empirical cost observations

The algorithms implemented in the EcoGrid EU experiment were subject to commercial confidentiality. However, some details are in the public domain, including that EMPC-based algorithms were used as a starting point [57]. Several iterations were tested, leading to a final version where controllers had 3°C comfort bounds by default and minimum on- and off-times of at least 60 and 30 minutes respectively [58]. Such long minimum on/off times ensured greater customer comfort, as requested by participants. It should be noted, however, that the comfort bounds are only virtual in that the heat pump will ignore such minimum on/off times if its internal minimum on/off times are already met and comfort bounds are breached.

Table 2.4 details the empirical cost observations, averaged per house and excluding taxes and tariffs, for each group during the period September-April inclusive (the heating season when DR is present). The demonstration includes three automated groups and a control group for comparison. Houses in the control group, also called the reference group, receive no pricing information, but houses are equipped with smart meters that report consumption with five minute intervals. The first automated group is comprised of houses that use heat pumps as their main source of heating and are fitted with automated controllers that react to real-time prices and price forecasts. Houses in the second automated group have older resistive-electric heating with automated controllers. Houses in the third group have resistive-electric heating, controllable PV and hot water boilers. The first row in Table 2.4 shows the average monthly cost for each group. The second row is this number normalised by dividing

it by the average consumption for each house (as used in paper B) and dividing the mean group consumption by the reference group cost, i.e.

$$A_i^{\text{norm}} = \frac{A_i}{A_i^{\mu}} \tag{2.18}$$

where A_i and A_i^{μ} are the real and mean costs for house i respectively. The normalised mean consumption for group g is then

$$A_g^{\text{norm}} = \frac{A_g^{\mu}}{A_{g1}^{\mu}} \tag{2.19}$$

where A_g^{μ} is the mean consumption of all normalised houses in the group and A_{g1}^{μ} is the mean consumption of all normalised houses in the reference group.

Table 2.4: Average monthly costs per house during winter months

Group	Reference	Group 1	Group 2	Group 3
Cost [€]	25.3	36.9	28.4	17.7
Cost norm [%]	100.0	99.3	99.6	98.8

The reference group does not, at first glance, appear to be a representative control group, since the automated households have significantly different costs. The normalised cost resizes load patterns to give similar average consumption and appears to allow comparison. It shows that the heat pump group, group 1, has a 0.7% reduction in normalised cost. Scaling this up to absolute costs equates to savings of €1.9 per year per household, a similar figure to the cost savings of a simulated 3°C comfort bound, but much lower than would be expected when considering the mean comfort bounds (4-5°C). Assuming that cost normalisation appropriately reveals the true cost savings of the automated groups, then the discrepancy between simulation and empirical results has many potential causes, including:

- More stringent minimum on/off times in the final algorithms tested in the experiment;
- Sporadic communication, market and thermometer failures in the experiment;
- Models for individual houses become highly unreliable when subject to human interactions [59];
- Obtaining model parameters for individual houses is unreliable, leading to additional structural uncertainty in the experiment;
- The mean comfort bounds estimated in Section 2.2 are overestimates and outliers are more prevalent than estimated here. It is possible that 3°C is the real mean comfort bound; and

- Demonstration participants may have other sources of heating, like a wood stove, that reduces the flexibility of a heat pump.

2.5 Household benefit conclusions

Space heating has been identified as the largest source of DR, in terms of power and energy, out of all domestic appliances in colder and moderate climates [60, 23]. Simulated and experimental results suggesting annual savings of €2-31 and €2 respectively are therefore a disappointment. These outcomes are lower than previous studies and should bring financial estimates for other price-responsive DERs into question.

The business case for automating heat pumps reacting to real-time pricing looks dire from this perspective. If equipment costs €350 and the savings are €2/year, then there is no possibility of a reasonable payback time. In this case, real-time pricing is not incentive enough to warrant investment by aggregators and households. The business case remains unclear even if a lower level of customer comfort can be accepted, leading to €20/year savings. Furthermore, the lifetime of the device may be compromised compared to a thermostat that optimises for reduced wear and tear, thus lowering the desirability of economic algorithms.

The balancing market pricing used is a guess at future pricing, but it's entirely possible that it underestimates future price volatility. With more volatility, the financial rewards for flexible consumers may be greater, since a consumer who increases and reduces their consumption during high and low price periods respectively will may reduce their bill more (compared to a customer who does not) as extreme prices become more frequent. However, the results of how often heat pumps were able to respond to the highest and lowest prices show that this is a double-edged sword. If heat pump customers take the risk of switching to real-time pricing, then they will also be exposed to extreme prices without being able to respond to them due to their internal constraints. If extreme prices are the main justification for DR, then CPP or direct control may be a lower risk form of activation, since if these events happen infrequently, then heat pumps may be able to respond every time.

From a controller perspective, the performance of hysteresis and EMPC algorithms are unexpectedly similar. In the case of older, resistive-electric heating, EMPC has previously been shown to outperform hysteresis controllers [46]. The impact of price forecast uncertainty and heat pump constraints clearly limit the benefit of EMPC, suggesting that the complexity of model-based control is unwarranted for residential loads. The idea that consumption patterns can be changed without affecting the user experience are also challenged by simulation results. A financial reward can only be realised with broader comfort bounds, which translates to lower user comfort. More advanced methods of control like artificial neural networks [61] and reinforcement learning [62] do not need a full model of the area being heated, and may therefore

be able to deliver additional financial gains at higher levels of comfort, although such controllers are also complex and do not solve the issue of increased on/off cycles.

Inverter based heat pumps, which are capable of delivering far more than an on/off response, are a promising target for future research, since they may offer significantly greater financial savings at a higher level of comfort. However, for now, these devices are not present in significant numbers and still have minimum production levels and minimum on- and off-times that limit their flexibility and complicate controller design.

CHAPTER 3

Aggregated response evaluation

Control of many small loads requires coordination or aggregation so that the response can be exploited in a useful way. This chapter presents the fundamental principles of indirect control with statistical models to forecast the load and to estimate DR volume and other DR characteristics. A validation method is discussed and evidence for a non-linear response is investigated. Finally, a clustering algorithm is used to identify well-performing loads from a larger, anonymous population.

3.1 Introduction

This chapter presents the models for evaluating DR and performing real-time load and DR forecasting. This work was motivated by a market that delegates responsibility for forecasting to a third party, to reduce the burden and risk for households who would not otherwise participate in the market. An operational forecast tool was developed and statistical analyses were performed to assess the size of the DR resource. Previous DR evaluation studies rely on baseload profiles of the load [63], which are well defined for medium- and large-sized commercial and industrial loads, but are unreliable for smaller residential loads. Historically, DR evaluation has focussed on peak-load reduction [64] with models that do not adequately describe the load shift (cross elasticity, frustrated demand) and quickness of delivery that are important for DR activated by a real-time price (RTP). New models with a more detailed description of the load are therefore needed.

Section 3.2 presents the fundamental theory of indirect control and how it applies to TCLs like those simulated in Chapter 2. Section 3.3 follows with linear models that can estimate flexibility and perform forecasting on an aggregated population of loads, which is the basis of paper A. This section also discusses how additional data sources can improve the model's performance. Section 3.4 then investigates how we can ensure that a linear model is a trustworthy and representative picture of reality.

A linear model has significant drawbacks in an operational environment, since DR must be bounded to make a control decision. As such, Section 3.5 presents evidence

for a non-linear response and how linear models can be adapted to include non-linear features for operational use.

Section 3.6 assesses DR from a bigger perspective, whereby well-performing loads are identified from a larger, anonymous population. The clustering methodology from paper B is used here to divide the load into subgroups that perform in a similar manner. Finally, Section 3.7 discusses forecasting responsibility.

3.2 The basics of indirect control

That a population of loads can be indirectly controlled in any meaningful way relies on the fact that they exhibit a somewhat homogeneous response to the control signal and that they have a range of different internal states. Figure 3.1 shows how this applies to thermostatically controlled loads. Red circles (devices, e.g. heat pumps) are on, blue circles are off. When the set-point is moved as a response to a price, a proportional fraction of the devices switch on or off. Constraints like minimum-on and -off times that are widely overlooked in the literature are represented in Figure 3.1 by the devices x and z respectively. The boundaries in this figure, $T_{\min}$ and $T_{\max}$, are normalised boundaries, i.e. they do not represent an absolute temperature, but rather the boundary temperature that each individual device respects. This, combined with different house heat capacities, house dynamics and device size, means that the individual circles in this figure will move up and down at different speeds, giving rise to the different internal states required for indirect control to succeed.

With a large enough population and a diverse enough range of internal states, a continuous and proportional change in demand could be expected from a continuous change in temperature set-point. It is important to note that, in spite of a large body of research on indirect control of TCLs, it remains an assumption that a population of loads will behave in a linear, predictable manner. To our knowledge, there exists no mathematical proof that this is the case.

3.3 Flexibility estimation and demand forecasting

Flexibility estimation of a population of loads such as the one in Figure 3.1 is a hotly discussed topic. A review of 15 dynamic pricing experiments in [64] focussed mostly on common TOU and CPP experiments. It was concluded that CPP programs with enabling technologies (typically automated control of TCLs) reduce the peak usage by an average of 36%. The one RTP experiment included in this survey, the famous Olympic Peninsula carried out by PNNL, showed a 15-17% reduction in peak demand - worse than TOU/CPP groups. However, the idea that peak load reduction should be the primary benchmark for the success of a DR program is outdated and inappropriate for RTP programs that aim to increase social welfare during all time periods,

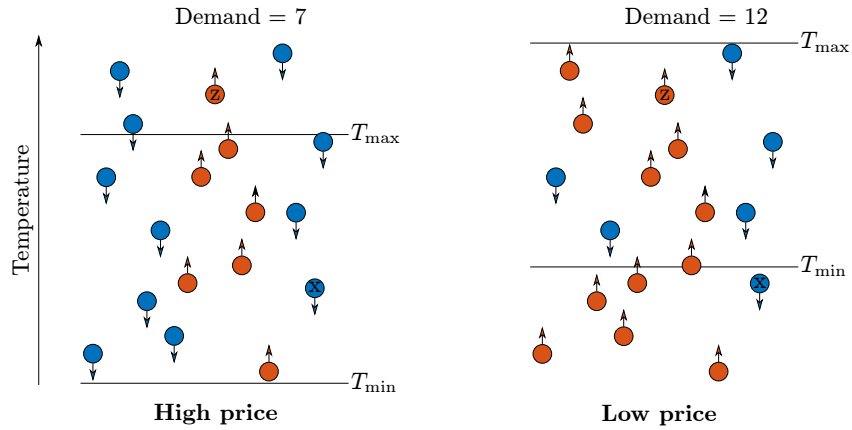

Figure 3.1: A population of thermostatic loads controlled by adjusting the temperature set-point proportionally to the price.

not just during peak hours. New benchmarks need therefore be designed to assess the wider value of RTP programs, including response time and energy shifted - two increasingly important indicators when dealing with RES integration.

Response time, energy shifted, peak response and time to peak response can all be described by the statistical models presented in paper A. The approach starts with the general linear model, which is

$$c_t = \tilde{\lambda}_t^\top \theta_\lambda + \tilde{z}_t^\top \theta_z + \tilde{\chi}_t^\top \theta_\chi + \epsilon_t = \boldsymbol{x}_t^\top \boldsymbol{\theta} + \epsilon_t \tag{3.1}$$

where $\tilde{\lambda}_t$ is a vector of forecast, instantaneous and historic electricity prices, $\tilde{z}_t$ is a vector of external variables like weather terms and a Fourier series that describe the independent baseload due to human behaviour, $\tilde{\chi}_t$ is a vector of interactions between different variables, and ϵ_t is normally distributed white noise with zero mean and finite variance. In this chapter, time-series analysis conventions are used; a variable is an exogenous object and a parameter is the object that must be found.

The parameters θ_λ describe the finite impulse response (FIR) for price. Such a FIR is analogous to plucking a guitar string. It resonates for a finite amount of time and the overall amplitude is impacted by how hard the string is plucked. Conceptually, however, a FIR for price can come to rest at a new steady state, whereas the guitar will always fall back to its initial state: silence.

The model in Equation (3.1) describes the entire load, not just the response to price, which is illustrated in Figure 3.2. Here, the load from Fourier terms, weather, day-ahead and real-time price are cumulatively added in the diagram. The peak DR

predicted by this model is 680kW on the coldest days from a load with an absolute peak consumption of 3154kW during the 2014/2015 heating season, suggesting 21.6% peak flexibility. The maximum energy shift capable is 586kWh/h and the ramping time to peak DR delivery is 15 minutes, although 99% of peak delivery is delivered after 10 minutes (i.e. the response plateaus temporarily). The observed load that this model estimates is also plotted. There is a noticeable gap between the model and the observations due to the structural deficits in the model and the fundamental uncertainty in nature, represented by ϵ_t in Equation (3.1). Despite the noise, price-response shapes and trends are still present in the observations.

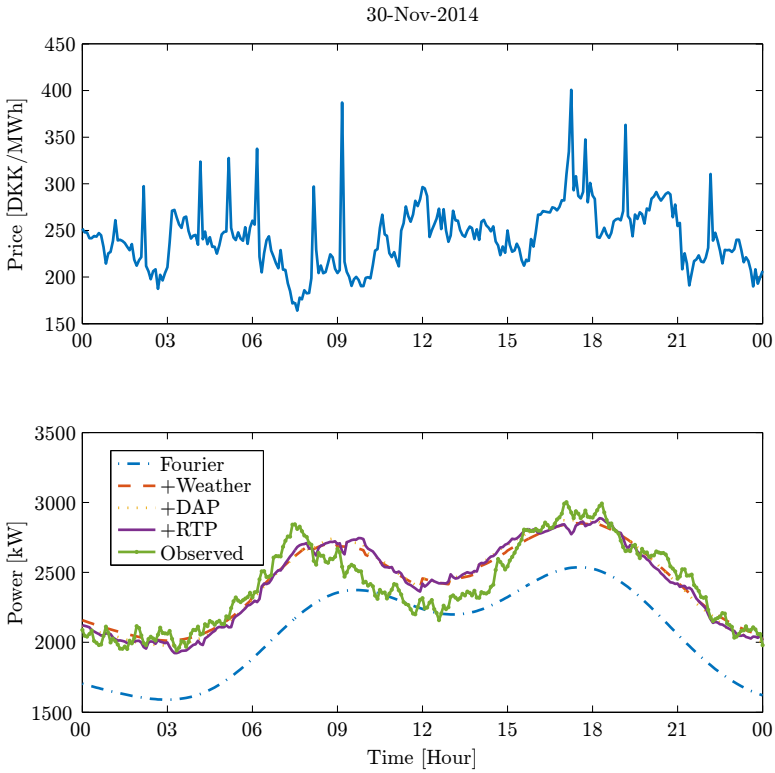

Figure 3.2: Example output of the general linear model from Equation (3.1).

The gap between the model output and the observations is analogous to forecast error, which is reduced as the load size increases. The benchmark for performance in the field of forecasting is the mean percentage absolute error (MAPE), defined as

$$\text{MAPE} = \frac{1}{n}\sum_{t=1}^{n}\left|\frac{c_t - c_t'}{c_t}\right| \tag{3.2}$$

where c_t is observed load and c'_t is the model-estimate for the load. Using this measure, [65] reported a 15% day-ahead MAPE for a 60kW load, [66] reported a 4% error for a 2GW load, while a 0.8% MAPE was observed for the Danish national load (5GW peak) in 2014 [67]. For a model built on a five month EcoGrid EU time-series (Figure 3.2 is an excerpt of this model), the error was 5.4%. Considering the peak-load for this time-series was 3.2MW, this error appears to be an appropriate size, larger than the error for larger loads and smaller than the error for smaller loads. It is therefore possible that the chance of DR from residential loads not delivering the response forecasted diminishes as the load increases in size, thanks to the lower MAPE.

Should DR forecasting continue to be a problem, then using additional state estimations of DERs and the load as an additional external input to the model is a promising approach. The market operator could incentivise aggregators to make anonymous internal state estimations available to the forecast responsible party in return for a reward proportional to the additional benefit these observations provide.

An example of state estimations are indoor temperature measurements which, when added to Equation 3.1 as an external regressor, reduced the MAPE by an additional 0.3%. This was in spite of a very small fraction of the 1900 houses being represented and very poor data quality from the available thermometers, as shown in Figure 3.3. Data quality was impacted by thermometers being wireless and powered by AA batteries, which regularly needed replacing, and difficult human behaviour, like placing a thermometer in the fridge when a participant wanted a warmer house instead of changing the thermostat settings. The value of internal state estimations, even if poor and limited in quality, is therefore high.

3.4 Linear model verification

Having identified a model, it becomes important to prove its trustworthiness, especially if the outcome of this model is to be used for real power system operation, as it was in the EcoGrid EU demonstration. In the experiment, the model was implemented in Java and delivered a new forecast every five minutes with a 36 hour forecast horizon.

A reliable way to validate a statistical model is to apply it to previously unseen data, but this proved difficult to do in real-time due to the fluctuating meter readings, as shown in the forecasting results of paper A. Thankfully, there exist other tools that can be used to determine the trustworthiness of the models used. Cross-validation is often used to assess a model but, in combination with parameter shrinkage, can also be used to help with model selection by way of discouraging over-parameterisation and encouraging a reproducible result when applied to new data (i.e. forecasting).

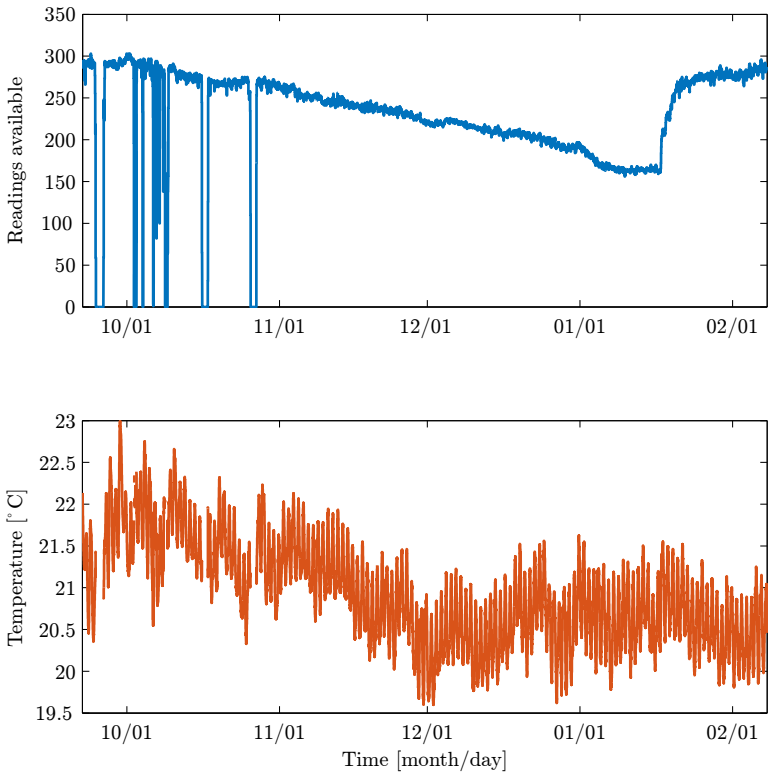

Figure 3.3: Indoor thermometer availability and temperature measurements from the EcoGrid EU population for the 2014/2015 winter.

Leave-one-out cross-validation (LOOCV) is a resampling technique used in paper A, where the time-series being modelled has a non-consecutive portion, or fold, of data removed and a model is built with the remaining data. The mean squared error is then assessed for this fold and the process was repeated for the other portions of data.

To start this process, the model parameters are found by minimizing the penalised least square error [68], i.e.,

$$\min_{\theta} \sum_{t=1}^{T} \left(c_t - \boldsymbol{x}_t^{\top} \boldsymbol{\theta}\right)^2 + \eta |\boldsymbol{\theta}| \tag{3.3}$$

where η is the tuning parameter that governs how heavily the parameters of the model, $\boldsymbol{\theta}$, should be reduced.

Figure 3.4 shows the outcome of this process when used to find the tuning parameter η. Each bar represents the range of mean square errors (MSE) from a 10-fold cross-validation tested with a unique value of η. The fact that the MSEs are similar for each fold in the cross-validation routine implies that the model is sound since the variance does not change much if you build the model on a limited sample of data. The η with the lowest average mean squared error, given at the dashed line in Figure 3.4, was then used. The process of finding the model is also the process for reducing the likelihood for over-parameterisation.

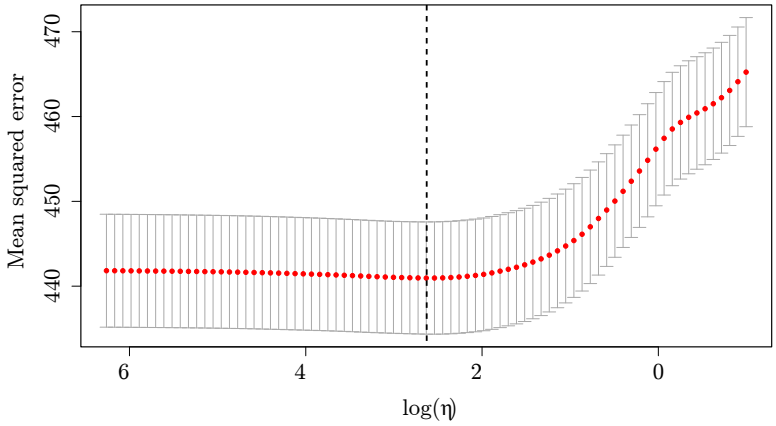

Figure 3.4: Cross-validation routine with different levels of parameter shrinkage.

There exist several additional methods that can assess the validity of a linear model. Such methods primarily analyse the residuals of the model and include a sign test, auto-correlation and partial auto-correlation functions, cumulative periodogram, quantile-quantile, scale-location and residual-leverage plots [69]. All these indicators suggested that a linear model was valid. However, Figure 3.5 shows that outliers exist, equidistantly spaced. Further investigation showed that these outliers were found every week at 6AM on a Monday morning. Discussion with a manufacturer revealed that this was a hot-water tank cleaning function that was enabled on all devices at exactly the same time. This five-minute spike was not identified by the models developed, highlighting a danger of synchronised behaviour of loads that are too similar causing an unforeseen imbalance and unavailable DR during certain time periods.

3.5 Evidence for a non-linear response

Model validation of the linear model largely supported its choice, yet common sense suggests that there must be bounds on the response to price. A linear model will

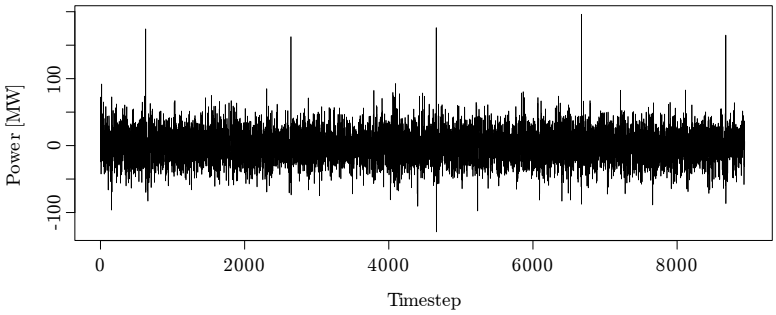

Figure 3.5: A time-series of the residuals, ϵ, from Equation 3.1.

forecast an infinite amount of DR, given an infinite price. In an operational environment, bounds on the response are therefore needed. Previous work has identified a non-linear response to pricing by simulating a population of houses with SDEs with controllable heating responding to a five-minute price [70] and modelling demand as a Markov process [71]. Evidence for non-linear behaviour can be shown in EcoGrid EU data by plotting residuals of a linear model with the price responsive data put back into the noise. To do so, residuals are combined with the price response according to the Equation (3.1), i.e.

$$\epsilon_t^* = \epsilon_t + \lambda_t \theta_\lambda \tag{3.4}$$

The residuals ϵ_t^* now include the predicted linear DR and, perhaps, non-linear components too. In this example, the price λ_t and linear price response θ_λ exclude lagged values. A smoothed interpolation through this cloud of points can subsequently be created to see the relationship between these residuals and the real-time price. A B-spline representation [72], $f = \boldsymbol{\lambda}^* \theta_b$, is found by minimising the penalized likelihood of the difference between the spline and the observations, i.e.

$$\min \left(\epsilon^* - f\right)' W \left(\epsilon^* - f\right) + \eta \theta_b' \Sigma \theta_b \tag{3.5}$$

where $\boldsymbol{\lambda}^*$ describes the B-splines, θ_b are the spline coefficients, W is the weight given to each node and is determined by the number of observations at that price, Σ is a matrix of the second order differential of coordinates of the B-splines, and η the tuning parameter found by performing a LOOCV. This algorithm was applied to the mean and standard deviation of prices λ_t grouped for €3 bins of ϵ_t^*. The end result can be seen in Figure 3.6.

For positive prices there is almost immediate saturation and significant non-linear behaviour. For negative prices, the price response appears reasonably linear, so it is likely that saturation lies beyond the range of negative prices used. The asymmetrical behaviour reflects the fact that many devices in the demonstration could only be turned on and not off, which equates to responding to lower prices rather than high

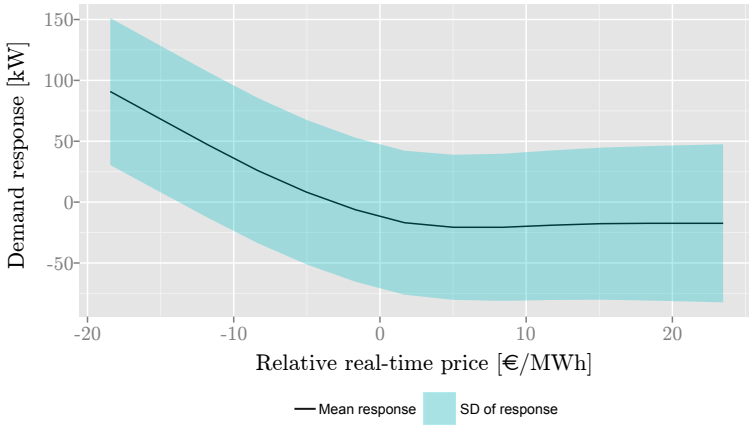

Figure 3.6: The non-linear relationship between relative real-time price and the load based on 2014/2015 winter observations. This excludes lagged prices, so overall DR activated is greater.

prices.

In the demonstration (and before the spline-based analysis was performed) this non-linear behaviour was assumed to be symmetrical and modelled through a logistic function. A logistic function has the desirable property of being described by just two variables (as opposed to three variables for an arctangent function of the same shape), making it easy to solve using the Levenberg-Marquardt algorithm [73]. A generalised logistic function was modelled in the form

$$\epsilon_t^* = \sum_{t'=1}^{n_\lambda} -\frac{A_{t'}}{2} + \frac{A_{t'}}{1 + e^{-B_{t'}\lambda_{t'}}} \tag{3.6}$$

where ϵ_t^* contains linear model residuals and linear price response for price lags t'. The shape parameter for each price lag is $B_{t'}$, while $A_{t'}$ is the range of the logistic function response. Half of this range gives the amplitude of the response, which in turn is the maximum DR predicted by this model for each cross-price elasticity. The maximum DR that can be delivered in theory is therefore

$$\Delta c^{\max} = \frac{\sum_{t'} |A_{t'}|}{2} \tag{3.7}$$

However, due to the computational complexity of solving (3.6) for more than three price lags, only the price lag with the most price elastic response is solved for (typically the first, second, or third price lag), which then bounds the entire FIR. For the

differenced model presented in paper A, all three price lags are bounded. The model can be expanded to give more detailed bounds when considering price interactions, such as the important price-temperature interaction modelled in paper C.

3.6 Clustering approach for identifying households delivering DR

In system operation, it is highly likely that loads need to be clustered, so that well-performing and problematic loads can be identified based upon similar behaviour. Paper B presents a clustering process that aims to do just this. It was initially used to identify houses that were price responsive in the first part of the EcoGrid EU demonstration. The paper is formulated assuming that we know which houses should be price responsive and which should not. This knowledge was only possible due to the efforts of the manufacturers in EcoGrid EU. Both price- and non-price responsive groups in this paper had the same automation equipment fitted and non-price responsive houses were identified by maintaining close contact with the customers about where and how their thermometers were being used and analysing individual communication problems on a day-by-day basis.

In a larger roll-out of DR, such close, personal analysis of individual customers is unlikely to be feasible. Using cost to identify a response, as in paper B, also has its difficulties, as identified by the small cost savings observed experimentally (see Table 2.4). It is therefore desirable to combine the clustering process with the models developed in paper A to identify price-responsive clusters in a manner that scales to larger populations and identifies price responsiveness based upon the FIR for price.

To show how such an approach could work, a minimal example that combines the clustering (paper B) and FIR (paper A) tools is presented here. To start with, 500 houses were selected from the EcoGrid EU population. Figure 3.7 shows the FIR for the houses selected in each group. Figure 3.8 then shows the dendrogram of how the houses are clustered, with an arbitrary cut-off giving six clusters. The height on the y-axis is normalised between zero and one and reflects the distance between the variance of each cluster. Figure 3.9 shows the time-series of each cluster for the input data (one week in December 2014). The shaded area represents 95% confidence intervals for these time-series, derived using a non-parametric method whereby individual house consumption is sampled with replacement (bootstrapping). The confidence intervals are narrow, suggesting that houses in each cluster are quite similar.

Following the clustering process, linear models were created for each cluster and the FIRs for price were picked out and shown in Figure 3.10. The clustering algorithm appears to identify houses that deliver the most DR, as seen in Figure 3.10. Despite having similar peak loads, clusters 2, 3 and 6 show significantly different response to prices. The DR volume in cluster 3 is over 8 times larger than the DR delivered

by clusters 2 and 6. The DR delivered by clusters 1 and 2 appears to present different characteristics to clusters 3 and 6, with a far more gentle rebound. Clusters 4 and 5 exhibit no DR and further inspection reveals that these houses are empty holiday homes, which suggests that the clustering algorithm is influenced by both DR characteristics as well as participant demographics, which in turn suggests that a clustering approach can be used for identifying houses in a wide range of applications.

The success of identifying cluster 3 as the best performing one by far means that, if additional financial incentives were to be paid to customers, e.g. in the form of an availability payment, then cluster 3 participants could be rewarded additionally for exhibiting a desirable response.

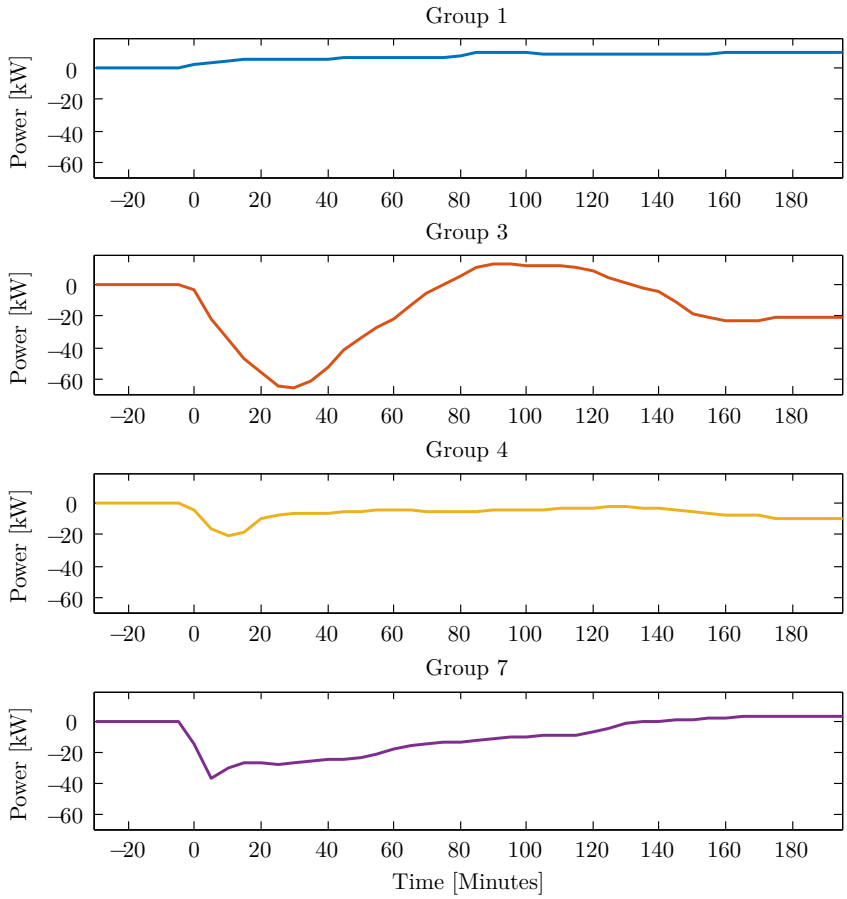

Figure 3.7: Finite impulse responses of the reference group and the automated groups.

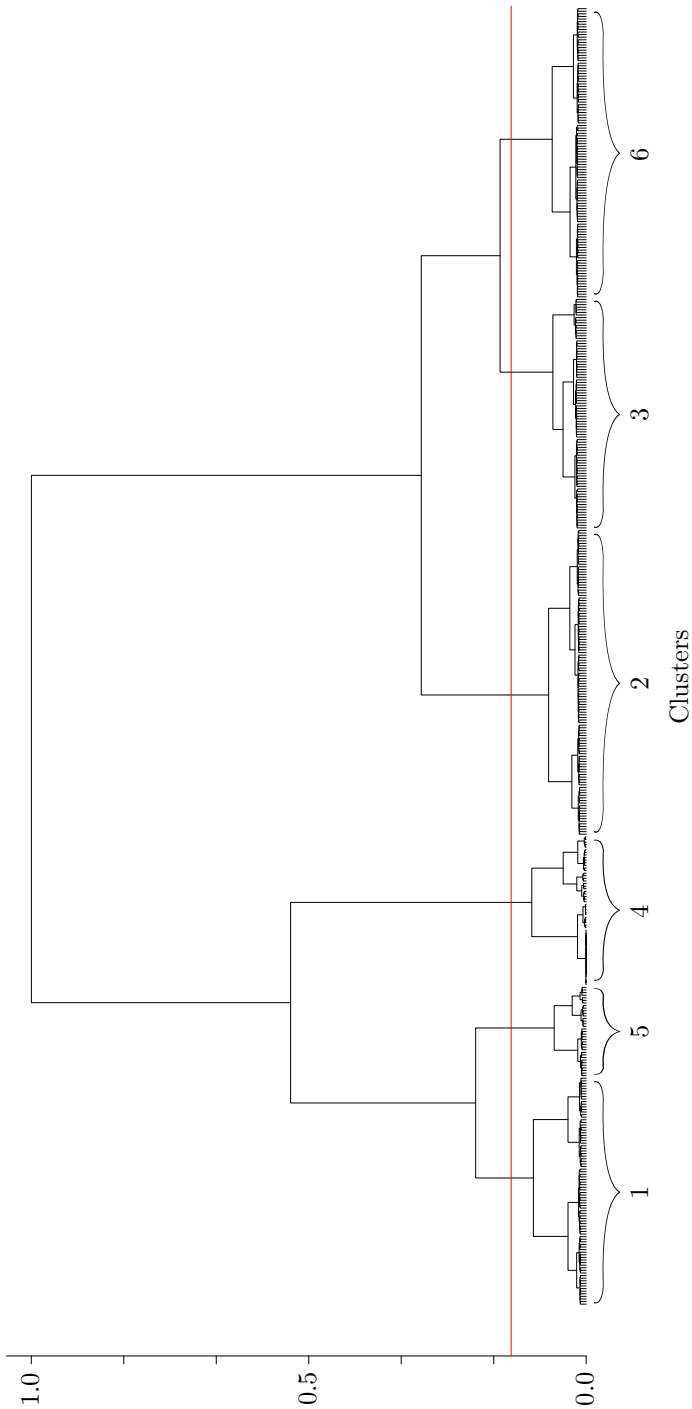

Figure 3.8: Clustering of 500 houses into six clusters. The red line shows the cut-off where the clusters are defined. The bottom row is individual houses, which become grouped as you move up the dendrogram.

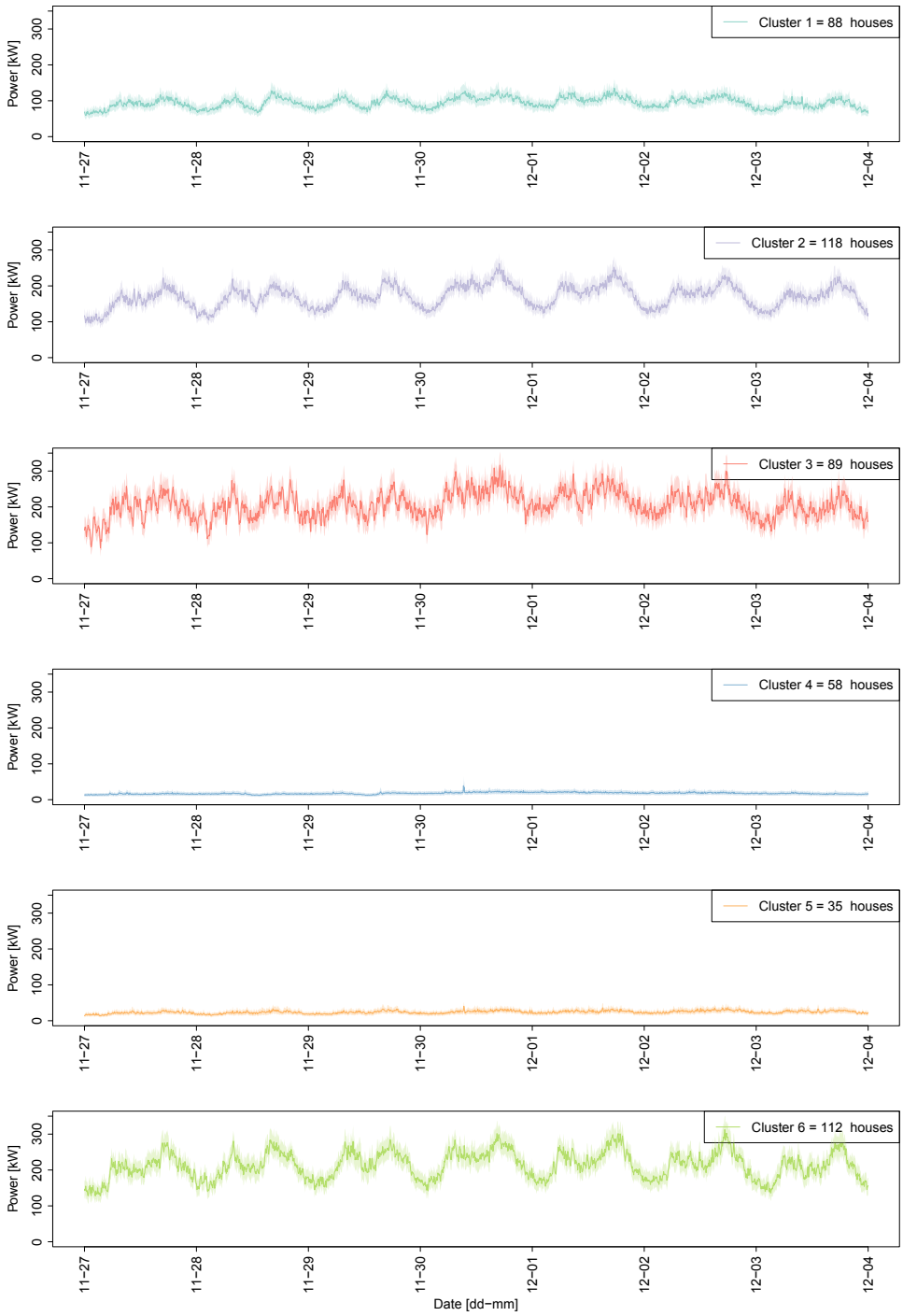

Figure 3.9: Clustering outcome from the 500 houses chosen.

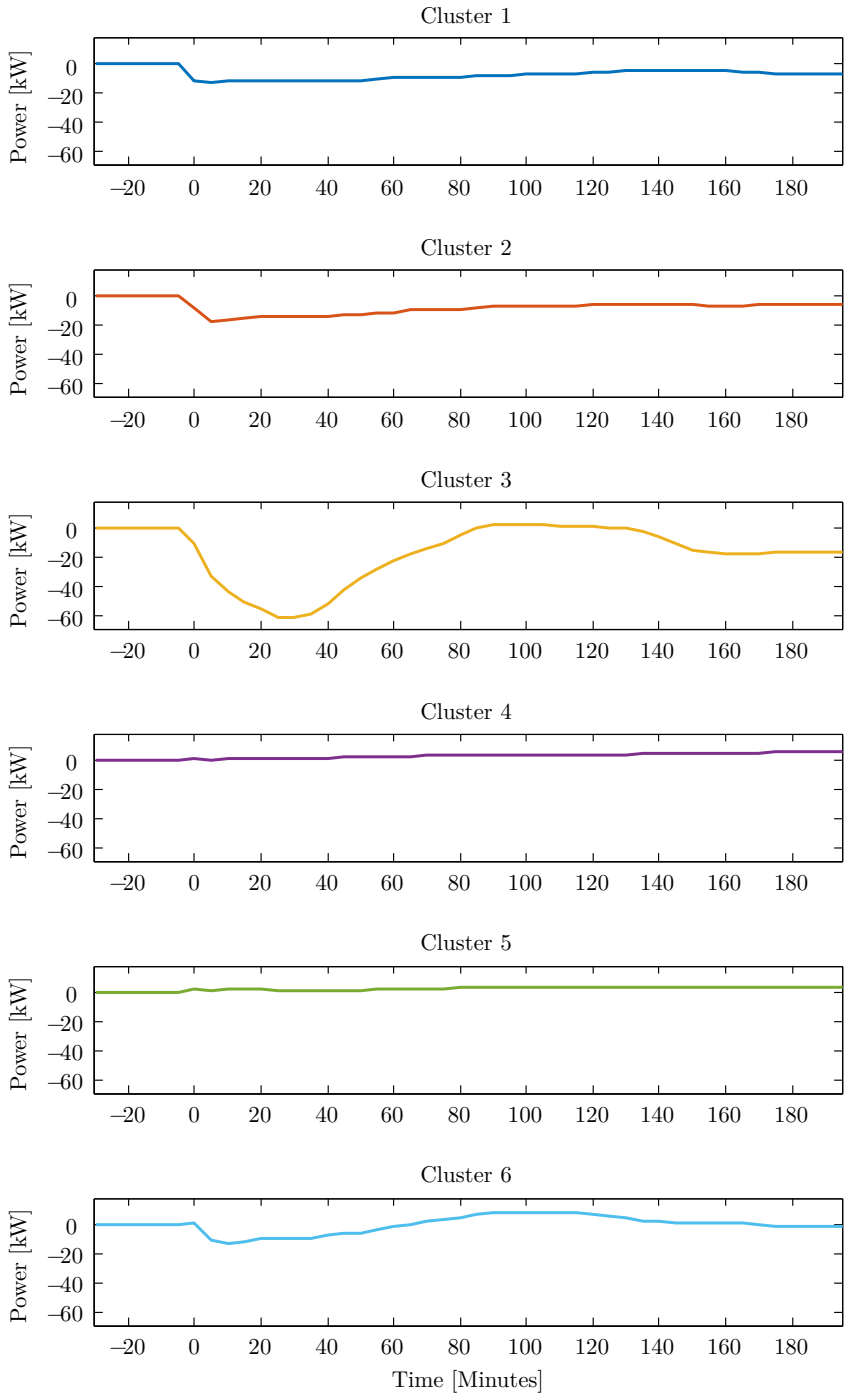

Figure 3.10: Finite impulse responses of the clustered groups.

3.7 Consequences for the forecast responsible party

In existing markets, loads must be a minimum size in order to participate, e.g. 10MW in Denmark. Each load then has a balance responsible party (BRP) who is accountable for forecasting consumption and remedying imbalances in their portfolio. The minimum size requirement precludes smaller loads such as individual houses from participating in the market. Markets can remove this barrier to entry by moving the responsibility for estimating bid size and price response to a third party, perhaps the market operator. This allows smaller loads entry to the market and removes the burden of bidding and the financial risk of not fulfilling the resulting bids, making DR an attractive and accessible proposition for a wide array of loads.

Forecasting is the key to making indirect control work. Without adequate forecasting accuracy, indirect control DR does not fulfil the goal of maintaining a reliable power system. The experiences learnt from identifying and validating a forecasting model suggested that, under certain conditions, the approach of having a third party taking forecasting responsibility leads to higher risk and lower efficiency than each load being forecast responsible. The source of risk were the large, unforeseen deviations due to synchronised device behaviour. This would not be an issue if there are a diverse enough range of device manufacturers, but if there are only a handful, then one botched firmware upgrade - or even schedule maintenance not communicated to the forecast responsible body - can wipe out significant flexibility, making DR an unreliable resource. Even if forecasting methods are more advanced and fully adaptive, there will at least be a five-minute period (and likely longer) where DR could disappear entirely, causing a major imbalance in the power system.

The source of lower efficiency comes from device manufacturers being reluctant to share useful, anonymous state-estimation data, such as indoor temperature readings, that would improve forecast accuracy. It may therefore be desirable that companies responsible for DER behaviour, e.g. aggregators, take a significant or entire part of the responsibility for forecasting load and DR.

Should the aggregator take forecasting responsibilities, then it could be rewarded by the market operator based upon forecast accuracy and DR delivered. These payments can subsequently be passed on to individual well-performing loads, identified using the clustering and linear models as in Section 3.6. Such an approach can retain the no-risk option of not penalising loads when they do not perform as forecast (analogous to delivering on a bid as promised) whilst encouraging good DER-controller design and strong forecasting algorithms, which in turn can promote competition between aggregators who win the additional income by competing with the best forecasting algorithms and for the most responsive and reliable customers.

CHAPTER 4

Electricity market design

Trading and activating DR in a market is a top priority for many TSOs and policy legislators. Yet fitting DR into a market structure and yielding a positive outcome is challenging from economic and technical perspectives. This chapter presents day-ahead and real-time markets with new constraints to fully describe flexible demand, followed by implementation-specific additions. The causes of inconsistent pricing for demand and supply are identified, and the impact on cost and reliability are estimated.

4.1 Introduction

An electricity market exists to ensure that supply equals demand at all times and everywhere in as economically efficient a manner as possible. This should be achieved reliably, while adhering to the fundamental market principle that revenue from demand equal revenue to supply [74]. The real world, however, invariably interposes significant discontinuities and non-linearities that make a balance hard to achieve optimally [75]. This chapter explores these challenges by integrating the load models developed in Chapter 3 into basic day-ahead and real-time market structures. The basic market framework is built up with implementation specific features added afterwards, which also form the basis for the market formulation in papers C and D. Results from the EcoGrid EU experiment are presented and a re-purposed tool for innovatively quantifying market based volatility is described. Regardless of how DR is controlled, so long as it is traded in a power pool, new types of DR have characteristics that market-traded consumption has not had previously, requiring changes to existing market structures.

Section 4.2 gives preliminary definitions for price and cross-price elasticity that are used in the remainder of the chapter. Section 4.3 introduces the basic concept of clearing day-ahead and real-time markets with DR. Section 4.4 demonstrates the impact of generation, demand and network constraints on price discovery. Section 4.5 discusses the unique challenges and design of the experimental market that operated in real-time on the Danish island of Bornholm in 2014 and 2015. Section 4.6 presents

empirical and simulated results, with a focus on market objectives such as social welfare, congestion management and volatility. Section 4.7 highlights the future research necessary for real-time pricing to become a reality.

4.2 Definitions of price and cross-price elasticity

Price elasticity, also called self or own elasticity [76], describes how sensitive a load is to a change in price [77]. It is traditionally defined as

$$\varepsilon = \frac{dC/C}{d\lambda/\lambda} \tag{4.1}$$

where C and λ are consumption and price respectively. This equation describes the how infinitesimal changes in price cause infinitesimal changes in consumption, which need not be a linear relationship. ε is dimensionless and is often used to describe how a 1% change in price relates to a 1% change in quantity.

For the purposes of operating a day-ahead and real-time market, we define price elasticity parameter that is a linear function of observed changes in load, ΔC, according to the models developed in Chapter 3, i.e.

$$\alpha^{DA} = \frac{\lambda^{DA}}{\Delta C^{DA}} \tag{4.2}$$

where λ^{DA} is day-ahead price. Real-time price elasticity is defined with respect to the day-ahead state, i.e.

$$\alpha = \frac{\lambda^{RT} - \lambda^{DA}}{\Delta C} \tag{4.3}$$

where λ^{DA} and λ^{RT} are day-ahead and real-time prices respectively. α^{DA} and α are the ratios of price to DR with units of €/MW^{2}h.

In most cases, demand price elasticity is negative. The more expensive the commodity, the lower the demand. However, there are occasions when positive elasticity occurs. Demand for luxury items can go up if the item is perceived as being more exclusive. From an electricity demand perspective, positive or positive-price elasticity can occur before and after a period of negative elasticity. Known as the rebound effect, or frustrated demand, this occurs because, at some point, demand must be satisfied at any cost. When applied to electric heating, after a long enough period of being exclusively turned on or off, thermostat limits will be reached and the opposite on/off status will occur, so that the house temperature stays in a comfortable range.

In traditional economics literature, cross elasticity, also called cross-price elasticity, describes how the demand for one item is affected by the price changes of another item. In this thesis, cross elasticity is defined as how sensitive demand for an item

is to changes in price that happen before or after a price was valid. For example, if a high price is valid in the period 22:00-23:00, consumption will be altered in the hours before and after it as a direct consequence of the high price. Conceptually, the impact of cross elasticity can be explained using the relationship

$$\Delta C_t = \sum_{t'=T_a}^{T_b} \frac{\lambda_{t'}}{\alpha_{t'}}, \qquad T_a \leq t \leq T_b \tag{4.4}$$

In Equation (4.4) there exist DR and price time-series of length T. There also exists a sliding window around each time-step with the index t'. The sliding window starts at T_a and goes on to T_b and DR (ΔC_t) is a function of all the prices valid from T_a to T_b. This process describes the energy shifted from each slice of time before and after now to now (time-step t). I.e., when summed over the whole sliding window, the entire energy shifted to the current time-step is added together.

4.3 Price discovery in a market environment

Broadly speaking, deregulated power systems give rise to two types of electricity market [78]. The first relies on bilateral contracts, which offer certainty to buyer and seller for the contract's duration. The other far more common type of market, the power pool, is presented here. While power pools benefit from potentially lower prices, they carry the risk of short-term volatility, and some require more information (such as start-up, shut-down and operating costs) at the time of bidding. Other power pools internalise these costs into a single, opaque bid constructed by the entity participating in the market. The two structures use fairly similar tools to determine market outcomes, and they face similar challenges. In Europe, bids that internalise these additional costs are the most common and are presented here.

Electricity pools that maximise social welfare yield a mathematical program with equilibrium constraints (MPEC) [79]. They can be conveniently formulated as linear programming (LP) and quadratically constrained programming (QCP) problems. Heuristic approaches like Piecewise Integration (PIES) [76] and the Bid Cut heuristic [75] also exist for price discovery. However, here we present minimal examples for the most common "textbook" formulations of day-ahead and balancing market clearing mechanisms [80].

4.3.1 Day-ahead market

In a day-ahead electricity pool, the market can be formulated as [81]

$$\max_{\Theta} \sum_{t} \left\{ \lambda_t^{\text{res}} \Delta C_t^{DA} + \frac{1}{2} \alpha^{DA} \Delta C_t^{DA\,2} - \sum_{g} \lambda_{g,t} P_{g,t}^{DA} \right\} \tag{4.5}$$

subject to

$$\sum_{g} P_{g,t}^{DA} + W_t^{DA} = C_t^F + \Delta C_t^{DA} \qquad \forall t \tag{4.6}$$

$$P_{g,t}^{DA} \leq Q_{g,t}^{\max} \qquad \forall g, t \tag{4.7}$$

where the set of decision variables includes DR and conventional generation, i.e. $\Theta = \left\{\Delta C_t^{DA}, P_{g,t}^{DA}\right\}$ for all $g \in G$ and $t \in T$. In this chapter, operations research conventions are used; a parameter is an exogenous object and a variable is the object that must be found.

The objective function, Equation (4.5), aims to increase customer utility and reduce the cost from generation. By maximising customer utility, the market increases consumption and reduces its price. Figure 4.1 shows the shape of customer utility (with additional boundaries for DR, which are not included in the constraints above) and the step-wise supply curve. When price elasticity is assumed to be linear, customer utility is the area of a trapeze, i.e. a rectangle, which is the height (the intercept or reservation price, λ_t^{res}, which is the highest supply bid price) multiplied by the width (DR, represented by ΔC_t^{DA}) plus a right-angled triangle, which is a half times the width (ΔC_t^{DA}) times the height (the price, represented by $\alpha^{DA}\Delta C_t^{DA}$).

The day-ahead price elasticity constant, α^{DA}, is equal to $1/\theta_\lambda$ in Equation (3.1) with only one price lag in a market that does not consider cross elasticity. The flexible and inflexible demand is ΔC_t^{DA} and C_t^F respectively. The bid price, bid quantity and

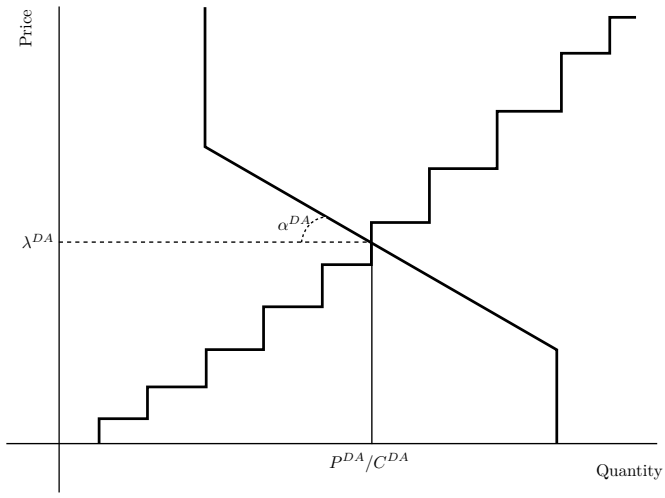

Figure 4.1: The basic equilibrium between supply and demand in a day-ahead power pool.

day-ahead power scheduled are $\lambda_{g,t}$, $Q_{g,t}^{\max}$ and $P_{g,t}^{DA}$ respectively. In this example, the day-ahead wind power forecast, W_t^{DA}, is treated as a free, negative load.

The balancing constraint in Equation (4.6) ensures that supply meets demand. The dual variable of this constraint (alternatively called a shadow price of the primal problem) sets the day-ahead price [79]. Constraint (4.7) describes the maximum boundary of each bid, assuming that a bid can be partly activated as in Nord Pool today.

4.3.2 Real-time market

Markets usually operate in several stages. A real-time market, also called a balancing or a regulating market, is the last market to clear before real-time operation, with faster reserves often following non-pool like structures. A minimal example of a real-time market can be structured as

$$\max_{\Theta} \sum_t \left\{ \left(\lambda_t^{DA} \Delta C_t + \frac{1}{2} \alpha {\Delta C_t}^2 \right) - \sum_g \left(\lambda_{g,t}^{\uparrow} P_{g,t}^{\uparrow} - \lambda_{g,t}^{\downarrow} P_{g,t}^{\downarrow} \right) \right\} \tag{4.8}$$

subject to

$$\sum_g \left(P_{g,t}^{DA} + P_{g,t}^{\uparrow} + P_{g,t}^{\downarrow} \right) + W_t^{DA} = C_t^{DA} + \Delta C_t + B_t \qquad \forall t \tag{4.9}$$

$$P_{g,t}^{\uparrow} \leq Q_{g,t}^{\uparrow,\max} \qquad \forall g,t \tag{4.10}$$

$$P_{g,t}^{\downarrow} \leq Q_{g,t}^{\downarrow,\max} \qquad \forall g,t \tag{4.11}$$

where the set of decision variables includes DR, up and down regulation, i.e. $\Theta = \left\{ \Delta C_t, P_{g,t}^{\uparrow}, P_{g,t}^{\downarrow} \right\}$. The prices $\lambda_{g,t}^{\uparrow}$ and $\lambda_{g,t}^{\downarrow}$ are the up- and down-regulating bid prices respectively, while quantities $Q_{g,t}^{\max}$ describe the maximum bid sizes. The day-ahead consumption is now a known parameter defined as $C_t^{DA} = C_t^F + \Delta C_t^{DA}$, while α describes the real-time price elasticity.

As in the day-ahead market, the objective function in Equation (4.8) aims to reduce costs from generation and increase customer utility, but with respect to the day-ahead market, illustrated in Figure 4.2 (with additional boundaries for DR). The shape that customer utility takes on is a trapeze, on one side of the day-ahead starting point, which is a square ($\lambda_t^{DA} \Delta C_t$) plus a right angled triangle ($\frac{1}{2} \alpha {\Delta C_t}^2$).

Deviations from the day-ahead schedule are represented by the imbalance variable B. If there is no imbalance, then the real-time price is equal to the day-ahead price. The imbalance variable is included in the balance constraint in Equation (4.9); the dual variable of this constraint gives the real-time price. Equations (4.10)-(4.11) define the maximum regulating bid sizes.

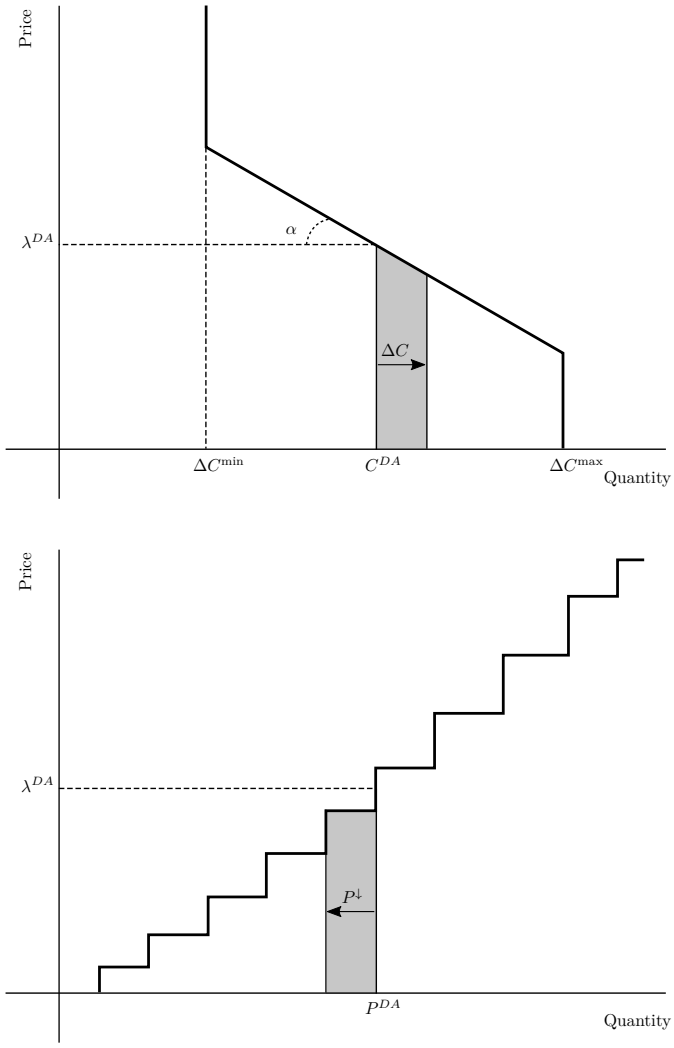

Figure 4.2: A real-time market maximising customer utility (top) and minimising cost (bottom).

4.4 General market constraints

When solved with quadratic programming solvers, the minimal examples in Section 4.3 produce prices that are at the intersection of supply and demand, but the resulting production cannot be met by any market participant. To ensure realistic production schedules, additional constraints are needed, as described in the market

formulation of papers C and D. This section discusses some of the constraints that impact supply, demand, transmission and distribution in a real-time market.

On the generation side, ramp rates, minimum on-times (or multi-period bids) and conditions excluding simultaneous up and down regulation are all needed for practical operation of the power system. On the demand side too, inter-temporal effects (i.e. cross elasticity) and other bounds are also needed. Without such constraints, production schedules cannot be followed, leading to significant imbalances that jeopardise stable power system operation. Paper D characterises the mismatch between market outcome and consumption in terms of social welfare, which was lower than a market without DR when inter-temporal effects were ignored.

The vast majority of generation and load constraints, including basic constraints like ramping, mean that the market clearing price is different from the marginal cost of energy, yet markets are efficient nonetheless [82]. What this usually means in practice is that the price sent to supply and demand is the marginal cost of energy - as calculated in a mixed integer quadratically constrained program (MIQCP) - plus an uplift price that ensures all market participants have their costs covered [83].
The following examples of generation, demand and network constraints illustrate the ramifications of this.

4.4.1 Generation constraint example: multi-period bids

Constraints that require binary variables (e.g., minimum on-times) can lead to behaviour that will strike some market participants as unfair. For example, linear minimum on-times can be added to the real-time market as follows

$$\sum_{t'\geq t}^{t'<t+z_g^{\text{on}}} x_{g,t'} \geq v_{g,t} z_g^{\text{on}} \qquad \forall g,t \tag{4.12}$$

where t' is an alias of t, i.e. it counts with respect to t, $x_{g,t}$ is a binary decision variable determining the status of generation unit g, $v_{g,t}$ is a binary variable that states when a bid was activated and z_g^{on} is the minimum on-time or the length of a block bid.

When such a constraint is included (typically, the thermal generating unit's physical limitations make it necessary), and when bids can have different minimum on-times or minimum activation conditions, the phenomenon of paradoxically rejected bids occurs [75], as illustrated in Figure 4.3. Here, an imbalance, B, occurs on the demand side due to an increase in inflexible consumption, which is remedied in the real-time market. Additional generation or a reduction in consumption, or both, causes supply and demand to reach a new equilibrium. The imbalance is forecast to last 30 minutes, but the next generator in the merit order curve (highlighted in red) has a minimum on-time of 60 minutes, and the following generator has a minimum on-time of 30 minutes. The cheaper generator is skipped and a more expensive unit is activated,

since this is more cost effective over the forecast horizon. This process leaves the cheaper bidder thinking that the market has treated him unfairly, since the market price should have activated him. Such a bid - the paradoxically rejected bid - can occur with any generation constraint (e.g., ramping, minimum bid-sizes).

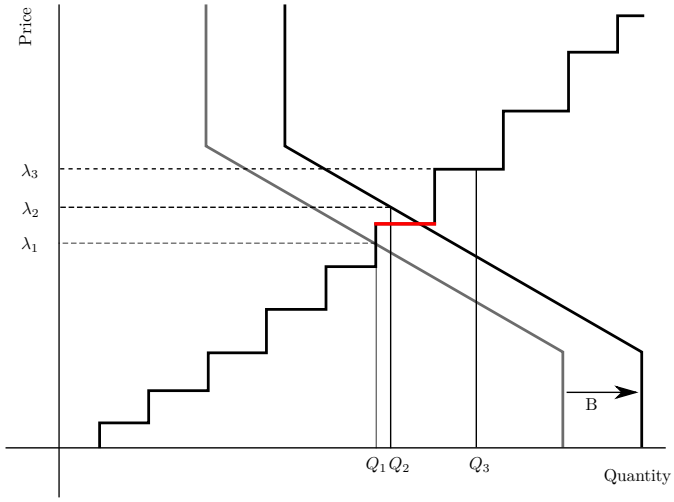

Figure 4.3: A paradoxically rejected bid (red) due to generation constraints.

To find a price in a mixed integer linear programming (MILP) or MIQCP environment with binary variables, the common academic approach is to solve the mixed integer problem first, then re-solve a linear or quadratic problem with the binary variables fixed as parameters and take the dual-variable of the balance constraint to yield a price [84]. The resulting system price, however, does not support the market outcome, as the marginal cost of energy is either lower than the marginal generator activated, or so high that it triggers a greater DR than required by the market. This phenomenon has led to widespread research of uplift payments [85], whereby heuristic algorithms are used to adjust the market outcomes after the market has cleared [86]. Alternatively, the problem can be relaxed and the gap between the relaxed and mixed integer problems can be reduced pending development of a solution with uniform prices that support the market outcome [87]. In both cases, the market loses a degree of transparency as to how a price was found. No uplift or reformulation has yet to deal with a demand that exhibits significant cross and positive elasticity.

4.4.2 Demand constraint example: cross elasticity

The impact of inter-temporal demand constraints on the marginal cost of energy is rarely included in the literature, especially for real-time markets in a mixed-integer

framework. Cross elasticity can be added to the minimal example of a real-time market by adding a new dimension to the objective function and modifying constraints. The new dimension is t' that is the sliding window that exists for every t. The social welfare considering every part of the sliding window is now optimised for by including t' trapezes to be summed over for each time step of customer utility, i.e.

$$\max_{\Theta} \sum_{t} \left\{ \lambda_t^{DA} \sum_{t'} \Omega_{t,t'} + \frac{1}{2} \sum_{t'} \alpha_{t,t'} \Omega_{t,t'} \sum_{t'} \Omega_{t,t'} - \sum_{g} \left(\lambda_{g,t}^{\uparrow} P_{g,t}^{\uparrow} - \lambda_{g,t}^{\downarrow} P_{g,t}^{\downarrow} \right) \right\} \quad (4.13)$$

subject to

$$\sum_{g} \left(P_{g,t}^{DA} + P_{g,t}^{\uparrow} + P_{g,t}^{\downarrow} \right) + W_t^{DA} = C_t^{DA} + \sum_{t'} \Omega_{t,t'} + B_t \quad \forall t \quad (4.14)$$

$$\Omega_{t,t'} = \Omega_{t-1,t'} \frac{\theta_{t,t'}}{\theta_{t-1,t'}} \quad t \neq t', \theta_{t,t'} \neq 0 \quad (4.15)$$

$$\Omega_{t,t'} = 0 \quad \forall t, t', \alpha_{t,t'} = 0 \quad (4.16)$$

$$\lambda_t^{RT} = \sum_{t'} \alpha_{t,t'} \Omega_{t,t'} + \lambda_t^{DA} \quad \forall t \quad (4.17)$$

$$-\Delta C^{\text{ramp}} \leq \sum_{t'} \left(\Omega_{t,t'} - \Omega_{t-1,t'} \right) \leq \Delta C^{\text{ramp}} \quad \forall t \quad (4.18)$$

where the set of decision variables includes DR, up and down regulation, i.e. $\Theta = \left\{ \Omega_{t,t'}, P_{g,t}^{\uparrow}, P_{g,t}^{\downarrow} \right\}$ for the sets $g \in G$, $t \in T$ and $t' \in T$. The matrix $\theta_{t,t'}$ has the FIR for price from Equation (3.1) given in every row. The price elasticity ratio, $\alpha_{t,t'}$, is now given as a matrix with the FIR for price and is the element-wise reciprocal of $(\theta_{t,t'})^{\dagger}$, i.e.

$$\theta_{t,t'} = \begin{bmatrix} \cdots & \theta_{\lambda_{-1}} & \theta_{\lambda_0} & \theta_{\lambda_1} \\ \theta_{\lambda_{-1}} & \theta_{\lambda_0} & \theta_{\lambda_1} & \theta_{\lambda_2} \\ \theta_{\lambda_0} & \theta_{\lambda_1} & \theta_{\lambda_2} & \theta_{\lambda_3} \\ \theta_{\lambda_1} & \theta_{\lambda_2} & \theta_{\lambda_3} & \cdots \end{bmatrix}, \quad \alpha_{t,t'} = \begin{bmatrix} \frac{1}{\theta_{\lambda_1}} & \frac{1}{\theta_{\lambda_0}} & \frac{1}{\theta_{\lambda_{-1}}} & \vdots \\ \frac{1}{\theta_{\lambda_2}} & \frac{1}{\theta_{\lambda_1}} & \frac{1}{\theta_{\lambda_0}} & \frac{1}{\theta_{\lambda_{-1}}} \\ \frac{1}{\theta_{\lambda_3}} & \frac{1}{\theta_{\lambda_2}} & \frac{1}{\theta_{\lambda_1}} & \frac{1}{\theta_{\lambda_0}} \\ \vdots & \frac{1}{\theta_{\lambda_3}} & \frac{1}{\theta_{\lambda_2}} & \frac{1}{\theta_{\lambda_1}} \end{bmatrix}$$

$\Omega_{t,t'}$ is square matrix decision variable that describes the load considering all cross elastic effects, so that when the sum over the sliding window is taken, it gives the instantaneous DR, ΔC. Matrix multiplication is done element-wise in the objective function and, since operations research problems are not well suited to dot product notation, the sums over t' are decoupled where needed.

Constraints (4.15) and (4.16) describe how the load responds for all prices. More specifically, Equation (4.15) ties the response of each time-step to the earlier one, considering the price elasticity ratio, i.e. the sequence of change in consumption must

be respected once a change has been initiated. This is needed because, although the objective function defines a desirable change in customer utility, it does not ensure an outcome that DR can follow. Equation (4.16) ensures that the resulting FIR is zero when price elasticity is zero. Equation (4.17) defines the real-time price needed to activate the DR scheduled in the optimization problem. Constraint (4.18) enforces DR ramp rates.

To show the consequence of cross elasticity on market outcomes, two different types or response are defined and shown in Figure 4.4. The first is a step response that exhibits no cross elasticity. It is defined by taking the average response to real-time price over the first hour. The second response is a FIR that comes from a model (see Equation (3.1)) of the aggregate population over the 2013/2014 winter season in the EcoGrid EU demonstration. This response was chosen rather than a newer one from 2014/2015 because the early EcoGrid EU load exhibited a significant rebound effect, leading to positive-price elasticity. DR with positive-price elasticity was chosen because market players do not exhibit such a response today, yet new sources of DR will exhibit it. In the following examples, an open loop system is considered and the dynamics and costs due to subsequent imbalances from feedback are ignored.

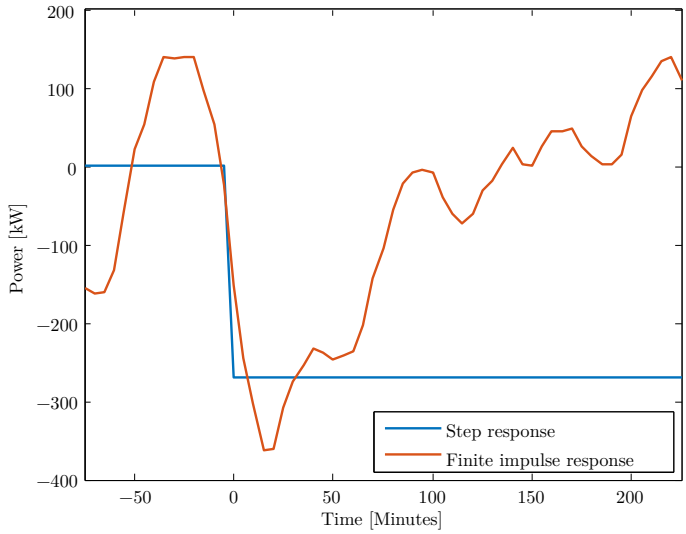

Figure 4.4: Price response used in the cross elasticity demand constraint example.

The outcomes in Figure 4.4 are observed when the step response is considered and imbalances from incorrectly modelled DR (i.e. feedback) are ignored. The top plot of Figure 4.5 represents the system imbalance from wind power and inflexible demand. The second plot shows the DR and up and down regulation scheduled. The third

plot shows the price of the most expensive up- and down-regulating bids activated at that point in time, as well as the price needed for demand to deliver as scheduled according to Equation (4.17) and the marginal cost for energy, which is the dual-variable of the balance constraint. When the marginal cost of energy is used as the price that supply and demand receives, then market outcomes are supported by the price (i.e. all market participants receive a price that meets their bid).

When the FIR with full cross elasticity is included, the market schedule and pricing outcomes are as shown in Figure 4.6. In this figure, the top plot shows the scheduled bids and DR and the second figure shows the prices needed to support each market outcome for up and down regulation, DR, and the marginal cost of energy. The third figure shows the prices for supply and demand, normalised as $\hat{\lambda}_t = \lambda_t - \lambda_t^{DA}$. Normalisation shows that the real-time prices needed to support market outcomes are on opposite sides of the day-ahead price during certain periods, leading to missing revenue if demand causes the imbalance.

Figure 4.6 shows that supply and demand regularly deliver a differing response to achieve a balanced system. Table 4.1 shows the impact of cross elasticity on supplier and consumer surplus [74] if the marginal cost of energy is sent to supply and demand. In the cross elastic case, suppliers appear to gain additional profit, while consumer utility is reduced dramatically. In markets where consumers are not compelled to deliver as scheduled (such as EcoGrid EU), such a surplus would not become a reality. Instead, an imbalance on the demand side would occur. The final row of Table 4.1 shows the additional revenue gained by the market operator if prices that support market outcomes were sent instead of the marginal cost of energy and if demand caused the imbalance. Prices to support market outcomes are the most expensive up-regulating bid, the cheapest down-regulating bid and the price to meet the DR expectation scheduled for each five-minute period. The reason for studying demand causing the imbalance is because if an external actor causes the imbalance, the average cost of energy is charged. But if it is demand (the only "internal" actor who can cause an imbalance), the different prices for supply and demand lead to a revenue imbalance. In the example analysed, significant missing revenue occurs when demand causes the imbalance.

Table 4.1: Impact of cross elasticity on revenue

	Step response	FIR
Supplier surplus [€]	964.5	1329.1
Consumer surplus [€]	1421.7	841.0
Excess revenue if demand causes imbalance [€]	0	-314.0

As an example of why this occurs, consider the time interval 3:55 - 4:00 in Figure 4.6.

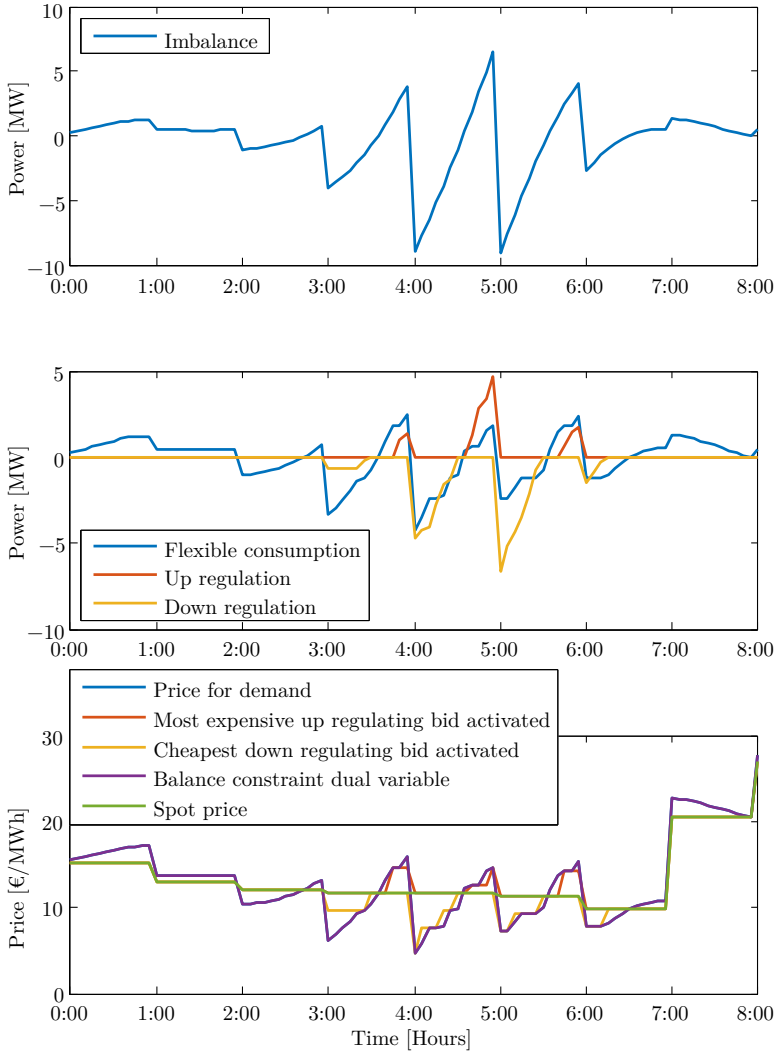

Figure 4.5: System imbalance, regulation scheduled and bid and system prices in a market that does not consider cross elasticity.

At this time, 4.7MW of up regulation and 0.8MW of increased consumption (down regulating DR) are scheduled. Prices that support market outcomes are 22.7 and 14.2€/MWh respectively, while the marginal price is 22.7€/MWh. If demand causes the imbalance, sending prices that support market outcomes leads to missing revenue, since paying supply costs 4.7*22.7 = €106.7, but revenue from demand is only 14.2*0.8 = €11.4. If the marginal price is sent, a new imbalance on the demand-side

arises, because sending a 22.7€/MWh price will activate an undesirable quantity of DR (the desirable quantity is activated at 14.2€/MWh).

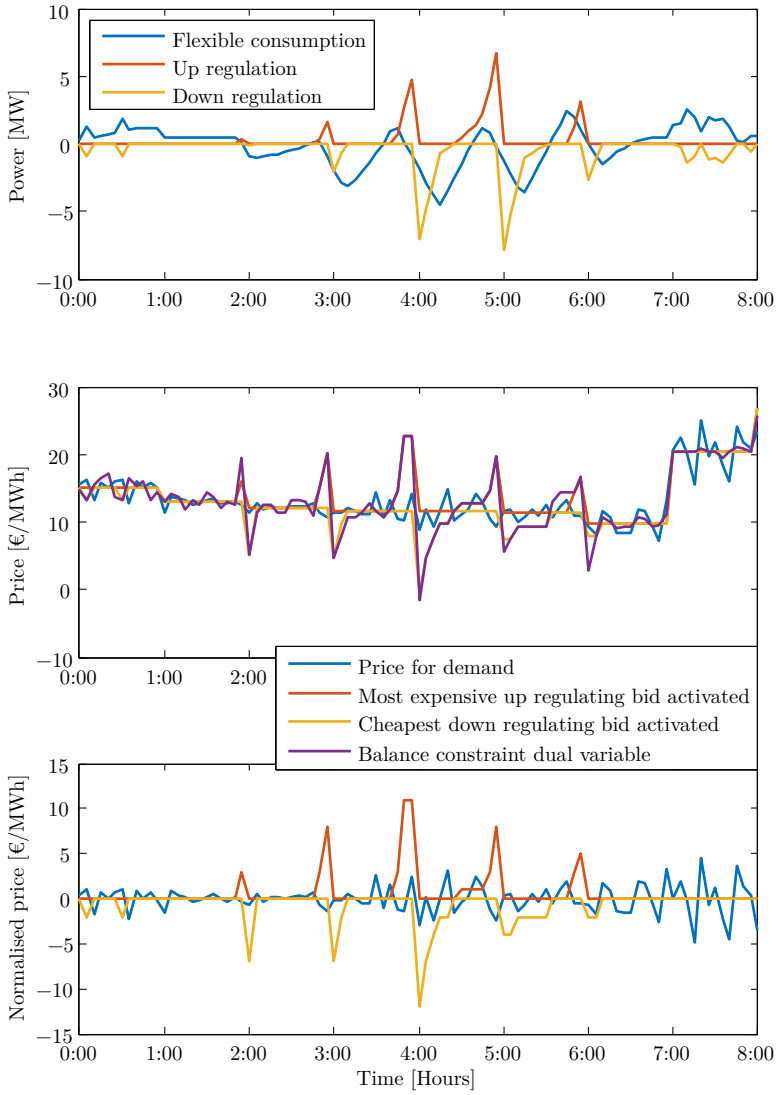

Figure 4.6: Regulation scheduled, bid and system prices and normalised prices needed to support the market outcome in a market that considers cross elasticity.

To put the revenue imbalance into perspective, generation constraints in Paper D causes -€223 of excess revenue if demand causes the imbalance. We therefore surmise that cross elasticity has a similar detrimental impact on cash flows or system balance as generation constraints do. Furthermore, not including cross elasticity leads to the Cobweb effect and lower social welfare, as shown in Paper D.

4.4.3 Network constraint example: low voltage feeder limits

Some electricity markets, most notably in parts of the USA, use locational marginal pricing (LMP) to send different prices to different parts of a transmission network to accommodate that network's physical limitations [78]. LMP, or nodal pricing, is only used in a minority of electricity markets, while the majority split this cost (or "socialise" it) among all market participants [78] in the name of fairness.

Network constraints and optimal power flow calculations are beyond the scope of this thesis, with the exception of low-voltage feeder limits, which were motivated by the EcoGrid EU experiment. The experimental setup to test low-voltage feeder constraints is described in paper C. The motivation for this study is congestion in the distribution network due to increased distributed activity such as EV charging and PV production. Such congestion threatens to reduce the lifetime of cables and transformers due to thermal limitations, or to cause voltage problems leading to poor power quality.

In order to support congestion management, the demand is first split into a set of loads, $l \in L$. The real-time market formulation is modified with new constraints as follows

$$\max_{\Theta} \sum_{t} \left\{ \sum_{l} \left(\lambda_t^{DA} \Delta C_{l,t} + \frac{1}{2} \alpha_l {\Delta C_{l,t}}^2 \right) - \sum_{g} \left(\lambda_{g,t}^{\uparrow} P_{g,t}^{\uparrow} - \lambda_{g,t}^{\downarrow} P_{g,t}^{\downarrow} \right) \right\} \tag{4.19}$$

subject to

$$\sum_{g} \left(P_{g,t}^{DA} + P_{g,t}^{\uparrow} + P_{g,t}^{\downarrow} \right) + W_t^{DA} = \sum_{l} \left(C_{l,t}^{DA} + \Delta C_{l,t} \right) + B_t \qquad \forall t \tag{4.20}$$

$$P_{g,t}^{\uparrow} \leq Q_{g,t}^{\uparrow,\max} \qquad \forall g,t \tag{4.21}$$

$$P_{g,t}^{\downarrow} \leq Q_{g,t}^{\downarrow,\max} \qquad \forall g,t \tag{4.22}$$

$$\sum_{t} \Delta c_{l,t} + \sum_{i} \Delta c_{l,i} = 0 \qquad \forall l \tag{4.23}$$

$$c_{l,t}^{\min} \leq c_{l,t} \leq c_{l,t}^{\max} \qquad \forall l,t \tag{4.24}$$

where the set of decision variables includes DR, up and down regulation, i.e. $\Theta = \left\{ \Omega_{t,t'}, P_{g,t}^{\uparrow}, P_{g,t}^{\downarrow} \right\}$ for the sets $g \in G$, $t \in T$ and $l \in L$.

The objective function and balancing constraints now have demand decomposed into multiple loads, but if every load is identical and constraints 4.23 and 4.24 are not included, this market gives the same outcome as the earlier market formulation.

Equation (4.23) sums over all DR scheduled over the forecast horizon, $\Delta c_{l,t}$, and all DR historically scheduled, $\Delta c_{l,i}$, for each load. This constraint has two purposes. The first is to increase the likelihood of a controllable response by avoiding TCL saturation (such saturation occurs when a continuous increase in consumption is requested for several hours, which the houses cannot deliver because they get too hot, resulting in a period longer than the FIR for price can accurately describe). The second purpose is to ensure that all loads receive the same average price (when all loads have the same price elasticity). Although it is extremely unlikely for all loads to be homogeneous, prices will be more equitable with this constraint than without it. Equation (4.24) sets the maximum and minimum feeder limits respectively beyond which congestion occurs.

Congestion management requiring separate prices for different loads inherently causes divergent pricing. The attempt to make pricing average out for different loads over a long enough time frame also causes supply and demand pricing to diverge. This happens because the gap between customer utility and generator cost (the two main terms in the objective function) widens as customer utility becomes restricted by Equations (4.23) and (4.24).

4.5 Specifics of the EcoGrid EU market

4.5.1 Design objectives

In the previous section, a general market that can facilitate DR was presented. In this section, the implemented market and its unique design objectives are discussed.

The market was initially designed to operate in parallel with the existing Danish regulating market and incorporate generators with a five-minute minimum on-time [88]. However, the DR potential is at least 100MW when Chapter 3 results are applied to all residential heat pumps in Denmark. This means that tertiary reserves traded in the regulating market are the only ancillary service with enough liquidity to assimilate distributed generation and DR, as shown in Table 4.2. Faster moving reserves are limited in size by the physical constraints of thermal generating units.

The implemented market was therefore designed to match the generator constraints in the existing Danish regulating market but reduce barriers to entry for smaller, distributed actors on the supply and demand-sides. New market players are those providing DR and the 2.3GW of distributed generation in Denmark that currently receive regulated prices via a feed-in tariff [90].

Table 4.2: Ancillary service availability in Denmark [89]

	DK1 (west)	DK2 (east)
Primary	27	23
Secondary	100	200
Tertiary	250	675*

*about half of this generation has very slow activation times

Today, the regulating market in Scandinavia is operated manually without an optimization problem scheduling bids. A bid is activated 15 minutes before every half hour or hour (depending on the system operator) and simultaneous up- and down-regulation is avoided. Bids under 10MW must be activated in full, while bids over 10MW can be activated in part. Constraints to emulate this behaviour were added to standard market clearing formulation shown in Section 4.4.

In the existing regulating market, pricing is calculated ex-post, i.e. the cost of electricity is decided the hour after activation. Two-price settlement for supply and imbalance-actor is used, with the most expensive up-regulating and cheapest down-regulating activated bids setting the price for the whole hour (either or both can be the day ahead price in case of no imbalance). In the EcoGrid EU market, such pricing is replaced with two-price settlement every five minutes, with separate prices for supply and demand (to improve DR controllability in the absence of appropriate uplift payments). To lower EcoGrid EU partners' computational and communicational burdens, the market was only cleared once per hour. How often the market clears is, however, merely a small formulation detail - it can be, and was, easily changed to compare market outcomes.

The market was formulated as a MIQCP problem, programmed in OPL and solved using CPLEX, with separate prices for supply and demand that support all market outcomes, as shown in Figure 4.6. The market ran on the Danish island of Bornholm in 2014 and 2015, sending five-minute pricing to EcoGrid EU's 1900 residential participants. Full documentation for this application can be found in report I, while paper C describes the implemented market formulation.

4.5.2 The missing money problem

A fundamental flaw with the EcoGrid EU market is that, even without demand, supply or network constraints, supply and demand revenue do not match. This is because the framework uses the real-time price for settlement, when actually the settlement price must be a function of the day-ahead and real-time prices, i.e.

$$\lambda_t^S = \frac{C_t^{DA}\lambda_t^{DA} + \Delta C \lambda_t^{RT}}{C_t^{DA} + \Delta C} \tag{4.25}$$

where λ_t^S is the theoretical settlement price that ensures consistent revenue from supply to demand. By sending λ_t^{RT} as the settlement price, the market assumes that this is also the settlement price for the energy purchased in the day-ahead market, leading to missing money issues. For example, if 200MWh is purchased in the day-ahead market at 30€/MWh and 20MWh is activated in the real-time market at 20€/MWh, sending the real-time price to demand as the settlement price leads to €2000 missing revenue.

EcoGrid EU reports [88, 91, 92] have proposed separate metering for devices delivering DR, but such an approach may be too costly and was not implemented in the demonstration.

To determine λ_t^S in the EcoGrid EU market and its price elasticity parameter α_t^S, the relationship in Equation (4.25) is built upon. First, consider the equation

$$\lambda_t^S = \alpha_t^S \Delta C + \lambda_t^{DA} \tag{4.26}$$

Substitution into Equation (4.25) gives

$$\alpha_t^S \Delta C^{RT} + \lambda_t^{DA} = \frac{C_t^{DA} \lambda_t^{DA} + \Delta C \lambda_t^{RT}}{C_t^{DA} + \Delta C} \tag{4.27}$$

Substituting for λ_t^{RT} and solving for α_t^S gives

$$\alpha_t^S = \frac{\alpha \Delta C_t}{C_t^{DA} + \Delta C_t} \tag{4.28}$$

where λ_t^{RT} is the market equilibrium price (assuming uniform prices can be found) used for settlement of market players with dual metering or dual accounting (i.e. generators and larger market actors) and α is the price elasticity ratio that reflects the real-time price for dual accounting customers. This relationship is rather intuitive; as more real-time DR is activated with respect to the day-ahead bid, so the settlement price tends towards a purely real-time price. However, adjusting the objective function (Equation (4.8)) so that the real-time price generated accurately reflects the true customer utility (based upon α^S) leads to a non-linear program with discontinuous derivatives. Although non-linear solvers can solve such a formulation, the market still does not have consistent revenue from supply to demand because of the non-linear customer utility is no longer comparable to linear generator utility, leading to DR-only activations for small to medium imbalances as $\alpha_t^S \to 0$ for moderate activations of DR.

Due to the asymmetry in regulating pricing, it is unlikely that a cash reserve could be a part of daily operation. For demonstration purposes, it was assumed that customers receive dual-price settlement, although in reality, participants' quarterly bills were not related to the broadcast price they responded to.

4.6 Empirical results and discussion

4.6.1 General outcome

From a larger perspective, the EcoGrid EU demonstration had many successes. The first success was achieving a peak flexibility of 21.6%, as calculated in Section 3.3, which appears to be higher than the 17% flexibility achieved in the PNNL GridWise experiment [64] - although it's not clear how the latter figure is calculated. This is doubly impressive considering that the EcoGrid EU peak flexibility figure comes from a population where only half the houses are price responsive. From a controllability perspective, the demonstration had moderate success. Paper A shows how controllable the load was and how much DR was activated. Briefly, when the largest increase in consumption was requested by the market, an increase was observed 100% of the time. When the largest decrease in consumption was requested, a decrease was observed 80% of the time. Controllability is impacted by the level of noise in the system and, as such, will presumably improve as the population grows.

Estimating the cost benefit of DR in a balancing market is best done by simulation, since empirical evidence of cost reductions would require an identical population not providing DR. Paper D shows potential social welfare increases of up to 70% for a population of houses that are fully responsive. This does not mean a reduction in cost of 70%, since customer utility is increased, but there does appear to be significant value in DR. Social welfare benefits were also calculated with congestion constraints in Paper C. In this paper, we simulated that congestion management reduced social welfare by €3 per day per low voltage feeder, where the low voltage feeder has a peak load of 100kW. The feeder limit in these simulations was set at 5% below the unconstrained peak load.

Calculations of social welfare in papers C and D are based upon several assumptions that may not hold true in a larger roll-out of DR. The calculations assume that all houses would be responsive, that the supply curve would remain the same in the presence of DR, and that primary frequency reserve costs will equal the highest and lowest costs of up and down regulation activated each hour, as in Denmark today. None of these assumptions may hold true in a future power system. Finally, it should be noted that volumes in a balancing market are a small fraction of volumes in a day-ahead market, which means that the overall benefit to customers is significantly smaller.

4.6.2 Empirical results from the congestion management test

The main demonstration results of congestion management obtained after Paper C was submitted were largely disappointing. In the demonstration, the population was split into two loads: 1872 houses receiving standard real-time pricing, and 28 houses receiving pricing adjusted for congestion. A model based upon Equation (3.1)

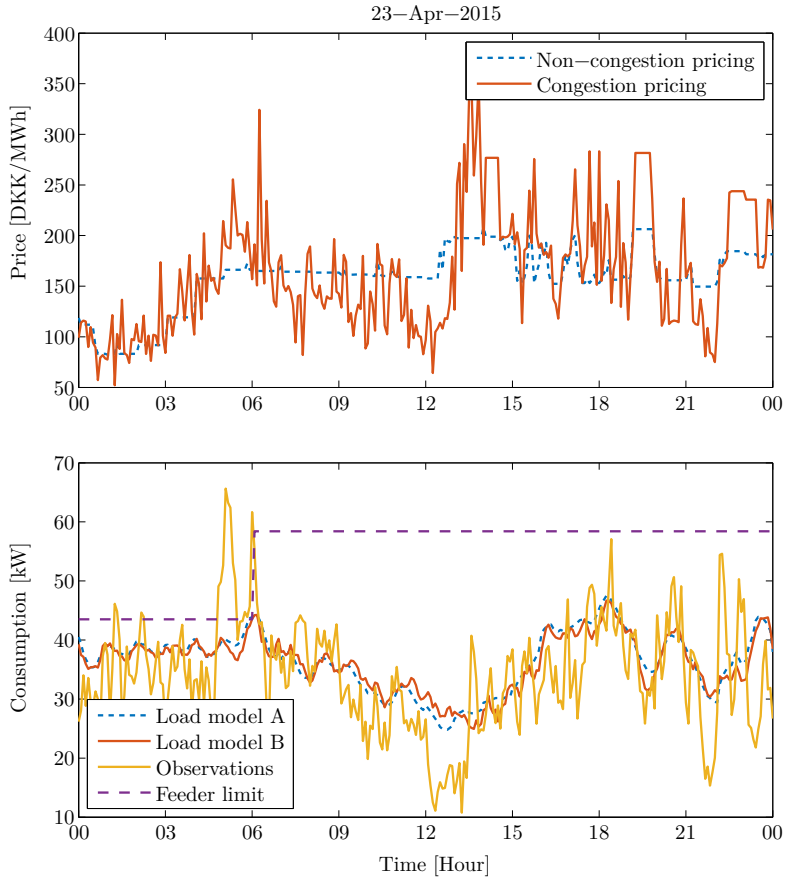

Figure 4.7: An example day of the congestion management experiment. The feeder limit was breached every day during the experiment.

was then built to compare observations with the expected response if the second load had received non-congestion pricing. When congestion pricing was higher than standard pricing, consumption was lower than a model of the load with non-congestion pricing only 51% of the time. In addition, over the two months of the congestion management experiment, consumption did not stay under the feeder limit on any single day. Figure 4.7 shows an example day from that two-month period. The top plot shows the prices sent to the main group and the group receiving congestion management pricing. The bottom plot shows the feeder limit (which changes once per day at 6:00 UTC), the observed load, and the models of the load assuming they received non-congestion pricing (model A) or congestion pricing (model B).

Possible causes for this poor performance might be

1. Poor small-sample modelling and forecasts. The tools developed may not have been adequate to control such a small (28 house) sample;
2. A 30 minute delay in measurements, during which time a congestion may have developed before the market could take a control decision; and
3. Smart meter jump, where the aggregated consumption for the virtual feeder changes as different meters contribute to aggregated consumption at different times. This is further explained in paper A.

4.6.3 System reliability

The ability of a market to truly maintain control of DR in a reliable manner and operated at lower cost than a market without DR remains unproven. Interest in secure operation of the power system has increased in Denmark since the 2003 blackout caused initially by the shut-down of a 1.2GW nuclear power plant [93]. Transient analysis of supply and transmission has been the primary focus of security investigations, yet the risk posed by new distributed activities is also gaining TSO interest [17]. A recent example was the threat of PV collapse in Germany, where 2011 grid codes led to 400,000 PV installations being retrofitted so that 9GW of PV production wouldn't cut out at a system frequency of 50.2Hz [94]. Any distributed devices acting in unison may lead to a significant loss of load and the method of activation, perhaps a real-time market, must be carefully designed to avoid such a scenario.

In paper D, simulations showed that markets that do not optimise for cross elasticity have higher costs when DR is added, due to the Cobweb effect. The Cobweb effect is the divergent oscillation of supply and demand, thwarting efforts to find a stable equilibrium [38, 95, 96, 97] and leading to unnecessary generator and DR activations that reduce social welfare. Simulations show that the Cobweb effect can lead to DR being fully activated in a cyclical manner. When scaled to all heat pumps in Denmark, this could mean a 100MW activation followed by a -100MW response 15 minutes later. Although such a 200MW drop isn't technically a loss of power, swings back and fourth could have undesirable consequences for system stability. This example is also small compared with the 1.2GW loss that preceded the last Danish blackout, but we assume that the DR potential is significantly larger when including other devices not studied in this thesis.

Previous methods to measure volatile swings in power generation and consumption are the Incremental Mean Volatility (IMV) and Incremental Aggregate Volatility (IAV) metrics, developed in [38]. IMV measures slow-decaying deviations from the moving average, while IAV measures fast-decaying deviations. To calculate these metrics, we

must first define the p-norm of a time-series which, for $p \geq 1$ is

$$\|\bar{x}\|_p = \left(\sum_{i=1}^{I} |x_i|^p \right)^{1/p} \tag{4.29}$$

A signal of interest, h, is then identified, which could be supply and demand power or prices time-series. The IMV of the signal of interest is defined as

$$\bar{V}(h) = \lim_{T \to \infty} \frac{1}{T} \sum_{t=0}^{T} \|h(t+1) - h(t)\| \tag{4.30}$$

while the IAV of the signal of interest is

$$V(h) = \sum_{t=0}^{\infty} \|h(t+1) - h(t)\| \tag{4.31}$$

These measures of volatility are abstract and the result can only be used to describe the phenomenon. As such, we developed a different way to measure power system volatility in Paper D: the rainflow-counting algorithm. The rainflow counter was historically designed to measure loading of materials [98]. Its result is intuitive, with units, that can then be used for further study. When measuring energy, the volatility outcome is cumulative energy, when measuring a price, the volatility outcome is a cumulative price which, when combined with energy, gives the total revenue of market transactions. For this reason, the result is easily applied to other studies, for example a real time digital simulator (RTDS) of the power system to see at what point volatility leads to stability problems.

Figure 4.8 shows a comparison of IMV, IAV and the range of the rainflow counter for simulations of the Danish power system with a market clearing that does not consider cross elasticity. The signals of interest are demand requested (demand which the market schedules), demand delivered (considering a non-linear and cross elastic response that is not modelled in the market), prices that support the demand scheduled, generation supplied and the marginal cost of generation (which is the price needed to support the generating bids activated). Volatility increases in all cases as DR penetration increases, with the exception of demand pricing, which increases dramatically and then falls away. This is because just a small level of DR inherently introduces new price variability. Low DR penetration subsequently requires a large price change to activate the same amount of DR as a power system with greater DR penetration.

As measured by the rainflow counter, volatility increases over 10 times for demand requested, 8 times for demand delivered, over 100 times for demand pricing, 3.5 times for generation delivered and 1.7 times for generation pricing, compared to a power system without DR (but where demand receives the regulating price without responding to it).

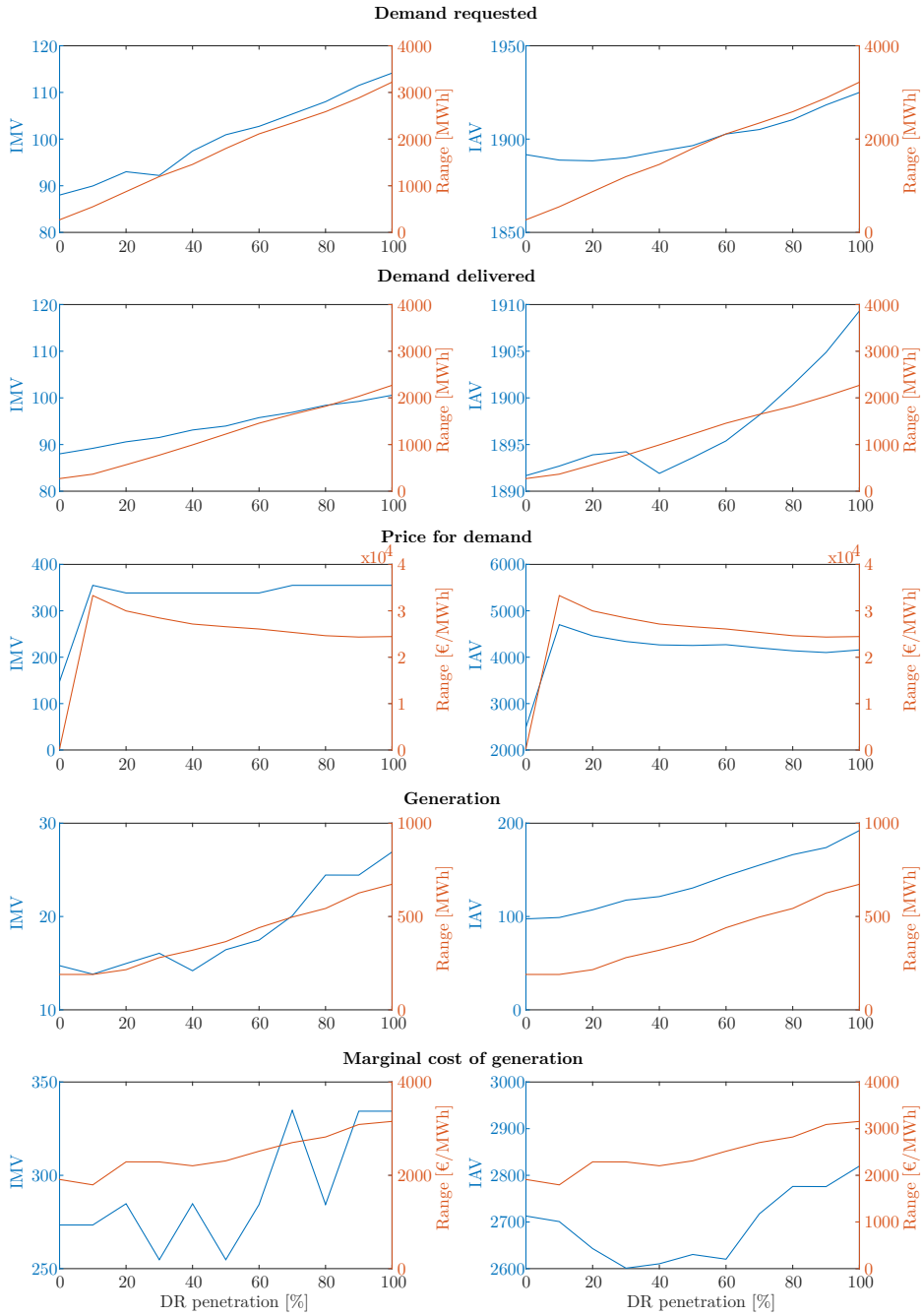

Figure 4.8: Rainflow counter compared with existing measures for volatility, which are incremental mean volatility (IMV) and incremental aggregate volatility (IAV).

The rainflow counter gives very similar results to the previously established measures of volatility, which suggests that this tool is a valid approach. If anything, it appears to give a more consistent, smooth result as DR penetration increases, while the IMV and IAV suggest more sporadic changes in volatility. Future work could assess the robustness of each measure by performing a LOOCV on the different signals of interest.

In the EcoGrid EU experiment, consumption volatility was 66% greater than simulated, suggesting that the Cobweb effect may even exceed our estimates in a real, dynamic system. However, additional factors hinder a direct comparison between the experiment and simulations: these include smart meter reliability, sporadic breaks in the experiment, additional market delays, and increased price elasticity over time as control algorithms improved. The experiment also consisted of a smaller population with greater uncertainty than simulated. Thus the Cobweb effect may diminish as uncertainty diminishes, as happens whenever a larger population of loads is forecast.

4.7 Market conclusions

The potential benefit of DR on the operational costs of the power system are enormous. Studies have consistently shown that DR can bring down the cost of electricity, especially during critical periods. Knowledge of how to activate DR in a pure-market setting is, however, still lacking. MPECs are difficult to solve when non-linear formulation is present, such as the conditions for single-price settlement in a two stage market, and fully describing a load that has a non-linear, autoregressive response to price. A recent example of this [97] showed that non-linear DR similar to the models developed in Chapter 3 integrated into an electricity market could not converge on a uniform market clearing price when just 10% of the load was price responsive.

As markets become subject to more discrete decisions, the requirements for uplift payments increase [85]. Results from this chapter show this to also be true for modelling of demand cross elasticity in the market. Even if uplift payments leading to revenue neutral market structures can be developed, also considering non-linear, cross elastic DR, then volatility may still present new challenges. By its very nature, flexible consumption is more volatile than inflexible consumption. Consider the two demand curves in Figure 4.9. Here, the high elasticity curve is cheaper to activate, since a larger quantity can be activated for a smaller price change than the low elasticity curve at the intersection with supply. But [38] proved that a higher ratio of demand elasticity to supply elasticity leads to undesirable volatility. This phenomenon implicitly suggests that it is purely coincidental whether or not a market has the right elasticities to facilitate DR.

The issues of volatility, cross elasticity and a poorly modelled response to price (i.e. approximating a curve as a linear) do not just impact markets where demand responds directly to the market price like EcoGrid EU. These issues can affect any real-time

market that trades demand-side flexibility, most specifically new sources of flexibility with significant cross elasticity. However, if an aggregator performs coordination using direct or indirect means (i.e. an additional control layer sits between DR and the market bid), then undesirable characteristics can be reduced by the aggregator. Grid codes can then be developed to enforce certain characteristics, such as the shape of the bid curve and the amount of cross- and positive-price elasticity, which in turn will affect the way aggregators perform control.

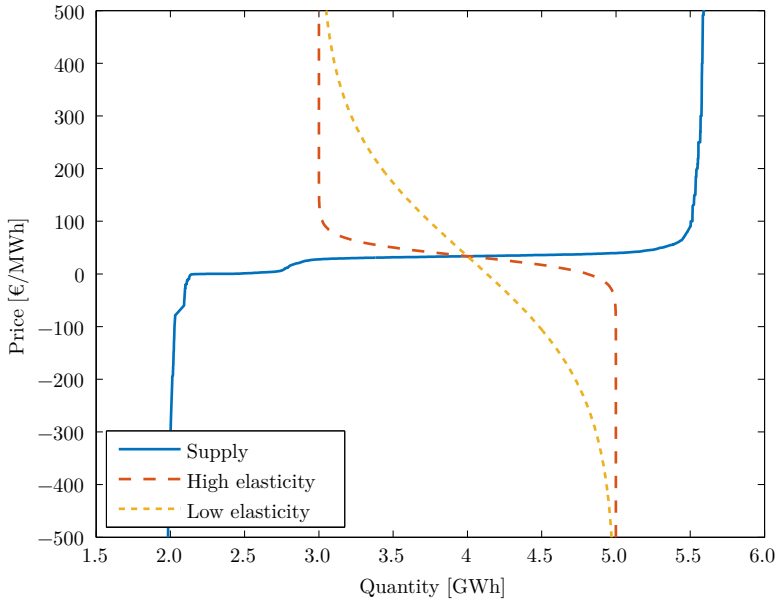

Figure 4.9: The Cobweb effect increases as the demand price elasticity increases with respect to supply elasticity.

CHAPTER 5

Conclusion

5.1 Discussion of key results and contributions

This PhD project developed and implemented tools for devices responding to a price signal, aggregating a distributed response, and integrating DR into an electricity pool. Results from the experiment on the Danish island of Bornholm were not always successful, but shortcomings were identified and a clearer path to market integration of DR may now be possible. Above all else, we managed to activate a significant level of flexibility from residential loads totalling over 20% of the load, and likely higher when control subjects and non-automated customers are removed.

Determining DR characteristics like volume was only made possible when parameter penalisation was applied to regression models, shaping model selection by reducing numerous parameters to zero. Without this, the number of external factors influencing the load and the unusually high resolution of data caused over-parameterisation. Load forecasting typically deals with hourly values and fewer external factors influencing the load. Five-minute observations with three concurrent prices (day-ahead forecast, real-time forecast and real-time settlement) lead to over-parameterised models and a meaningless result in the absence of parameter penalisation. Going forward, such methods will become an invaluable part of every load forecasting toolbox.

At a customer level, simulations and experimental observations revealed poor annual savings for automated heat pumps. Typical cost reductions of €2/year diverge from previous estimates of up to €71/year due to the inclusion of realistic constraints like minimum on- and off-times and price and weather uncertainty. However, a positive outcome of heat pump simulations was that basic hysteresis controllers are able to deliver similar comfort and economic performance as EMPC algorithms. EMPC is vulnerable to uncertainty, present in weather and pricing data in our simulations, and requires an accurate model of the area being heated, which is difficult to obtain. Since hysteresis algorithms can match EMPC, and probably surpass them when model uncertainty is considered, this simplifies the design of price-responsive algorithms.

From a market perspective, large increases in social welfare were estimated, once new inter-temporal demand constraints were developed for the real-time market. Paper D's estimate of a 60% increase in social welfare, equal to €3.5/day, is seemingly high. This estimate is for a balancing market for a winter month and assumes every house has some form of automated electric heating. Real, year-round estimates will

be lower when considering all other power system costs, such as day-ahead market energy purchases, and considering a lower level of DR penetration. Nonetheless, the impact on system costs is extremely promising.

The market benefit appears to contradict the financial savings individual customers can achieve. How can households only reduce costs by 0.7% from automating their heat pumps, yet the power system see a 60% increase in social welfare? This is mainly because the heat pump study considers customers responding to pricing generated by a market that already has new pricing-patterns as a result of DR (i.e. lower average pricing). The market study, on the other hand, compares social welfare of a market whose marginal prices have changed as a result of DR to a market whose pricing hasn't changed (i.e. higher average pricing). This means that the heat pump study assumes that customers are price takers, while the market study assumes customer behaviour contributes to setting the price.

The cost/benefit paradox is also affected by the free rider phenomenon. Free riders have been identified in previous DR programmes as those who benefit from DR incentives without having to change their behaviour [99]. Applied to the cost/benefit paradox, the flexibility of some customers makes electricity cheaper for all customers, also those who aren't flexible. This is because the marginal cost of generation decreases as DR penetration increases. Applied to Denmark, if 100,000 households responded to the regulating price, then the operational costs of the power system will actually be lower for all 2.6 million Danish households. If the benefit of reducing consumption by 100W a dozen times a day is €20/year and only 1 in 20 loads reduce their consumption, then the €20 is spread across all 20 loads. The loads reducing their consumption get some additional benefit, but this pales in comparison to the system-wide reduction in costs.

The congestion management experiment controlled with a centralised market was not successful, with meter delays being the main suspect for failure. This work developed new constraints for fairer locational pricing, since the basic principles of fairness are challenged by price discrimination for residential loads. Electricity distribution is a natural monopoly - you do not have multiple cables coming into your home - and so receiving high pricing that your neighbour does not because you are on a different feeder is incompatible with the principle of equal access to utilities for all. A fairer and potentially more effective option to reduce low-voltage congestion already exists in many countries: demand charges based upon peak consumption [7]. Demand charges may be an effective way to compel new distributed activity to reduce congestion, and are fair if every customer is bound by the same tariff.

TSOs hope that DSM can mitigate the threat to security of supply from new distributed activity [17], yet we showed that market-based DR can have undesirable consequences for stability. In a balancing market, increased volatility from DR is unavoidable, but detrimental effects are avoidable if demand is properly modelled

within market constraints. This thesis developed a new way to measure volatility in the power system, using a rainflow-counting algorithm to measure the amplitude and frequency of supply and demand oscillations. The end result is intuitive and may have many other applications in power system studies.

5.2 Future work

The low reward for residential customers automating their DERs makes investment unattractive. The appeal of DR schemes could be increased with additional incentives, such as availability payments that support equipment installation and reward customers for the full benefit they provide. Availability payments could be based on the volume of DR delivered by each customer, identified by clustering and statistical models. More volatile real-time pricing might also be more attractive, which can be achieved by making taxes and tariffs proportional to the price (while still allowing tax authorities, the TSO and DSOs to obtain the same revenue). Future research should therefore build a better business case for automating households. The benefit of being a first mover should also be investigated, since there may or may not be a benefit to doing so, depending on the level of high pricing and the ability of loads to respond sufficiently to extreme pricing.

In view of more frequent activations of heat pumps under real-time pricing, algorithms for automating TCLs must also evolve further to consider this, since customers may not want to sacrifice the lifetime of their devices in return for relatively little compensation.

Real-time pricing has a lot of hype behind it, but it is currently no cheaper than other forms of DR. All equipment installed in the EcoGrid EU demonstration had two-way rather than low-cost, one-way communication. The complexities of forecasting and the benefits of using internal state estimates to improve forecasting accuracy, i.e. data collected via two-way communication systems, leads to the conclusion that the stated benefits of real-time pricing simply don't exist at this point. Risk and reward are coupled for DR, since without being a reliable resource, DR has little value. For this reason, more reliable forms of activation, such as direct control or CPP, may be naturally better suited to DR providing ancillary services in the power system, while not actually being more expensive than indirect control. Irregular price spikes are often cited as the motivation for future DR developments [100], which indirect control is poorly suited to and which further justifies future research into coordinated control by direct means or CPP.

Uncertainty is a significant problem in all aspects of indirect control, from the activation of devices, to the identification of a response, to the scheduling of DR in a market. At controller level, stochastic approaches already exist [45]. Identifying the level of uncertainty associated with the DR that a statistical model predicts is

more problematic. LOOCV is a potential solution for estimating the true level of uncertainty of a statistical model [101], but is currently too computationally intensive when dealing with five-minute time-series. For now, we are left with a poor estimate based on standard errors, which future research should urgently address.

Once uncertainty has been quantified, effectively managing it in a market framework is a big challenge. Stochastic optimisation was extensively pursued when running market clearing simulations, but the cost benefit of stochastic optimisation is small relative to correctly modelling demand constraints. From an implementation perspective, the computational burden of stochastic optimisation was the most problematic. Each additional scenario can double the number of decision variables that an optimisation problem must solve for, making it impossible to clear the market in a reasonable time scale when hundreds of generators with hundreds of thousands of discrete variables exist, as in real world power systems.

Forecast responsibility also beleaguers stochastic optimisation. It remains unknown who should be responsible for scenario generation and, if it is a renewable power producer who does so, how their scenarios should be evaluated, since bidders can game the market by revealing false information [102]. Future research should therefore focus on usable tools that can manage the uncertain nature of DR.

For identifying and forecasting DR, more advance statistical models could be developed. Modelling the price response as a stationary FIR has many limitations, including that the length of the response and time to the FIR maximum is always the same, regardless of how big a price change happens. Understanding how DR evolves with external factors like weather and time-of-day is also important, since this may implicitly reduce the uncertainty present. There appears to be evidence of an asymmetrical response from residential DR and new tools to identify this are important for reliable power system operation.

It is possible that many types of DR, activated by direct or indirect means, will at some point be traded in an electricity market. For this reason, uplift payment mechanisms that can find a solution in markets with cross elasticity will be needed. Without uplift payments, revenue from demand to supply will not match, leading to market failure. Volatility is also likely to increase whenever DR is traded in the market. Levels of volatility that are acceptable and do not lead to power system voltage and frequency instability should therefore by defined. This could be done by simulating increasingly volatile consumption patterns in a real time digital simulator (RTDS).

Finally, if market-based pricing is to be sent directly to consumers, then new market structures should be found that reveal a settlement price that satisfies the energy purchased in all markets from day-ahead to real-time. A two-step market currently requires loads to be capable of two-price settlement, which is impractical for an indi-

vidual residential load. Until there is a significant simplification and cost reduction of the systems required for consumers, the suggestion of separate metering for DERs [103] is also unrealistic, since the costs of doing so would undo the low-cost appeal of indirect control. Bi-level optimisation structures that consider day-ahead and balancing outcomes [104] are a promising research direction that may lead to a single price and also schedule DR in a more efficient manner.

5.3 Opportunities for DR growth

A general lesson learnt from the experimental work was that it is extremely time consuming to retrofit houses with new equipment and teach users how to use it. To avoid this, one option would be to install DR control and communication equipment in all new homes with heat pumps. This would accompany the Danish law on green heating sources (predominantly heat pumps) in all new builds. Such an approach would allow small-scale DR to grow organically over time and is likely a cheaper option to retrofitting existing houses.

From an activation perspective, the quickest way to integrate DR is for aggregators to participate in existing electricity markets. Coordinated activation of heat pumps to meet bids in Scandinavian day-ahead and regulating markets has previously been shown [105] and may be an effective way of activating DR. Such an approach would require an aggregator, also acting as a balance responsible party, to bid on behalf of a larger population of loads. Grid codes could encourage aggregators to use control strategies that result in little or no positive-price and cross-price elasticity, potentially mitigating the need for electricity market changes. The financial rewards would be too low to make small-scale DR attractive, but aggregators could be paid an additional availability payments based on the accuracy of their bid forecast (this directly impacts reliability of the power system) and the amount of energy delivered. To support availability payments, loads could be clustered and the best performing flexible loads identified. Additional availability funding could come from a tariff on non-price responsive loads, since such loads would benefit from lower power system costs and would not experience a higher price than if there was no DR.

Long term, the way we use energy could change out of all recognition. Telephony is one of the few public utilities that was revolutionised by deregulation, competition and new technology. Electricity has the potential to undergo the same transformation. Ubiquitous installation of smart meters is the first step towards a closer interaction with electricity suppliers and network operators. EVs, PVs, home batteries, heat pumps and the like are also forcing the issue. Home automation is getting so cheap and so pervasive - from light bulbs to fridges - that exploiting residential devices for their flexibility should be cheap. The only thing missing is a centralised, regulated marketplace, like the Affordable Care Act in the USA, which allows health insurance to be compared and bought through a single website. In a similar vein, customers

could switch suppliers on a regular basis through a single portal, getting deals that suit their energy use best, or allowing them to take a moral standpoint on where their energy comes from, considering geopolitical and environmental concerns. Political and social initiatives to promote changing energy behaviour are therefore as important as technological developments.

Bibliography

[1] C. He-rui and W. Di, "The study on the relationship between energy consumption and economy growth in China based on VAR model," *2009 First International Workshop on Database Technology and Applications*, 2009.

[2] V. Costantini and C. Martini, "The causality between energy consumption and economic growth: A multi-sectoral analysis using non-stationary cointegrated panel data," *Energy Economics*, vol. 32, pp. 591–603, 2010.

[3] *BP Statistical Review of World Energy.* British Petroleum, 2015.

[4] *World energy outlook. Executive summary.* IEA, 2013. [Online]. Available: http://www.iea.org/Textbase/npsum/WEO2013SUM.pdf

[5] "Energy and climate change," International Energy Agency, Tech. Rep., 2015.

[6] "Energistatistik 2011," Danish Energy Agency, Tech. Rep., 2011, ISBN: 9788778449429.

[7] A. Faruqui, *The case for introducing demand charges in residential tariffs.* The Brattle Group, 2015.

[8] *The future requirements for flexibility in the energy system.* Ea Energianalyse, 2012.

[9] S. Becker, R. a. Rodriguez, G. B. Andresen, S. Schramm, and M. Greiner, "Transmission grid extensions during the build-up of a fully renewable pan-European electricity supply," *Energy*, vol. 64, pp. 404–418, 2014.

[10] *Fact Sheet 13: Blackouts and electricity deregulation.* Clearwater, 2001. [Online]. Available: http://www.clearwater.org/news/dereg.html

[11] W. B. Marcus, *Does deregulation raise electric rates? - A cross sectional analysis of state-by-state data.* BS Energy, Inc., 2011. [Online]. Available: http://citeseerx.ist.psu.edu/viewdoc/download?doi=10.1.1.307.9970&rep=rep1&type=pdf

[12] T. Slocum, *The failure of electricity deregulation: History, status and needed reforms.* Public Citizen, 2007.

[13] J. Vickers and G. Yarrow, "Economic perspectives on privatization," *Journal of Economic Perspectives*, vol. 5, no. 2, pp. 111–132, 1991.

[14] T. H. Arimura, S. Li, R. G. Newell, and K. Palmer, "Cost-effectiveness of electricity energy efficiency programs," *Energy Journal*, vol. 33, no. 2, pp. 63–99, 2012.

[15] "Electric power sales, revenue, and energy efficiency Form EIA-861 detailed data files," U.S. Energy Information Administration, Tech. Rep. [Online]. Available: http://www.eia.gov/electricity/data/eia861/

[16] C. A. Goldman, I. M. Hoffman, M. Billingsley, and G. L. Barbose, *On a rising tide: The future of US utility customer-funded energy efficiency programs*. Lawrence Berkeley National Laboratory, 2012.

[17] V. V. Thong, C. Latour, M. Norton, E. Larsen, H. Vandenbroucke, C. Dyke, and S. Banares, "Demand side response - ENTSO-E policy paper," ENTSO-E, Tech. Rep., 2014.

[18] W. W. Hogan, "Demand response pricing in organized wholesale markets," Federal Energy Regulatory Commission, Tech. Rep., 2010.

[19] "Implementation proposal for the national action plan on demand response," Federal Energy Regulatory Commission, Tech. Rep., 2011.

[20] D. S. Loughran and J. Kulick, "Demand-side management and energy efficiency in the United States," vol. 25, no. 1, pp. 19–43, 2004.

[21] *Lower taxes on electric heating.* Danish Tax Authority, 2013. [Online]. Available: http://www.skm.dk/public/dokumenter/presse/FL13/1d.pdf

[22] *Heat pumps in Denmark - How oil-fired boilers will be converted by 2035.* Dansk Energi, 2013.

[23] F. Sossan, "Indirect controlled flexible demand for power system applications," Ph.D. dissertation, 2013.

[24] K. Heussen, S. You, B. Biegel, L. H. Hansen, and K. B. Andersen, "Indirect control for demand side management - A conceptual introduction," in *IEEE PES Innovative Smart Grid Technologies Conference Europe*, 2012.

[25] J. Hopkinson, "The cost of electric supply," *Transactions of The Junior Engineering Society*, pp. 33–46, 1892.

[26] L. Hancher, X. He, I. Azevedo, N. Keyaerts, L. Meeus, J.-M. Clachant, W. Mielxzarski, and F. Leveque, "Shift, not drift: Towards active demand response and beyond," Tech. Rep., 2013. [Online]. Available: http://cadmus.eui.eu/bitstream/handle/1814/28998/SomeTHINKingonEuropeanEnergyPolicyJan2012-May2013.pdf?sequence=1

[27] H. A. Aalami, M. P. Moghaddam, and G. R. Yousefi, "Demand response modeling considering interruptible/curtailable loads and capacity market programs," *Applied Energy*, vol. 87, pp. 243–250, 2010.

[28] F. A. Wolak, *An experimental comparison of critical peak and hourly pricing: The PowerCentsDC Program*, 2010.

[29] P. O. Steiner, "Peak loads and efficient pricing," *The Quarterly Journal of Economics*, vol. 71, no. 4, pp. 585–610, 1957.

[30] J. A. Hausmann, M. Kinnucan, and D. McFaddden, "A two-level electricity demand model: Evaluation of the Connecticut time-of-day pricing test," *Journal of Econometrics*, vol. 10, no. 3, pp. 263–289, 1979.

[31] J. Schleich and M. Klobasa, *Peak demand and time-of-use pricing in a field study of residential electricity demand in Germany.* Grenoble Ecole de Managment, 2013. [Online]. Available: http://www.diw.de/documents/dokumentenarchiv/17/diw_01.c.430441.de/schleich_klobasa_applied_micro_seminar_okt2013.pdf

[32] J. Torriti, M. G. Hassan, and M. Leach, "Demand response experience in Europe: Policies, programmes and implementation," *Energy*, vol. 35, no. 4, pp. 1575–1583, 2009.

[33] "Danish experiences in setting up charging infrastructure for electric vehicles with a special focus on battery swap stations," North sea region electricty mobility network, Tech. Rep., 2013.

[34] D. J. Hammerstrom, , R. Ambrosio, T. A. Carlon, J. G. Desteese, R. Kajfasz, and R. G. Pratt, "Pacific Northwest GridWise testbed demonstration projects part I . Olympic Peninsula project," 2007. [Online]. Available: http://www.gridwise.pnl.gov/docs/op_project_final_report_pnnl17167.pdf

[35] G. R. Horst and R. Kajfasz, "Pacific Northwest GridWise testbed demonstration projects part II . Grid friendly appliance project," 2007. [Online]. Available: http://www.pnl.gov/main/publications/external/technical_reports/PNNL-17079.pdf

[36] H. Allcott, "Rethinking real-time electricity pricing," *Resource and Energy Economics*, vol. 33, pp. 820–842, 2011.

[37] ——, *Real-time pricing and electricity market design.* New York University, 2013.

[38] M. Roozbehani, M. A. Dahleh, and S. K. Mitter, "Volatility of power grids under real-time pricing," *IEEE Transactions on Power Systems*, vol. 27, no. 4, pp. 1926–1940, 2012.

[39] C. Y. Chong and A. S. Debs, "Statistical synthesis of power system functional load models," *1979 18th IEEE Conference on Decision and Control including the Symposium on Adaptive Processes*, vol. 18, 1979.

[40] S. Ihara and F. Schweppe, "Physically based modeling of cold load pickup," *IEEE Transactions on Power Apparatus and Systems*, vol. PAS-100, no. 9, pp. 4142–4150, 1981.

[41] F. Schweppe, R. Tabors, J. Kirtley, H. Outhred, F. Pickel, and a.J. Cox, "Homeostatic utility control," *IEEE Transactions on Power Apparatus and Systems*, vol. PAS-99, no. 3, pp. 1151–1163, 1980.

[42] P. Nyeng and J. Ø stergaard, "Information and communications systems for control-by-price of distributed energy resources and flexible demand," *IEEE Transactions on Smart Grid*, vol. 2, no. 2, pp. 334–341, 2011.

[43] Y. Zong, D. Kullmann, A. Thavlov, O. Gehrke, and H. Bindner, "Model predictive control strategy for a load management research facility in the distributed power system with high wind penetration - towards a Danish power system with 50% wind penetration," *2011 Asia-Pacific Power and Energy Engineering Conference*, 2011.

[44] R. Halvgaard, N. K. Poulsen, H. Madsen, and J. B. Jorgensen, "Economic model predictive control for building climate control in a smart grid," *2012 IEEE PES Innovative Smart Grid Technologies (ISGT)*, 2012.

[45] N. Good, A. Navarro-Espinosa, P. Mancarella, and E. Karangelos, "Participation of electric heat pump resources in electricity markets under uncertainty," *International Conference on the European Energy Market, EEM*, 2013.

[46] F. Sossan and H. Bindner, "A comparison of algorithms for controlling DSRs in a control by price context using hardware-in-the-loop simulation," in *IEEE Power and Energy Society General Meeting*, 2012.

[47] G. Papaefthymiou, B. Hasche, and C. Nabe, "Potential of heat pumps for demand side management and wind power integration in the German electricity market," *IEEE Transactions on Sustainable Energy*, vol. 3, no. 4, pp. 636–642, 2012.

[48] B. Biegel, P. Andersen, T. S. Pedersen, K. M. Nielsen, J. Stoustrup, and L. H. Hansen, "Electricity market optimization of heat pump portfolio," 2013, pp. 294–301.

[49] J. L. Mathieu, M. Dyson, and D. S. Callaway, "Using residential electric loads for fast demand response: The potential resource and revenues, the costs, and policy recommendations," in *Proceedings of the ACEEE Summer Study on Buildings*, 2012, pp. 189–203.

[50] M. Loesch, D. Hufnagel, and S. Steuer, "Demand side management in smart buildings by intelligent scheduling of heat pumps," in *IEEE International Conference on Intelligent Energy and Power Systems*, 2014.

[51] M. C. Vlot, J. D. Knigge, and J. G. Slootweg, "Economical regulation power through load shifting with smart energy appliances," *IEEE Transactions on Smart Grid*, vol. 4, no. 3, pp. 1705–1712, 2013.

[52] P. Bacher and H. Madsen, "Identifying suitable models for the heat dynamics of buildings," *Energy and Buildings*, vol. 43, no. 7, pp. 1511–1522, 2011.

[53] C. F. Mieritz, "Aggregate modeling and simulation of price responsive heat pumps," Master's thesis, Technical University of Denmark, 2010.

[54] "Panasonic CS-HE9GKE operating instructions," 2008. [Online]. Available: https://support.panasonic.co.nz/docstore/CS-HE9GKEOperatingInstructions.pdf

[55] "Toshiba RAS-B13SKVP-E owner's manual." [Online]. Available: http://www.toshiba-aircon.co.uk/assets/uploads/product_assets/SuperDaiseikaiOwnersManual.pdf

[56] J.-C. Hadorn, *Solar and Heat Pump Systems for Residential Buildings*. John Wiley & Sons, 2015, ISBN: 3433604851.

[57] F. Mueller, O. Sundstroem, and D. Gantenbein, "IBM EcoGrid direct-price agent implementation status," IBM, Zurich, Tech. Rep., 2013. [Online]. Available: http://www.zurich.ibm.com/pdf/ecogrid/priceAgent.pdf

[58] ——, "IBM EcoGrid direct-price agent implementation status," IBM, Zurich, Tech. Rep., 2014. [Online]. Available: http://www.zurich.ibm.com/pdf/ecogrid/IBM-priceAgent_v3.1.pdf

[59] P. Andersen, T. S. Pedersen, and K. M. Nielsen, "An investigation of energy storage possibilities in single family houses for smart grid purposes," in *Proceedings of the 19th IFAC World Congress*, 2014.

[60] B. Drysdale, J. Wu, and N. Jenkins, "Flexible demand in the GB domestic electricity sector in 2030," *International Conference on Applied Energy, Pretoria, South Africa*, vol. 139, pp. 281–290, 2013.

[61] N. Morel, M. Bauer, M. El-Khoury, and J. Krauss, "Neurobat, a predictive and adaptive heating control system using artificial neural networks," *International Journal of Solar Energy*, vol. 21, no. 2-3, pp. 161–201, 2001.

[62] F. Ruelens, B. J. Claessens, S. Vandael, S. Iacovella, P. Vingerhoets, and R. Belmans, "Demand response of a heterogeneous cluster of electric water heaters using batch reinforcement learning," in *Power Systems Computation Conference (PSCC)*, Wroclaw, 2014.

[63] J. L. Mathieu, D. S. Callaway, and S. Kiliccote, "Examining uncertainty in demand response baseline models and variability in automated responses to dynamic pricing," in *IEEE Conference on Decision and Control and European Control Conference*, Dec. 2011, pp. 4332–4339.

[64] A. Faruqui and S. Sergici, "Household response to dynamic pricing of electricity: A survey of 15 experiments," vol. 38, no. 2, pp. 193–225, 2010.

[65] J. R. M. Hosking, R. Natarajan, S. Ghosh, S. Subramanian, and X. Zhang, "Short-term forecasting of the daily load curve for residential electricity usage in the Smart Grid," *Applied Stochastic Models in Business and Industry*, vol. 29, no. 6, pp. 604–620, 2013.

[66] A. Harvey and S. J. Koopman, "Forecasting hourly electricity demand using time-varying splines," *Journal of the American Statistical Association*, vol. 88, no. 424, pp. 1228–1236, 1993.

[67] *Udtræk af markedsdata*. Energinet.dk. [Online]. Available: http://www.energinet.dk/EN/El/Engrosmarked/Udtraek-af-markedsdata/Sider/default.aspx

[68] G. James, D. Witten, T. Hastie, and R. Tibshirani, *An introduction to statistical learning*. Springer, 2006, vol. 102, ISBN: 9780387781884.

[69] H. Madsen, *Time series analysis*. CRC Press, 2007.

[70] O. Corradi, H. Ochsenfeld, H. Madsen, and P. Pinson, "Controlling electricity consumption by forecasting its response to varying prices," *IEEE Transactions on Power Systems*, vol. 28, no. 1, pp. 421–429, 2012.

[71] J.-Y. L. Boudec and D.-C. Tomozei, "Satisfiability of elastic demand in the smart grid," in *The First International Conference on Smart Grids, Green communications and IT Energy-aware Technologies*.

[72] J. M. Chambers and T. Hastie, *Statistical Models in S*, ser. Wadsworth & Brooks/Cole computer science series. Wadsworth & Brooks/Cole Advanced Books & Software, 1992, ISBN: 9780534167646.

[73] J. Nocedal and S. J. Wright, *Numerical optimization*. Springer, 2006, ISBN: 0387303030.

[74] D. Kirschen and G. Strbac, *Fundamentals of power system economics*. Wiley, 2004, ISBN: 0470845724.

[75] A. Martin, J. C. Müller, and S. Pokutta, "Strict linear prices in non-convex European day-ahead electricity markets," vol. 29, no. 1, pp. 189–221, 2012. [Online]. Available: http://arxiv.org/abs/1203.4177

[76] C. D. Jonghe, B. F. Hobbs, and R. Belmans, "Optimal generation mix with short-term demand response and wind penetration," *IEEE Transactions on Power Systems*, vol. 27, no. 2, pp. 830–839, 2012.

[77] M. G. Lijesen, "The real-time price elasticity of electricity," *Energy Economics*, vol. 29, no. 2, pp. 249–258, Mar. 2007.

[78] L. A. Barroso, T. H. Cavalcanti, P. Giesbertz, and K. Purchala, "Classification of electricity market models worldwide," *2005 CIGRE/IEEE PES International Symposium*, no. i, pp. 9–16, 2005.

[79] J. M. Morales, A. J. Conejo, H. Madsen, P. Pinson, and M. Zugno, *Integrating renewables in electricity markets: Operational problems*, 2013, ISBN: 08848289.

[80] R. H. Kwon and D. Frances, "Optimization-based bidding in day-ahead electricity auction markets: A review of models for power producers," in *Handbook of networks in power systems I, Energy Systems*. Springer, 2012, ISBN: 9783642231926.

[81] G. B. Shrestha and P. a. J. Fonseka, "Congestion-driven transmission expansion in competitive power markets," *IEEE Transactions on Power Systems*, vol. 19, no. 3, pp. 1658–1665, 2004.

[82] I. K. Cho and S. Meyn, "Efficiency and marginal cost pricing in dynamic competitive markets with friction," *Proceedings of the IEEE Conference on Decision and Control*, vol. 5, pp. 771–778, 2007.

[83] M. Carey, C. Houghton, M. Jabłońska, and J. Kinsella, "Uplift quadratic program in Irish electricity price setting," in *Proceedings of the seventieth European study group with industry*, Limerick, Ireland, 2009, pp. 65–84.

[84] G. Wang, U. V. Shanbhag, T. Zheng, E. Litvinov, and S. Meyn, "An extreme-point subdifferential method for convex hull pricing in energy and reserve markets-part ii: Convergence analysis and numerical performance," *IEEE Transactions on Power Systems*, vol. 28, no. 3, pp. 2121–2127, 2013.

[85] P. Gribik, W. Hogan, and S. Pope, "Market-clearing electricity prices and energy uplift," 2007. [Online]. Available: http://www.hks.harvard.edu/fs/whogan/

[86] P. Andrianesis, G. Liberopoulos, G. Kozanidis, and A. D. Papalexopoulos, "Recovery mechanisms in day-ahead electricity markets with non-convexities — Part I : Design and evaluation methodology," vol. 28, no. 2, pp. 960–968, 2013.

[87] C. Ruiz, A. J. Conejo, and S. A. Gabriel, "Pricing non-convexities in an electricity pool," *IEEE Transactions on Power Systems*, vol. 27, no. 3, pp. 1334–1342, 2012.

[88] Y. Ding, S. Morente, J. Ø stergaard, E. Larsen, P. Nyeng, U. Mø ller, A. Arendt, H. Cech, M. Reischboeck, D. Gantenbein, O. Sundstroem, and K. Kok, "EcoGrid EU Deliverable 1.2b: Real-time market concept architecture," 2011.

[89] "Energinet.dk's ancillary services strategy," Energinet.dk, Fredericia, Tech. Rep., 2011.

[90] H. Parbo, *Distributed generation trends and regulation: The Danish experience*. Energinet.dk, 2014.

[91] Y. Ding, S. Morente, J. Ø stergaard, E. Larsen, P. Nyeng, U. Mø ller, A. Arendt, H. Cech, M. Reischboeck, D. Gantenbein, O. Sundstroem, and K. Kok, "EcoGrid EU Deliverable 1.2c: Real-time market concept architecture," 2014.

[92] O. Grande, S. Pineda, P. Nyeng, K. Kok, S. Otjacques, M. Cuk, J. Sprooten, B. Hebb, and F. Niewenhout, "Task force EcoGrid EU market model – final report," EcoGrid EU, Tech. Rep., 2013.

[93] H. Jóhannsson, "Development of early warning methods for electric power systems," Ph.D. dissertation, Technical University of Denmark, 2011. [Online]. Available: https://www.etde.org/etdeweb/details_open.jsp?osti_id=1033692

[94] J. C. Boemer, K. Burges, P. Zolotarev, J. Lehner, P. Wajant, M. Fürst, R. Brohm, and T. Kumm, "Overview of German grid issues and retrofit of photovoltaic power plants in Germany for the prevention of frequency stability problems in abnormal system conditions of the ENTSO-E region continental Europe," in *1st International Workshop on Integration of Solar Power into Power Systems*, 2011, pp. 1,6.

[95] C. H. Hommes, "Dynamics of the cobweb model with adaptive expectations and nonlinear supply and demand," *Journal of Economic Behavior & Organization*, vol. 24, no. 3, pp. 315–335, 1994.

[96] J. Nutaro and V. Protopopescu, "The impact of market clearing time and price signal delay on the stability of electric power markets," *IEEE Transactions on Power Systems*, vol. 24, no. 3, pp. 1337–1345, 2009.

[97] Z. Zhao, L. Wu, and G. Song, "Convergence of volatile power markets with price-based demand response," *IEEE Transactions on Power Systems*, vol. 29, no. 5, pp. 2107–2118, 2014.

[98] S. D. Downing and D. F. Socie, "Simple rainflow counting algorithms," *International Journal of Fatigue*, no. January, pp. 31–40, 1982.

[99] R. Orans, "Phase I results: Incentives and rate design for energy efficiency and demand response," Tech. Rep. April, 2006.

[100] "Danish action plan for demand response," Nordel, Elkraft System a.m.b.a., Tech. Rep., 2004.

[101] J. L. Mathieu, P. N. Price, S. Kiliccote, and M. A. Piette, "Quantifying changes in building electricity use, with application to demand response," *IEEE Transactions on Smart Grid*, vol. 2, no. 3, pp. 507–518, 2011.

[102] S. S. Oren, *Market design and gaming in competitive electricity markets.* Iowa State University, 2005.

[103] "Main conclusions and recommendations," EcoGrid EU, Tech. Rep., 2015.

[104] S. Soleymani, A. M. Ranjbar, and A. R. Shirani, "New approach for strategic bidding of Gencos in energy and spinning reserve markets," *Energy Conversion and Management*, vol. 48, no. 7, pp. 2044–2052, 2007.

[105] T. S. Pedersen, K. M. Nielsen, and P. Andersen, "Maximizing storage flexibility in an aggregated heat pump portfolio," in *IEEE Conference on Control Applications*, Antibes, France, 2014, pp. 286–291.

PAPER A

From demand response evaluation to forecasting - Methods and results from the EcoGrid EU experiment

This paper has been submitted for publication in IEEE Transactions on Power Systems.

From Demand Response Evaluation to Forecasting - Methods and Results from the EcoGrid EU Experiment

Emil M. Larsen, Pierre Pinson, *Senior Member, IEEE*, Fabian Leimgruber, Florian Judex

***Abstract*—Understanding electricity consumers participating in new demand response schemes is important for investment decisions, and the and design and operation of electricity markets. Important metrics include peak response, time to peak response, energy delivered, ramping, and how the response changes with respect to external conditions. Such characteristics dictate the services DR is capable of offering, like primary frequency reserves, peak load shaving, and system balancing. In this paper, we develop methods to characterise price-responsive demand from the EcoGrid EU demonstration in a way that was bid into a real-time market. EcoGrid EU is a smart grid experiment with 1900 residential customers who are equipped with smart meters and automated devices reacting to five-minute electricity pricing. Customers are grouped by the manufacturer that provided the smart control equipment and analysed over several months. A number of advanced statistical models are used to show significant flexibility in the load, peaking at 27% for the best performing groups.**

***Index Terms*—Demand response (DR), real-time pricing, demand forecasting, smart grid.**

I. Introduction

INTEREST in Demand Response (DR) has grown in recent years as system operators look for new tools to meet the needs of a rapidly changing power system. Changes include increased production from renewables, tighter market coupling, and a surge in decentralised production and consumption from photovoltaics (PV) and electric vehicles. The changing needs of the power system can broadly benefit from DR in two ways: through emergency use, where a reliable reduction in demand is needed during infrequent critical periods, and through economic use, where demand exhibits continuous flexibility to bring down average costs in the power system.

There are many ways of changing consumption patterns, but dynamic tariffs in particular are gaining interest due to their potential to respond quickly to fluctuating production from renewable energy sources (RES) [1]. Indirect control is one such dynamic tariff that uses an incentive signal, e.g. a real-time price, to influence the load. Indirect control does not require an exact response from any one customer, but with a large number of loads that exhibit somewhat similar behaviour, a statistically likely response can be forecast [2]. The value of indirect control therefore depends heavily on being able to accurately foresee its response to the incentive signal, which has previously been proven complicated [3].

The challenge of determining how much DR there is in a load has previously been done using baseline profiling [4]–[7]. Baseline profiling requires a prediction of the load under non-DR conditions which is then subtracted from the observed consumption under a DR event. A key drawback of existing methods is the need for data from non-DR days, data for which will not always exist, or may be unreliable since new equipment and interaction with customers can make non-DR data unrepresentative. Existing baseline methods are also unsuitable for evaluating fast moving DR that is conditional on a wide range of historical prices and price forecasts. Existing methods typically look a load curtailment, while we consider both increases and decreases in consumption due to decreases and increases in real-time pricing. Finally, existing methods may be susceptible to overfitting, often relying on just one or two dozen observations per parameter.

Demand forecasting literature is a well developed area that is useful in predicting the price-elasticity of a load, e.g. see [8], [9], but many modern approaches involve black box schemes like artificial neural networks (ANN), that obscure our understanding of the dynamics. Therefore, to get a full understanding of the controllable resources requires disaggregating the load into its constituent parts. Flexibility can then be interpreted in a useful way, so that it can be exploited for use in different services, or bid into a market. There are no existing methods that are appropriate for evaluating and integrating residential DR into a balancing market, in particular when data for non-DR days is unavailable, which was the task we had to achieve in the large scale smart grid experiment, EcoGrid EU.

We cultivate modelling approaches that determine how much DR a load is capable of delivering in terms of power and energy, and under what external conditions, e.g. ambient temperature. More specifically, DR is characterised in terms of peak response, time to peak response, energy delivered and ramping. Our primary motivation was to compare the performance of groups of houses with different hardware and software that receive real-time pricing. The tools developed were used to give feedback to hardware and software manufacturers so that their algorithms could be improved. Our second objective was to apply these attributes in the constraints of a balancing market so that the load could be controlled. With

Manuscript submitted 27/05/2015. This work was partly supported by the European Commission through the project EcoGrid EU (grant ENER/FP7/268199).

E.M. Larsen and P. Pinson are with the Centre for Electric Power and Energy, Technical University of Denmark, Kgs. Lyngby, Denmark (email: {emlar,ppin}@dtu.dk). F. Leimgruber and F Judex are with the Energy Department, Austrian Institute of Technology, Vienna, Austria (email: {fabian.leimgruber,florian.judex}@ait.ac.at).

a balancing market scheduling DR, we sought to validate our method by comparing the observed response to the scheduled DR. Aside from the approach, an additional contribution is the application that results in state-of-the-art estimates of residential flexibility used in a five minute balancing market.

The paper is structured as follows: section II investigates existing approaches for evaluating the success of DR, as well as previous work that was relevant when developing our own methodology. Section III introduces the experimental setup and the data gathered from the demonstration. Section IV describes the models developed to analyse the DR activated during the demonstration. Section V presents DR analysis for different groups and results from real-time forecasting in the demonstration. Section VI discusses uncertainty, future work and concludes.

II. Demand modelling

There are several lines or research that are relevant when assessing a DR program, including previous experimental studies, load forecasting research, and energy disaggregation research. Previous experimental analyses have looked at different types of DR, like critical-peak pricing (CPP) and time-of-use (TOU) pricing, and often consider human demographics and behaviour as an impact on DR. Forecasting literature has a wide-spread use in operation of power systems and offers a deeper insight into the statistical tools available, with a greater focus on weather conditions, calendar effects and economic variables. Energy disaggregation research is an up and coming area driven by new sources of data, like high resolution smart meter data from thousands or millions of customers.

A. Previous DR studies

The study of residential loads responding to prices goes all the way back to the 1970s and many fundamental aspects, like accounting for the time of day and ambient temperature in a statistical model, remain in use today. Studies have also included home type, size, income and smart thermostat ownership as model inputs [10], [11], but residential DR studies have not been able to give concrete numbers in terms of power and energy the load is capable of delivering.

For medium and large commercial and industrial loads, baseline methods are widely used to determine financial settlement for participating customers. The baseline is simply the prediction of consumption under the assumption that no DR was present. The baseline is then subtracted from the observed consumption to determine the amount of load shed the customer was able to deliver during a critical period. Baseline models are created by regressing on historical data before DR events. This has been done with hourly interval data [4] and 15 minute interval data [6]. In the latter case, it was observed that including parameters for load shed directly into the model did not give a reliable result, possibly because the model was too primitive or due to over parameterisation. Another approach is to average consumption for just 5-10 days before a DR event [5], yet such few observations may mean that this approach lacks robustness.

B. Forecasting approaches

Short-term load forecasting presents a number of useful tools that can be used to predict how load changes with respect to price. Classical approaches to solving hour-ahead and day-ahead load forecasting problem include time-series methods like auto-regressive integrated moving average (ARIMA) models and exponential smoothing, also including geographical factors [12] and seasonal variations [13].

Recent advances in forecasting methods include spline-based methods [9], which avoid over-parametrisation by relying on a handful of splines to describe the baseload, although authors in [9] noted that some fidelity was lost during peak load periods. This work was applied to a price responsive load in New York, with parameters for price and, in theory, these parameters should allow a full evaluation of the DR volume, although this was not explored in practice.

Other modern advances in forecasting include multivariate state-space models [14], which feature time-varying regression coefficients that may be useful for analysing DR. Semi-parametric methods to predict the contribution of load from some non-linear variables [15] may also be useful for DR volume evaluation, although [15] did not apply the methodology to a price-responsive load.

Machine learning approaches like artificial neural networks (ANN) are also popular for forecasting, with positive results reported in [16]. The benefit from ANN includes being able to capture unspecified non-linear relationships between external variables like weather. It is likely that such an approach becomes increasingly valuable as demand becomes more non-linear and volatile with new external incentives like price and the growth of distributed energy resources (DERs). ANNs have, however, been criticised for leading to over-parametrised models [17] and do not necessarily outperform linear regression models [18]. From a DR evaluation perspective, ANN's black box form makes picking out price influences complex, especially when bidding a price response into an electricity market.

C. Energy disaggregation

Energy disaggregation has gained interest as automatic metering infrastructure becomes ubiquitous in many countries. Energy disaggregation tools can be used to see beyond the meter and uncover which devices are turned on despite only seeing a noisy, aggregated snapshot of the load. The stated goal of disaggregation is to better understand the load and make well-targeted energy efficiency plans.

Of particular relevance to our study is the success in [19] of detecting air-conditioning use from 1-minute interval smart meter data. However, such a disaggregation technique is not well proven with external influences, such as price, or with variable speed devices. Methods that rely on a dictionary of devices describing the real and reactive power each consumes have previously been developed [20]. Grey-box, markovian stochastic, bayesian and logistic adoption models are also promising ways of identifying human behaviour and price-responsive devices in metering data [21].

TABLE I
SUMMARY OF ECOGRID EU CUSTOMER GROUPS

Reference group	Manual group	IBM HP	IBM EH	TNO HP	Siemens EH
253 households with smart meters	455 households with smart meters	195 households with smart meters and automation equipment	322 households with smart meters and automation equipment	84 households with smart meters and automation equipment	398 households with smart meters and automation equipment
No pricing information	Receive real-time pricing, but must alter consumption manually	Heat pumps react autonomously to prices	Resistive electric heating reacts autonomously to prices	Heat pumps react autonomously to prices	Resistive electric heating, water boilers and controllable PV react to aggregator control
279 / 621kW average / peak load	287 / 750kW average / peak load	317 / 710kW average / peak load	394 / 854kW average / peak load	123 / 293kW average / peak load	300 / 810kW average / peak load

III. DATA AND EXPERIMENTAL SETUP

Data for this work comes from EcoGrid EU, which is an indirect control experiment on the Danish island of Bornholm. The experiment uses a market framework to schedule regulating power from conventional generation and DR to meet the real-time balancing needs of the system, needs which are growing due to increased wind power production. DR is activated with a five minute price signal sent to 1900 houses. Houses are equipped with smart meters that collect data every 5 minutes, which in turn is used as an input to forecast demand in real-time. A mathematical introduction to price generation in the EcoGrid EU market can be found in [22].

Demonstration houses are fitted with a wide range of small-scale DERs like PV, heat pumps (HPs), resistive electric heating (EH) and hot water boilers. Heating is the main source of flexibility and is expected to grow due to electrification of heating systems. Flexibility of such installations comes from houses retaining heat and heating devices therefore only needing to be turned on sporadically to meet customer comfort requirements.

Table I shows the group composition that is the basis of our analysis. The IBM HP, IBM EH and TNO HP groups all use the same smart thermostat hardware, while the Siemens EH group uses different smart thermostat hardware. Different control algorithms were used in each group.

The reference group was designed be a control group for all other groups, yet the demographics of each test group were so different that the reference group's baseline profile was not representative in any case. An example of this is shown in Fig. 1, where the prices sent to customers is shown on the top plot, and the consumption of the reference group and Siemens EH group are on the bottom plot. Fourier time-series on the bottom plot are baseline behaviour due to the group demographics. The methodology section describes how to extract this baseline profile. Several customer surveys showed that HP owners have significantly higher incomes, much larger houses, are more likely to own their homes, and are younger than customers who use EH, which explains some of the demographic differences between groups. Unrepresentative reference groups are a key driver for the development of a comprehensive modelling approach.

Smart meter data was filtered to remove houses with fewer than 80% of measurements, leaving 1707 out of 1900 houses. It is never the case that all smart meters report consumption in each time period, so consumption was normalised to the full population of each group. Periods where fewer than 85% of houses reported their consumption were left out, leaving 40,000 observations for each group. The analysis period covers September 22nd 2014 to February 8th 2015, with ambient temperatures spanning -10.6°C to 18.0°C.

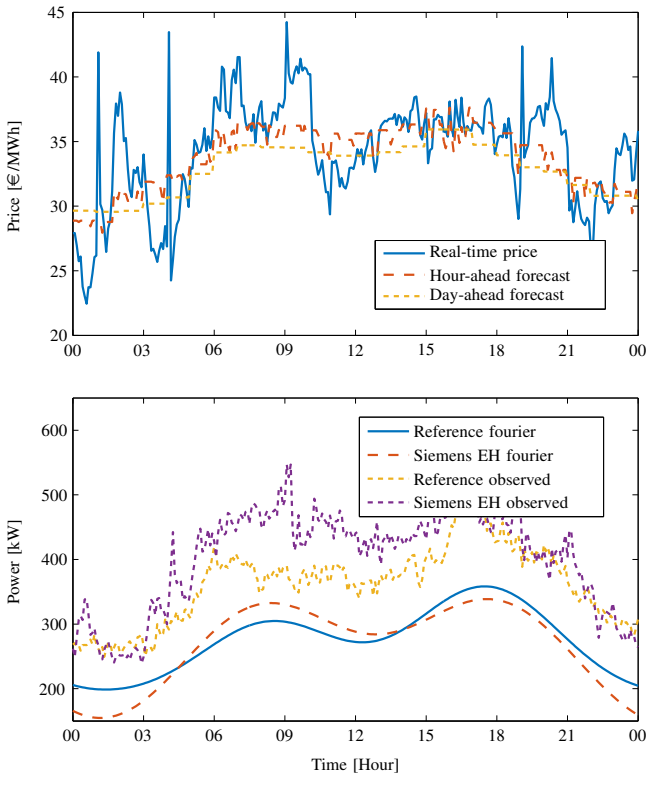

Fig. 1. Single day example of the reference group and a group of automated houses showing profiles that are too different for direct comparison.

IV. Methodology

To evaluate the DR potential of each group, we started with a standard general linear model with additive terms. Linear models have been previously noted to be competitive with newer methods, like probabilistic linear regression and ANN [18]. Unlike some newer methods, parameters of a linear model offer a clear and simple description of how different variables contribute to the load. We also expanded the model with non-linear terms for prices, which bound the response, since linear parameters otherwise predict an infinite response to prices, given infinite prices.

A key challenge with linear models is collinearity, which means that different external variables, for example solar irradiance and ambient temperature, explain the same outcome. This is particularly troublesome for the day-ahead prices, which came directly from the Nord Pool spot market and were not controlled by the experimental market. Day-ahead pricing is correlated with the inflexible part of the load, while the flexible part of the load reacts to the subsequent pricing. Separating active DR from a correlation that would be there anyway, i.e. cause and effect, is therefore difficult. Yet it is necessary to determine the price sensitivity when bidding into a day-ahead market, i.e. [23]. Likewise, determining the price sensitivity to real-time prices is also needed to bid into the balancing market, i.e. [22].

A second model that relies upon differenced variables was applied and found to be less susceptible to collinearity. Our experience taught us that the differenced model had a lower short-term forecast error, which made it well suited to trying to control the load every five minutes in the experiment. It also appears to capture the fast moving price-dynamics more accurately.

Despite the benefits of the second model, the standard model is still needed because it gives a different result. The standard model gives the absolute value for DR and is more accurate for long-term forecasting. The differenced model tells us the maximum change in DR in any five minute interval, which is needed when scheduling DR in an operational environment, like the EcoGrid EU experiment.

A. Cross validation

To ensure that our models are not overfitted, and to test the data for consistency with respect to time, a cross-validation approach was used. Specifically, a ten-fold cross-validation was employed. The data was randomly divided into 10 approximately equally sized subsets or folds. For each fold (validation fold), the remaining other 9 folds were used to first train the model. The model was then applied to the observations in the validation fold, resulting in a mean squared error (MSE) for the validation fold. This procedure is repeated for the other 9 folds respectively, resulting in 10 estimates of the test error (MSE) in total. These estimates are averaged, resulting in the CV estimate MSE_{CV}. To assess model performance with respect to time, this cross-validation estimate is compared to the MSE obtained by fitting the model to the full data. The relative difference of the full-data MSE and the MSE estimated by CV is then used as a measure of model consistency with respect to time. Table II shows the CV outcome for the standard model. The almost identical results for 10-fold MSE and full-sample MSE means that the model is consistent over time and less likely to be overfitted.

TABLE II
10-fold cross-validation by group

	MSE	$\mathrm{MSE_{CV}}$
Reference	111.72	110.66
Manual	122.24	119.68
IBM HP	226.06	228.88
IBM EH	205.17	204.05
TNO HP	263.95	265.50
Siemens EH	65.50	65.87

B. Standard general linear model

Initially, demand is conceptionally split into a component dependent on external variables and a component that is dependent on external variables and prices using the notation from [24], i.e.

$$c_t = f\left(\tilde{z}_t\right) + g\left(\tilde{\lambda}_t, \tilde{z}_t\right) \tag{1}$$

with

$$\tilde{\lambda}_t = \begin{bmatrix} \lambda^D_{t+u^D_\lambda}, \ldots, \lambda^D_{t-n^D_\lambda} \\ \lambda^R_{t+u^R_\lambda}, \ldots, \lambda^R_{t-n^R_\lambda} \end{bmatrix}$$
$$\tilde{z}_t = \left[z_{t+u_z}, \ldots, z_{t-n_z}\right]$$

where n^D_λ, n^R_λ and n_z are a finite number of lagged values of day-ahead price, λ^D, real-time price, λ^R, and external variables, z. There are also u^D_λ, u^R_λ and u_z forecast values, which capture the scheduling dynamics of DERs. All variables are first centered by subtracting their mean value, while price forecasts are converted to relative prices each time a new price forecast is made. The day-ahead price $\lambda^{\mathrm{D,raw}}$ is normalised to a value between 0 and 1, so that

$$\lambda^{\mathrm{D}}_t = \frac{\lambda^{\mathrm{D,raw}}_t - \tilde{\lambda}^{\mathrm{D,min}}_t}{\tilde{\lambda}^{\mathrm{D,max}}_t - \tilde{\lambda}^{\mathrm{D,min}}_t} \tag{2}$$

Real-time prices and real-time forecasts are also converted to relative prices, but with respect to the absolute day-ahead price, i.e.

$$\lambda^{\mathrm{R}}_t = \lambda^{\mathrm{R,raw}}_t - \lambda^{\mathrm{D,raw}}_t \tag{3}$$

External variables, z, include weather data such as wind speed, solar irradiance, temperature, Φ, and a base load term, y. A non-linear transformation is applied to temperature, whereby it is modelled as a third-order polynomial, as has previously been proven successful in [25], such that

$$\tilde{\Phi}_t = \Phi_t + \Phi^2_t + \Phi^3_t \tag{4}$$

Exponentially weighted smoothing is also performed on weather variables, so that

$$z_t = \frac{\sum_{i=n_z}^{u_z} \alpha^{i-1} z_{t-i}}{\sum_{i=n_z}^{u_z} \alpha^{i-1}} \tag{5}$$

The steps to find the number of lags, i, and the smoothing factor, α, are found experimentally (as described in [18]), where the lowest error is the determining factor.

The base load, y, is a Fourier series that describes demand due to the time of day, day of the week, and day of the month [26], such that, for a given time t,

$$y_t = \sum_{k=1}^{K} a_k \sin\left(\frac{2\pi k t}{T}\right) + b_k \cos\left(\frac{2\pi k t}{T}\right) \tag{6}$$

where T must be suitably large to cover different seasonal variations (for example 288 when capturing trends of different hours of the day using five minute data) and K is increased until enough high-resolution detail is captured.

Additional terms are added to capture the interaction between the base load and temperature, $y\Phi$, and the price and temperature, $\lambda\Phi$, included in the array of variables $\tilde{\chi}$. The full model for demand can be expressed in general linear model form, i.e.

$$c_t = \tilde{\lambda}_t^\top \theta_\lambda + \tilde{z}_t^\top \theta_z \epsilon_t + \tilde{\chi}_t^\top \theta_\chi = \boldsymbol{x}_t^\top \boldsymbol{\theta} + \epsilon_t \tag{7}$$

where ϵ is Gaussian noise with zero mean and finite variance. Relying on a conventional least squares regression with five minute data and several lags for external variables can lead to a model with hundreds of parameters and suspicions of overfitting, even in light of the 40,000 observations that the model is fitted to. As a result, we found the only way to solve the model and get reasonable parameter estimates was to minimizing the residual sum of squares while shrinking parameters using the Lasso penalisation [27]. The objective of this is

$$\min \sum_{t=1}^{T} \left(c_t - \boldsymbol{x}_t^\top \boldsymbol{\theta}\right)^2 + \eta|\boldsymbol{\theta}| \tag{8}$$

where η is the tuning parameter and is found using a 10-fold cross-validation routine, minimising MSE_{CV}. Given a model with 200 input parameters, the Lasso penalisation gave just 50-70 non-zero parameters for each group using both the standard and the differenced model.

C. Differenced model

The difference model relates how consumption changes with respect to how the variables change through time, i.e. gradients of external variables like price and temperature affect the gradient of consumption. Conceptionally, the split becomes

$$\dot{c}_t = f\left(\tilde{\dot{z}}_t\right) + g\left(\tilde{\dot{\lambda}}_t, \tilde{\dot{z}}_t\right) \tag{9}$$

where $\dot{c}_t$, $\dot{z}_t$ and $\dot{\lambda}_t$ are the change in consumption, external variables and prices at time t respectively. The interaction terms between temperature and price should be interpreted as how fast the change in consumption occurs due to how fast the price and temperature are changing. As a result, to better understand ambient temperature effects, the parameters of the general linear model are found in equation (8) for three different ambient temperature bins of equal population, which means that the parameters are found with 13,000 observations each time.

D. Non-linear terms for price

In an operational environment, specifically the market within which DR in EcoGrid EU is controlled, bounds for the price-response must be given for each five minute period. Without bounds, it is impossible to maintain control over the DR in the demonstration. The relationship between price and demand has previously been observed to be non-linear [24] and this can be modelled by redefining the price terms in a generalised logistic function that is centred around zero. To find non-linear price terms, the residuals are combined with the price response according to the Equation (7), i.e.

$$\epsilon_t^* = \epsilon_t + \lambda_t \theta_\lambda \tag{10}$$

The residuals ϵ^* now include the predicted linear DR and non-linear components too. The objective to find the logistic function parameters is given by

$$\min \sum_{t=1}^{T} \left(\epsilon_t^* - \left(\sum_{n=1}^{N} -\frac{A_n}{2} + \frac{A_n}{1 + e^{-\varepsilon_n \tilde{\lambda}_n}}\right)\right) \tag{11}$$

where the N most important lags are chosen. $A_n/2$ is the maximum amplitude of the response due to price lag n, while ε_n describes the price-elasticity. Parameters are found by minimising the sum of square errors using the Levenberg-Marquardt algorithm [28], with the linear parameters for price used as starting estimates for ε_n. Fig. 2 illustrates the impact of non-linear terms for price, where the top plot shows the boundary of DR, and the bottom plot shows the accumulated impact on the finite impulse response (FIR), that is the change in load due to price, through time, when given the data obtained in the EcoGrid EU demonstration. If non-bounded price terms are used, then the linear prediction (dashed red line in top plot) will tend to infinity if the prices tend to infinity. The non-linear model enforces bounds on this response, beyond which consumption cannot change further in the presence of extreme prices.

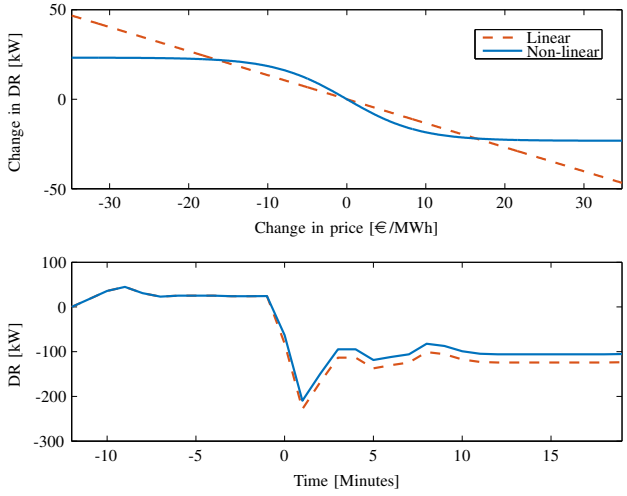

Fig. 2. A comparison of a linear parameter for price and a novel non-linear model for price. The response of the non-linear model (bottom plot) is bounded for very high electricity prices.

Non-linear terms reduce DR for each group by 2 to 16% compared with linear terms for DR, given the maximum prices seen, while the mean average percentage error (MAPE) is only fractionally reduced (0.05%). In a differenced model, the initial change to price gives the biggest DR load contribution, since it impacts all subsequent price lags. In the standard model, the biggest change to price is assumed to be largest parameter for price, which happens 10-30 minutes after a price change.

E. Deriving useful DR measures

The statistical models developed can now be used to bid DR into day-ahead and real-time markets assuming standard quadratic programming structures, as is in use today [29]. For the EcoGrid EU demonstration, this meant bidding the price sensitivity of the entire population into a real-time balancing market, which are the parameters associated with λ^{R}.

To evaluate DR, more specifically to determine peak response, energy delivered and ramping, the statistical models with non-linear terms for price where filled with observations and meteorological data and calculated as follows. For the peak real-time DR delivered

$$\text{Maximum DR} = \max \frac{|A_n|}{2} \tag{12}$$

For the initial ramping, we consider only the price lag for the instantaneous price, i.e.,

$$\text{Initial ramping} = \frac{|A_1|}{2} \tag{13}$$

For the energy delivered in one hour, we integrate over the first 12 values of the FIR, while the time to peak response is simply the time, n, for which A_n is largest.

V. Results

The power and energy that can be delivered by each group is presented here, using the two modelling approaches developed. We also present the outcome of forecasting the load using the differenced model. Fig. 3 shows the outcome of the non-difference model, with Fourier terms, weather, day-ahead and real-time price effects cumulatively added "on top" of each other.

A. Group FIR visualisation

The FIRs related to price parameters from the differenced model are shown for the different automated groups in Fig. 4 for three different temperature bins. In this figure, at time zero, the relative real-time price changes from 0 to the maximum price change observed in the experiment. The load responds immediately, reaching a peak, then rebounding, then arriving at a new steady state after approximately 50 minutes. Before the price change, real-time price forecasts cause consumption to increase, causing load to shift. This figure could also be given as a mirror image, showing load increase for a reduction in price. The Siemens EH group exhibited the largest and fastest response to prices, while the IBM groups exhibited a slower response to the price increase. We observed no change

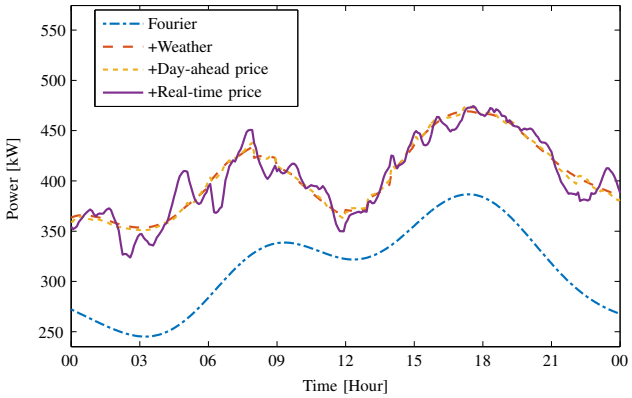

Fig. 3. Load contributions according to the general linear model. Each contribution to the load is added to the previous one.

in consumption for TNO HP houses. For the warmest periods, which averaged 11.3°C, the Siemens EH group exhibited significant DR, while IBM EH houses also exhibited a small but noticeable change in consumption. There was no DR from the other groups during warm conditions.

B. DR evaluation

Table III shows the peak DR according to the standard general linear model, also normalised with respect to the peak consumption of each group. In absolute terms, the Siemens EH group exhibits the biggest DR, while when normalised for the peak consumption, the IBM HP group appears to give the biggest response, totalling 27% of peak load. The reference group shows no DR, as expected, while the manual group shows a very small amount of DR. No DR was detected for TNO HP houses.

In Table IV, the consumption due to day-ahead pricing is shown for the standard and differenced models. A negative sign indicates that consumption and price are positively correlated. The differenced model shows less positive correlation across all groups, indicating that there is less collinearity between base load and price, i.e. the base load terms are better capturing demand rather than the day-ahead price. The benefit of the differenced model is especially noticeable for Siemens EH houses, which appears to exhibit the largest response to day-ahead pricing, followed by IBM HP houses.

Table V states the load shifting characteristics of each group, based upon the price-related parameters in the differenced model. The first column shows the average DR volume shifted

TABLE III
Maximum real-time DR

Group	DR	Normalised DR
Reference	0kW	0
Manual	4.0kW	0.005
IBM HP	190.1kW	0.268
IBM EH	114.4kW	0.134
TNO HP	0kW	0
Siemens EH	198.0kW	0.244

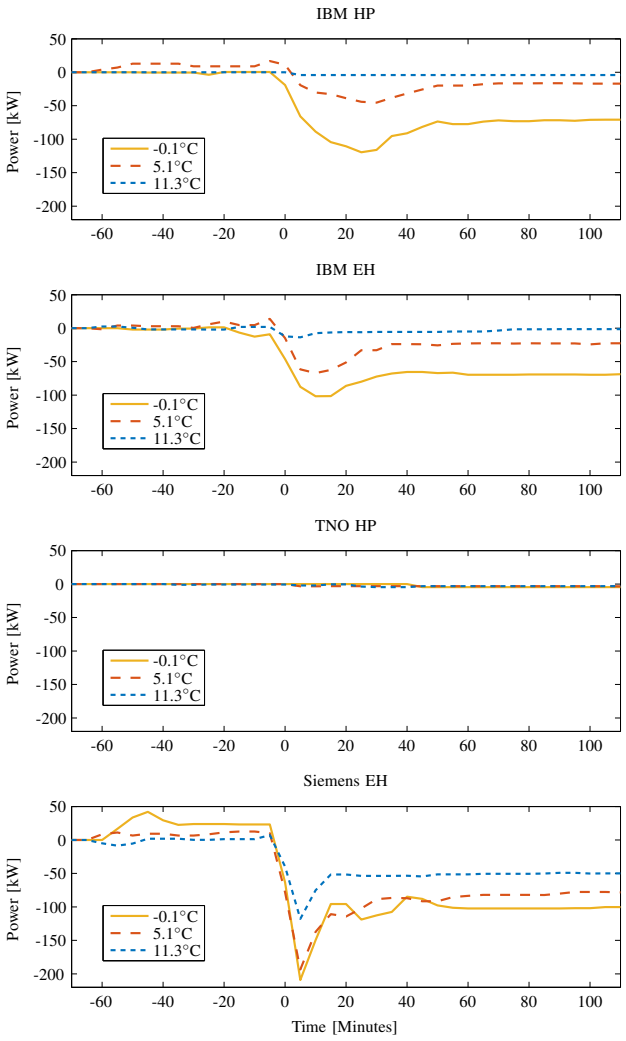

Fig. 4. The response to price for different groups, given the largest price change observed.

per hour throughout the test period. The second column normalises this value by the average energy consumed by each group. The final column states the maximum load shift in a single hour, when given the maximum price change observed. This is the area under the FIR curves show in Fig. 4. The average volume for Siemens EH houses, the best performing group, appears to be twice that of IBM HP houses, but it is only 19% higher in terms of maximum volume. This can be attributed to the faster ramping abilities of the Siemens EH group, which means its DR is exploited more by the market, since quick, small changes are activated more in a market framework.

TABLE V
REAL-TIME DR VOLUME

Group	Volume	Volume normalised	Volume max
Reference	0.4kWh/h	0.010	-9.8kWh
Manual	0.3kWh/h	0.006	-1.2kWh
IBM HP	4.9kWh/h	0.115	93.0kWh
IBM EH	3.9kWh/h	0.078	73.5kWh
TNO HP	0.1kWh/h	0.008	1.2kWh
Siemens EH	9.5kWh/h	0.206	110.3kWh

C. Forecasting application

The differenced model with additional auto-regressive components was used to forecast aggregate consumption of all houses in real-time in the EcoGrid EU demonstration, using real-time meteorological forecasts from the Danish Meteorological Institute (DMI). The MAPE for one step ahead was 1.6%, compared with persistence of 2% and hindcasting of 1.1% and 1.4% for models with and without price terms. Hindcasting with the standard linear model without auto-regressive terms gave a MAPE of 5.5%. Fig. 5 shows how the MAPE evolves with forecast horizon. We witnessed large errors for longer forecast horizons due to smart meter aggregation variability. For one five minute period, 250 smart meters might report in, with their load normalised to 1900 houses (the full population). In the next five minute period, 1700 houses might report in, which also causes the earlier observations to change. Smart meters contain a Sim card and report consumption over standard mobile phone networks. Varying delays are caused by cost and bandwidth limitations and patchy signals for some houses. The average jump in meter data for any five minute time period is 7% and, in the worst periods, this reaches 25% of the load; the results given above are for where the recent historical meter readings for the normalised aggregate population did not change by more than 0.5%. With such volatility, the auto-regressive contribution to the load forecast was extremely misleading, causing large errors for longer forecast horizons. In a full-scale roll-out, grid measurements such as system frequency could be used instead of smart meter data in our models. If smart meters were still

TABLE IV
MAXIMUM DAY-AHEAD DR

Group	DR	DR (differenced model)
Reference	-29.1kW	-25.6kW
Manual	-28.9kW	-24.0kW
IBM HP	7.3kW	10.6kW
IBM EH	-39.9kW	-30.4kW
TNO HP	-8.3kW	-4.5kW
Siemens EH	0kW	35.7kW

TABLE VI
RAMPING AND TIME TO PEAK RESPONSE

Group	Initial ramping	Time to peak response
Reference	-4.4kW	N/A
Manual	0kW	N/A
IBM HP	19.1kW	30 mins
IBM EH	46.2kW	15 mins
TNO HP	0kW	N/A
Siemens EH	63.4kW	10 mins

to be relied upon, then the most representative smart meters should be identified, made robust and be relied upon.

In spite of poor long-horizon forecasting performance due to smart meter collection variability, the five minute ahead forecast was good enough to see a real-time response. Fig. 6 shows the change in DR requested by the market, binned into 20kW groups, which is subsequently converted to a price based on the demand models created here and sent to customers. The change in load observed shows the raw consumption data that includes all other sources of uncertainty, like baseload, weather and human behaviour. Despite these sources of noise, there appears to be a clear trend where demand is following the price. For the largest requests in a reduction in consumption, a reduction in consumption occured 80% of the time, while for the largest requests for an increase in consumption, an increase in consumption occurred 100% of the time.

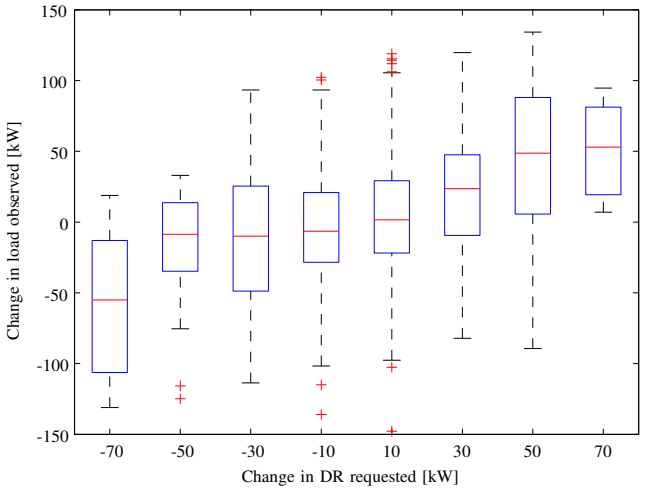

Fig. 6. Change in load observed, binned for different levels of DR activation based upon the forecasting model. Each boxplot shows the median as a red bar and the blue box showing the two middle quantiles.

D. Result uncertainty

Uncertainty is clearly present in our results and best observed in Table V, where the reference group appears to exhibit small amounts of DR, despite not receiving the real-time price. This is due to spurious correlation, but it is an order of magnitude smaller than the automated groups.

There are many sources of error in a residential DR system, the most significant of which is likely structural, i.e. models do not capture the full dynamics and all interactions in the load. Experimental errors include that the model is unaware when smart control equipment is off for maintenance or due to communication errors, which raises the possibility that the maximum DR potential is underestimated here. Weather observation and forecast errors are also present, since weather data comes from a single point that will not be representative of the entire population.

Previous DR error analyses have relied on standard errors [4]. Methods to derive standard errors from a Lasso regression have also been developed [30], yet the scientific community and leading journals are rejecting such significance tests since they are often interpreted incorrectly. In [3], standard errors for DR evaluation were identified as underestimating the uncertainty for a number of reasons. In our case, these include correlation between Fourier terms, temperature, and day-ahead pricing. Regression residuals are also autocorrelated, especially since we do not include auto-regressive or moving-average terms in our models (these terms are only meaningful in a forecasting environment). Regression residuals for baseline models have also been identified as being heteroscedastic; i.e. the error is dependent on external variables like the time. Leave one out cross validation (LOOCV) is a good solution for estimating the true level of uncertainty in a baseline framework with observations averaged over several hours [6]. It is, however, far too computationally intensive when dealing with the five minute interval data and the 40,000 observations that we rely upon. We are therefore left without an appropriate toolbox to assess uncertainty, and this should be a major focus of future work in this field.

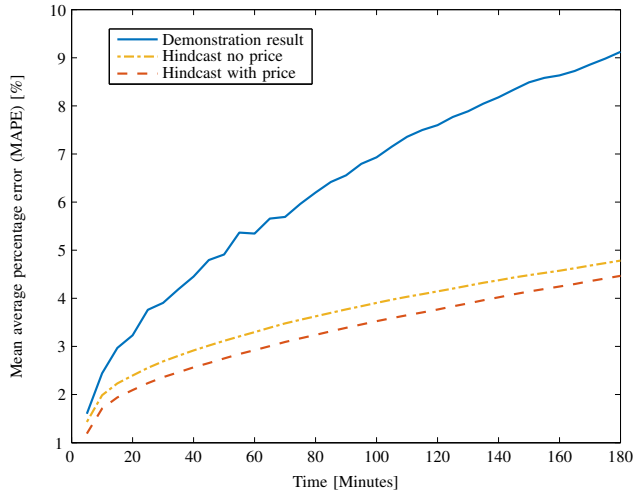

Fig. 5. Mean absolute percentage error (MAPE) from the experiment and from hindcasting on historical data.

VI. Conclusion

We have determined that our load is capable of delivering significant DR, where up to 27% of the peak load is flexible for the best performing groups. The software algorithm for the TNO HP group, which did not exhibit any DR, was subsequently changed following our findings and a response to price was observed in a later time period. This highlights how such statistical models could be used in the future; Revenue from following dynamic pricing may not be enough to justify the high investment cost needed to fit houses with automation equipment, which raises the possibility of availability payments being made to support initial DR installations. The statistical models developed here could therefore be used to determine financial settlement based on peak response and average energy provided. We did not see noticeable DR from the manual customers, but this could be due to the design of the experiment: customers were guaranteed an electricity

bill no higher than if they were not in the demonstration. A large scale roll-out of dynamic pricing would have no such guarantee and would penalise as well as incentivise customers, which would likely result in increased DR from customers with no automation equipment.

Future work should look to advanced machine learning models, since our models likely ignore significant non-linearities in the load. This is especially relevant for analysing the DR potential of IBM HP, IBM EH and TNO HP groups, since the hardware used in these groups can only turn off heating devices, not on. In a large enough population, with a diverse range of internal states, this may not mean a significant asymmetrical response for thermostatic loads, but it warrants investigation nonetheless.

ACKNOWLEDGMENT

The authors thank our EcoGrid EU partners for supporting this work. The authors also thank DMI and ECMWF for weather forecast data.

REFERENCES

[1] N. O'Connell, P. Pinson, H. Madsen, and M. O'Malley, "Benefits and challenges of electric demand response: A critical review," *Renewable and Sustainable Energy Reviews*, vol. 39, pp. 686–699, 2014.

[2] K. Heussen, S. You, B. Biegel, L. H. Hansen, and K. B. Andersen, "Indirect control for demand side management - A conceptual introduction," *IEEE PES Innovative Smart Grid Technologies Conference Europe*, pp. 1–8, 2012.

[3] J. L. Mathieu, D. S. Callaway, and S. Kiliccote, "Examining uncertainty in demand response baseline models and variability in automated responses to dynamic pricing," in *IEEE Conference on Decision and Control and European Control Conference*, Dec. 2011, pp. 4332–4339.

[4] S. D. Braithwait, D. G. Hansen, and J. D. Reaser, "Load impact evaluation of California statewide demand bidding programs (DBP) for non-residential customers: Ex post and ex ante report," Christensen Associates Energy Consulting, Madison, WI, Tech. Rep., 2011.

[5] M. L. Goldberg and G. K. Agnew, "Commission protocol development for demand response calculation - California," California Energy Commission, Tech. Rep. February, 2003.

[6] J. L. Mathieu, P. N. Price, S. Kiliccote, and M. A. Piette, "Quantifying changes in building electricity use, with application to demand response," *IEEE Transactions on Smart Grid*, vol. 2, no. 3, pp. 507–518, 2011.

[7] K. Coughlin, M. A. Piette, C. Goldman, and S. Kiliccote, "Statistical analysis of baseline load models for non-residential buildings," *Energy and Buildings*, vol. 41, no. 4, pp. 374–381, 2009.

[8] R. Weron, *Modeling and forecasting electricity loads and prices: A statistical approach*. John Wiley & Sons Ltd., 2006.

[9] J. R. M. Hosking, R. Natarajan, S. Ghosh, S. Subramanian, and X. Zhang, "Short-term forecasting of the daily load curve for residential electricity usage in the Smart Grid," *Applied Stochastic Models in Business and Industry*, vol. 29, no. 6, pp. 604–620, 2013.

[10] J. A. Hausmann, M. Kinnucan, and D. McFaddden, "A two-level electricity demand model: Evaluation of the connecticut time-of-day pricing test," *Journal of Econometrics*, vol. 10, no. 3, pp. 263–289, 1979.

[11] F. A. Wolak, "An experimental comparison of critical peak and hourly pricing: The PowerCentsDC Program," Stanford University, Stanford, Tech. Rep., 2010.

[12] S. Fan, K. Methaprayoon, and W. J. Lee, "Multiregion load forecasting for system with large geographical area," *IEEE Transactions on Industry Applications*, vol. 45, no. 4, pp. 1452–1459, 2009.

[13] J. W. Taylor, "Triple seasonal methods for short-term electricity demand forecasting," *European Journal of Operational Research*, vol. 204, no. 1, pp. 139–152, 2010.

[14] V. Dordonnat, S. J. Koopman, and M. Ooms, "Dynamic factors in periodic time-varying regressions with an application to hourly electricity load modelling," *Computational Statistics and Data Analysis*, vol. 56, no. 11, pp. 3134–3152, 2012.

[15] S. Fan and R. J. Hyndman, "Short-term load forecasting based on a semi-parametric additive model," *IEEE Transactions on Power Systems*, vol. 27, no. 1, pp. 134–141, 2012.

[16] N. Amjady, "Day-ahead price forecasting of electricity markets by a new fuzzy neural network," *IEEE Transactions on Power Systems*, vol. 21, no. 2, pp. 887–896, 2006.

[17] H. S. Hippert, C. E. Pedreira, and R. C. Souza, "Neural networks for short-term load forecasting: A review and evaluation," *IEEE Transactions on Power Systems*, vol. 16, no. 1, pp. 44–55, 2001.

[18] T. Hong, "Short term electric load forecasting," Ph.D. dissertation, North Carolina State University, 2010.

[19] K. X. Perez, W. J. Cole, J. D. Rhodes, A. Ondeck, M. Webber, M. Baldea, and T. F. Edgar, "Nonintrusive disaggregation of residential air-conditioning loads from sub-hourly smart meter data," *Energy and Buildings*, vol. 81, pp. 316–325, 2014.

[20] D. Benyoucef, P. Klein, and T. Bier, "Smart Meter with non-intrusive load monitoring for use in Smart Homes," *2010 IEEE International Energy Conference and Exhibition, EnergyCon 2010*, pp. 96–101, 2010.

[21] F. Farzan, M. a. Jafari, J. Gong, F. Farzan, and A. Stryker, "A multi-scale adaptive model of residential energy demand," *Applied Energy*, vol. 150, pp. 258–273, 2015.

[22] Y. Ding, S. Pineda, P. Nyeng, J. Ø stergaard, E. M. Larsen, and Q. Wu, "Real-time market concept architecture for EcoGrid EU - A prototype for European smart grids," *IEEE Transactions on Smart Grid*, vol. 4, no. 4, pp. 2006–2016, 2013.

[23] G. B. Shrestha and P. a. J. Fonseka, "Congestion-driven transmission expansion in competitive power markets," *IEEE Transactions on Power Systems*, vol. 19, no. 3, pp. 1658–1665, 2004.

[24] O. Corradi, H. Ochsenfeld, H. Madsen, and P. Pinson, "Controlling electricity consumption by forecasting its response to varying prices," *IEEE Transactions on Power Systems*, vol. 28, no. 1, pp. 421–429, 2012.

[25] M. T. Hagan and S. M. Behr, "The time series approach to short term load forecasting," *IEEE Transactions on Power Systems*, vol. 2, no. 3, pp. 785–791, 1987.

[26] S. A.-h. Soliman and A. M. Al-Kandari, *Electrical load forecasting: Modeling and model construction*. Elsevier, 2010.

[27] G. James, D. Witten, T. Hastie, and R. Tibshirani, *An introduction to statistical learning*. Springer, 2006, vol. 102.

[28] J. Nocedal and S. J. Wright, *Numerical optimization*. Springer, 2006.

[29] A. Martin, J. C. Müller, and S. Pokutta, "Strict linear prices in non-convex European day-ahead electricity markets," *Optimization Methods and Software*, vol. 29, no. 1, pp. 189–221, 2012.

[30] R. Lockhart, R. J. Tibshirani, R. Tibshirani, and J. Taylor, "A significance test for the lasso," 2014.

PAPER B

Evaluating price-based demand response in practice - with application to the EcoGrid EU experiment

This paper has been submitted for publication in IEEE Transactions on Smart Grid.

Evaluating price-based demand response in practice — with application to the EcoGrid EU Experiment

Guillaume Le Ray, Emil M. Larsen, Pierre Pinson, *Senior Member, IEEE*

***Abstract*—Increased emphasis is placed today on various types of demand response, motivated by the integration of renewable energy generation and efficiency improvements in electricity markets. Some advocated for the development of price-based approaches, where the conditional dynamic elasticity of final users is exploited in the power system, e.g. for system balancing. However, very few real-world experiments have been carried out and price-based demand response has consistently been found difficult to assess and quantify. It is our aim here to describe an approach to do so, as motivated by the large-scale EcoGrid EU experiment. In this project, 1900 houses were equipped with smart meters and other automation devices in order to adapt consumption to real-time electricity prices every five minutes, while monitoring it with the same resolution. Our approach first relies on the clustering of residential load observations that behave similarly within a given experiment. Then, a clinical testing approach, based on a test and a control group, is adapted to assess whether price-responsive loads were actually responsive or not. Interestingly, in the deployment phase of the project, the results show that houses could be deemed price-responsive on some test days, while results were inconclusive on some others.**

***Index Terms*—Demand response, clustering, time-series analysis, smart grid, electric load modelling**

I. Introduction

TARGETS TO increase the proportion of renewable energy production to 27% by 2030 across all 28 EU member states [1] present significant technical challenges, since existing markets, services and technologies are unlikely to be robust enough to cope with the expansion of variable power generation, also with limited predictability. Among the various options to support large-scale renewables penetration like wind and solar power, Demand Response (DR) has emerged as a popular approach, with its natural advantages and caveats [2]. Recent developments in that direction follow the concepts of *(i)* direct control, where a higher-level operator would somehow operate these electric loads, and *(ii)* control by price, where advantage is taken of the elasticity and cross-elasticity of electric power consumers. There obviously are obstacles in rolling out DR, including the non-flexibility of demand [3] and the low participation due to information asymmetries [4]. Control by price has additional difficulties over direct control due to the complexity in predicting response to price variations [5], although forecasting models and control schemes that make effective use of them have been researched [6]. Techniques that can readily identify whether a population (or a sub-population) of electric loads is price-responsive remain lacking, while this may be crucial in practice. This issue is of particular relevance during the deployment phase of demand response equipment and programs. Indeed a logical subsequent step after deploying necessary hardware and software is to control that the different elements communicate as expected, react to the right information, or simply to verify that the overall concept functions.

With that context in mind, we introduce a proposal test-control method to assess whether or not electric loads are price-responsive or not. The principle of comparing control and test groups has been extensively used in the medical industry to evaluate the efficiency of a treatment for over 200 years [7], and more recently in the electricity field, industrials working on load research practices have been using this approach to develop Customer Base Line (CBL) and evaluate candidate customers under DR [8]. This method has the advantage of having both the candidate customers and CBL to be exposed to the same weather conditions. Such an approach aims at assessing through hypothesis testing whether loads are responsive or not, which is a basic question to answer before to aim for a quantification and characterization of that response.

Prior to undergoing this test-control analysis, electrical loads are clustered based on similar behavior within a given experiment (i.e., a test day with a given price profile). This allows to identify electric loads that do not respond as expected, while sorting subgroups of responsive households. The value of the clustering step of our methodology also lies in the dimension reduction of the problem since, instead of trying to assess whether each and every household in a large-scale demand response experiment (with 1000 households or more) is responsive or not, a fully data-driven clustering step narrows down the analysis by focusing on a low number of subgroups of households with similar dynamic characteristics. This may also be seen as having the side benefit of pinpointing electric loads that could be useful in providing specific grid services such as balancing and congestion management, in view of the characteristics of their response.

Existing literature related to clustering applications (also referred to as segmentation) focuses on profiling, to group the consumers with similar energy consumption patterns [9], [10], or on modelling, to obtain more homogeneous data to improve forecasting accuracy [11], [12]. However, similar approaches using clustering to exclude electric loads that are not responding to the price have not been found in the literature, despite interest from industry in knowing whether a

G. Le Ray, E.M. Larsen and P. Pinson are with the Centre for Electric Power and Energy, Technical University of Denmark, Kgs. Lyngby, Denmark (email: {gleray,emlar,ppin}@elektro.dtu.dk).

This work was partly supported by the European Commission through the project EcoGrid EU (grant ENER/FP7/268199).

Manuscript submitted ...

smart controller is responsive or not [8].

The development of this methodology was originally motivated by, and then applied to, the EcoGrid EU demand response experiment, in which 1900 houses and 100 industrial loads receive new electricity prices every five minutes [13]. On the Danish island of Bornholm where the experiment takes place, the majority of the participants have resistive electric heating and heat pumps installed. Their controllability, combined with the heat capacity of the buildings, yields virtual electric power storage. Houses are equipped with smart meters reporting consumption in real-time, as well as a range of automated controllers that make provision of DR convenient by enabling controllability of a wide range of small-scale Distributed Energy Resources (DERs) in a cost-efficient manner. The automated controllers are proprietary and were developed by different companies. In this study, they are therefore considered as black boxes. However, it is know that these rely on state-of-the-art control techniques used for DR, like hysteresis control and economic model predictive control, allowing to schedule consumption optimally considering weather and price forecasts, as well as customer preferences in terms of comfort.

The prices seen by these electric loads originate from the EcoGrid EU market. It was primarily designed to support balancing when larger shares of renewables are present in the power system, yielding additional and more variable balancing needs. In EcoGrid EU, knowledge of the power system state is updated every five minutes. This higher temporal resolution, compared to the hourly time units broadly used in deregulated power systems today, naturally allow to better adapt to dynamic balancing needs. Another key aspect of the market is that it is bidless for demand, hence reducing risk and increasing convenience for small customers who would not otherwise participate. A full introduction to the market behind price generation in the EcoGrid EU experiment is given in [14]. The first phase of the EcoGrid EU project was completed in early 2014, where price-responsive controllers from two different manufacturers were installed in 1200 houses. The price-responsiness of participants was analysed and eventually validated using the clustering and test-control methods presented here.

The paper is structured as following. Section II presents the empirical framework of the experiment, with particular emphasis on the data and various test-cases to be analyzed. Our methodology is described in Section III, by first introducing the clustering approach for identifying fully non-responsive households and subgroups of responsive electric loads, followed by the test-control method to assess whether these reponsiveness can be seen as genuine price-responsiveness. The results for the roll-out phase of the EcoGrid EU experiment are used as an illustration in Section IV. The paper ends with conclusions and perspectives for future work in Section V.

II. Empirical framework

The datasets consist of electricity consumption for each candidate household with a resolution of 5 minutes. Real-time price series have the same temporal resolution, allowing for the joint analysis of the dynamics of both price and consumption series. Only consumption related to space heating varies as a function of prices based on the controllers deployed for heat pumps and resistive electric heating.

Throughout the initial phase of the demonstration, households were recruited and then made price-responsive gradually. Some households had their automation disabled deliberately, while others had their automation disabled due to technical problems. These households were used to form the CBL. Due to the random nature of technical problems, the composition of the test and CBL groups varied from one test-case to the next. Test and CBL groups also varied according to the number of households using one of two control-equipment types and according to different heating types (heat pump or resistive electric heating). As the size of the CBL and participant groups differ throughout the overall experiment, this influences the resulting data analysis and especially the estimated confidence intervals and hypothesis tests performed.

In order to test the controllers, test cases were designed to stress and assess their price-responsiveness with extreme price variations. As the energy consumption should be a function of the price, a significant change in the electricity consumption is expected when such extreme price variations occur [15]. More precisely, a variation in price is to be seen as an incentive for modification of electricity consumption: upwards when the price goes down, and downwards when the price goes up. Table I gives a summary of the price variations applied during each test case.

TABLE I: Price variations during the test-cases [15].

Test period	Extreme values (€/MWh)	Baseline (€/MWh)
25/10/2013	-53.7 / 148.0	47.2
07/11/2013	-53.7 / 148.0	47.2
21/11/2013	-61.3 / 140.3	39.4
27/11/2013	37.4 / 41.4	39.4
06/12/2013	-134.5 / 134.5	0
10/12/2013	-134.5 / 134.5	0
11/12/2013	-134.5 / 134.5	0
12/12/2013	-134.5 / 134.5	0
20/01/2014	-134.5 / 134.5	0
21/01/2014	-134.5 / 134.5	0
22/01/2014	-134.5 / 134.5	0
23/01/2014	-134.5 / 134.5	0
08/03/2014	-61.3 / 140.3	39.4
11/03/2014	37.4 / 41.4	39.4
09/04/2014	-61.3 / 140.3	39.4
13/04/2014	-61.3 / 140.3	39.4

III. Methodology for Assessing Price-responsive Behavior

A. A Non-supervised Classification for Dimension Reduction and to Identify Sub-populations

A natural way to reduce dimension and to extract information from a large and noisy dataset is to group it into more homogeneous clusters. Each of these clusters exhibit more homogeneous characteristics of its individuals than the overall dataset does [16]. Consequently, clustering can be used to exclude groups which could be considered as outliers [8]. In

addition, it emphasizes characteristic patterns in consumption, which may implicitly include the consumption variations due to changes in price.

As it is most likely the case for any real-world experiment, it was observed within the EcoGrid EU demonstration that uncertainty existed in the actual price-responsiveness of heat appliance controllers during DR experiments. This may be due to customers being able to interact with controllers - turning them off or changing comfort settings. Other issues, e.g., bad choice of location for temperature sensors used by controllers, can also result in households not being responsive (or just a little) at certain times. A number of other punctual technical problems can affect the responsiveness of these heat appliance controllers. Therefore, employing clustering for identifying and isolating these outliers can focus our analysis on the DR of well-functioning installations. On a more practical level it generates a list of targets to trouble shoot for the technicians.

Clustering approaches have been extensively described in the literature. The interested reader is for instance referred to [17] for an overview of clustering algorithms and [16] for applications in electric load analysis. Out of this wealth of algorithms, the most suitable one to be used depends upon the data setup and our a priori knowledge of the expected output (e.g., the number of clusters to be obtained) [18]. Hierarchical clustering permits to effectively choose the number of clusters, a posteriori, according to the so-called dendrogram, which is a clustering tree where the level of details (and the number of clusters) is increasing as its branches are further divided. An example dendogram used to cluster an original population of 35 households in one of the EcoGrid EU experiment is shown in Fig. 1. Hierarchical clustering is a non-supervised classification method where individuals are grouped according to their relative distances in a similarity space determined by a set of variables [19]. Hierarchical clustering can be performed in an agglomerative or divisive manner. The former approach starts with each household as a cluster and ends up with one cluster (bottom-up approach), while the latter one sees the whole population as one cluster to start with and eventually ending with each household as a cluster (top-down approach). Their outputs are similar, but Hierarchical Agglomerative Clustering (HAC) is known to be faster to compute.

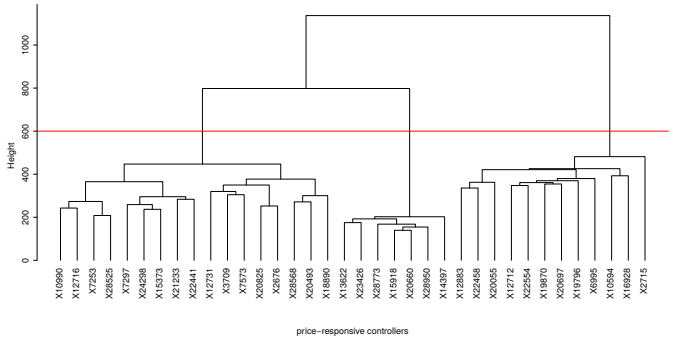

Fig. 1: Dendogram for the clustering of an original population of 35 households in one of the EcoGrid EU experiment. The red line indicates the cut to be made to obtain 3 clusters.

Here our households may naturally have different average consumption levels depending on the house types, number of inhabitants and human behavior. Consequently, some form of alignment is needed to make them all comparable in order to measure some kind of distances between them. However the variance σ_i^2 of the time-series from each household i should not be affected, as the variability in amplitude of the adjustment in consumption during DR events is of high importance. For each and every test case in the experiment, electric power consumption series were centered on their average consumption, by subtracting the mean consumption on a per-household basis, over the entire test case. Considering the original power consumption series $\mathbf{x}'_i = \{x'_{i,1}, \ldots, x'_{i,t}, \ldots, x'_{i,T}\}$ for household i ($i = 1, \ldots, I$), with t the time index, this reads

$$x_{i,t} = x'_{i,t} - \frac{1}{T}\sum_{t=1}^{T} x'_{i,t}, \quad i = 1, \ldots, I, \ t = 1, \ldots, T \qquad (1)$$

$\mathbf{x}_i = \{x_{i,1}, \ldots, x_{i,t}, \ldots, x_{i,T}\}$ is the resulting centered power consumption series for household i, with I the number of households at time t. The series $\mathbf{x}_i$ has the same dynamics and amplitude as $\mathbf{x}'_i$, though centered on 0, thus allowing to better compare the higher-order dynamics of the various households [20], [21].

In our experimental framework, the hypothesis is that if a household is active and receives a price variation during a DR event, the consumption should be affected. The variation in consumption is not expected the same for all houses because of their prior status (e.g. temperature, controller setup), nevertheless it should be possible to cluster similar patterns of consumptions' variation as they are expected to react. In that context, the chosen distance for the clustering approach ought to account for covariances between the consumption series. In our experimental framework, the space we have to explore has the dimension of the number of measurements performed in time. With a temporal resolution of 5 minutes and a test case duration typically of 24 hours, this translates to fairly large dimensions. However, it is expected that power consumption observations are serially correlated, i.e., not independent from one time instant to others. In other words, the effective dimension of the space within which the consumption patterns are observed is clearly less than the number of time steps T. The chosen distance for the clustering approach ought to reflect that aspect. The Mahalanobis distance [22], which fulfills this requirement, is then adopted. For two series $\mathbf{x}_i$ and $\mathbf{x}_j$, it is defined as

$$d(\mathbf{x}_i, \mathbf{x}_j) = (\mathbf{x}_i - \mathbf{x}_j)^\top S_{ij}^{-1} (\mathbf{x}_i - \mathbf{x}_j) \qquad (2)$$

where S_{ij} is the covariance matrix between the two time-series. However, the covariance matrix S_{ij} may happen to be singular when the number of households (I) is smaller or about the same as the number of data points (T) in the time-series [23]. This problem arises often while working with time-series as the number of data points can be extensive compared to the number of households. To prevent such issues with singularity, S_{ij} is replaced in (2) by a shrunk covariance matrix S^*_{ij}. Shrinkage is an efficient way to obtain a non-singular closest estimate of the original covariance matrix S_{ij}. It is calculated as

$$S^*_{ij} = \lambda T_{ij} + (1 - \lambda) S_{ij} \qquad (3)$$

where T_{ij}, commonly referred to as the target, is a diagonal matrix formed with the element on the main diagonal of the original covariance matrix S_{ij} [23]. λ is the shrinkage coefficient. S^*_{ij} is a trade-off between a highly-structured matrix (T_{ij}) and a non-organized one (S_{ij}), while λ allows controlling the balance between the two [24]. We set

$$\lambda = \begin{cases} \lambda^*, & \text{if } \lambda^* \leqslant 1 \\ 1, & \text{otherwise} \end{cases} \tag{4}$$

with

$$\lambda^* = \frac{\sum_{m \neq n} \widehat{\sigma}(c_{mn})}{\sum_{m \neq n} c_{mn}^2} \tag{5}$$

where c_{mn} are the components of the (sample) covariance matrix S_{ij} and $\widehat{\sigma}(c_{mn})$ their estimated variance [25].

HAC is a fairly general framework, given a metric suitable for the data at hand (e.g., the Mahalanobis one used here). Similarly, one may flexibly choose the way to regroup individuals within clusters. The most common one is the Ward's method, also known as minimum-variance method. It aims to minimize the increase of the within-cluster sum of squared distances, E, at each iteration of the agglomerative process [17],

$$E = \sum_{k=1}^{K} \sum_{\mathbf{x}_i \in C_k} d(\mathbf{x}_i, \mathbf{g}_k)^2 \tag{6}$$

where K is the number of clusters, $\mathbf{x}_i \in C_k$ the households in cluster C_k and $\mathbf{g}_k$ the center of gravity of cluster C_k, defined as

$$\mathbf{g}_k = \frac{1}{n_k} \sum_{\mathbf{x}_i \in C_k} \mathbf{x}_i \tag{7}$$

where n_k is the number of households in C_k.

Following [26], the total variance of a set of households, after clustering, can be expressed as the sum of the within-cluster variance plus the between-cluster's center variance. Consequently, since the Ward's method aims at minimizing the increase of within-cluster variance at each iteration, it also maximizes the variance between cluster centers. The resulting clusters can then be seen the most homogeneous possible subgroups from the full population. The HAC algorithm is illustrated in Fig. 2, starting with each household being its own cluster. It then iterates until all households are merged into a single cluster. The result of the HAC is conveniently represented in a dendrogram such as that in Fig. 1. The dendogram is a basis to decide on how many clusters should be chosen. The decision of where to cut the tree depends on the structure of the tree and the goal of clustering. If the goal is to have a clear and precise information on each clusters, a higher number of cluster will be favored. Conversely, if the goal is to isolate outliers, a lower number of clusters will be favored. It is then difficult to implement an automated routine to select the number of clusters.

After computing the HAC, the information contained in the different clusters should be summarized. When it comes to time-series, the clusters' averaged time-series is a suitable way to represent the specificities of each cluster. One of our test cases, with 5 averaged cluster time-series identified from the dendogram, is shown in Fig. 3 together with the averaged time-series of the CBL, as well as the corresponding price signal. Such representation allows clusters with reactive adjustment to the price variations (if compared to CBL) to be sorted apart from those that do not adjust during the DR event or show erratic patterns (e.g., due to technical problems). These are consequently not considered in the subsequent analysis. In the example of Fig. 3, the households from the clusters 2 and 5 are to be excluded from the test group, since cluster 2 follows the CBL while cluster 5 has no daily variations which most likely means that the households are empty. As these outliers are removed, the data quality of the treatment group is improved and eases the subsequent qualitative and quantitative analysis. When mentioning test groups in the remainder of the paper, we refer to those subgroups selected after the clustering was performed.

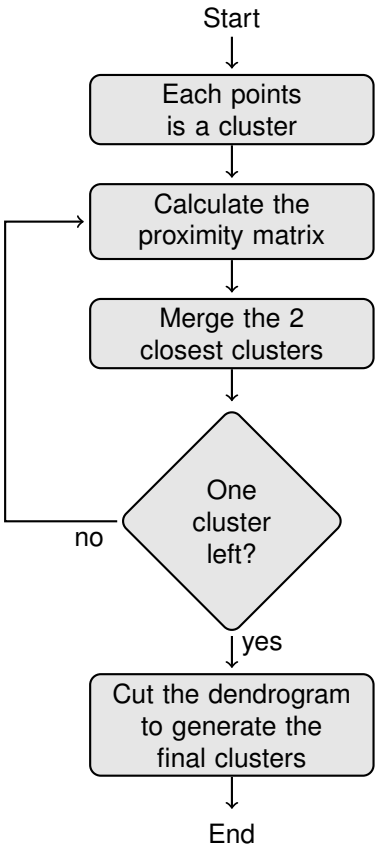

Fig. 2: The Hierarchical Agglomerative Clustering (HAC) algorithm.

B. A Clinical Trial Test Approach

Clinical trials were historically developed in the pharmaceutical industry. Owing to the variety of potential responses of biological organisms as individuals, it became common to perform tests on populations instead, thereby smoothing the potential negative effect of individual features on an overall assessment. In the present case, we can employ a similar clinical trial test approach since our data comes from a reference (CBL) and a test group, while our interest lies in the difference

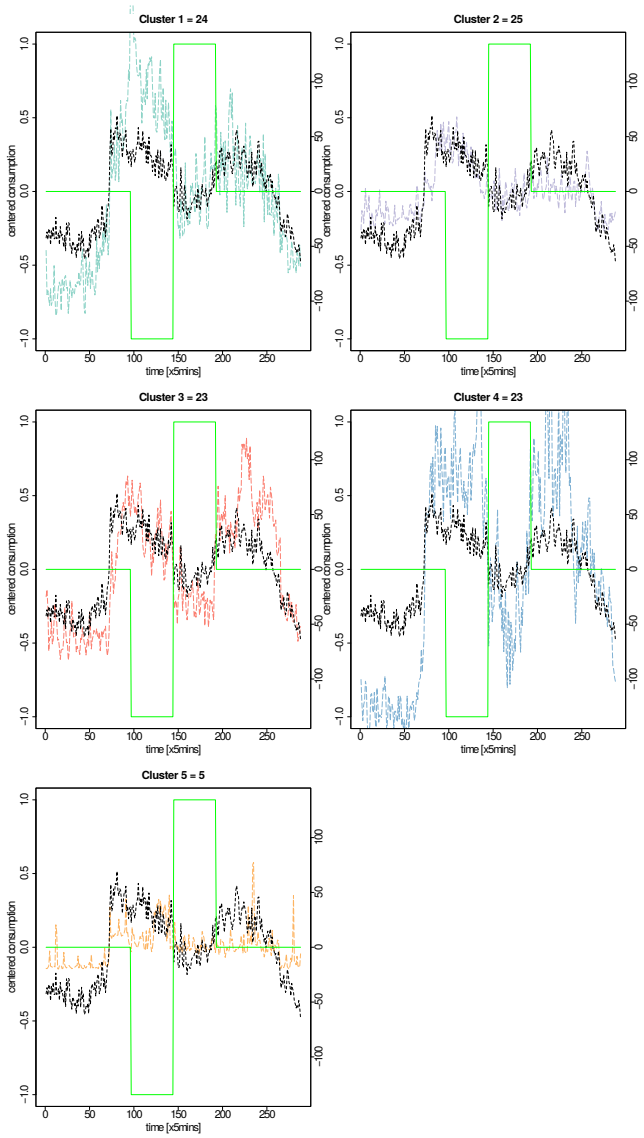

Fig. 3: The averaged time-series is calculated for each cluster in the test group and displayed as a colored dashed line. The black dashed line is the averaged time-series of the CBL and the green line is the price.

in consumption between these two groups. Moreover, the inherent uncertainty on the responsiveness (response to a treatment) resulting from the absence of homogeneity in the test group as well as in the reference group (e.g., behavior of the user, thermal confort setup, energetic profile of the buildings), supports the idea that a clinical trial approach is relevant here. The question we aim to answer can be formulated as *Do price variations induce significant changes in power consumption patterns?*

The results of the clustering on households recruited in the DR program from the different groups exposed in Table II, can be analyzed in two different ways. On the one hand, one can visually assess whether the average response of the selected clusters from each group is responsive by direct comparison with the CBL during the DR event. The purpose of visual inspection is to show that DR works for some clusters, and not for others, to a non-scientific audience who is not familiar with more objective statistical methods. However such an analysis cannot conclude on the significance of the response observed, while relying on expert knowledge at evaluating variation in patterns. On the other hand, this can be tested more rigorously in an hypothesis testing framework (see Section III-C). The purpose of hypothesis testing is to satisfy a scientific audience who requires a degree of objectivity when the results (e.g., lower unit electricity costs for the consumer) are presented.

Fig. 4 is an example of a case used for visual evaluation of a given test case. By observing the dynamics of the mean consumption series of the test group compared to the CBL, one may conclude on the responsiveness of that test group based on confidence intervals. Experience with such consumption data shows that it does not follow a Gaussian distribution. Hence, a nonparametric approach (Non-Studentized pivotal method) is used to obtain confidence intervals. More specifically, we employ a common resampling technique known as bootstrap [20] to generate them. From all the 5000 resampled average time-series, 95% confidence intervals defined by 2.5% and 97.5% quantiles of the distributions of bootstrap samples are obtained.

From visual inspection of Fig. 4, one may infer that the behavior of the test group is different from that of the CBL when the confidence intervals are not overlapping (for example, from 7:05 to 8:05). In other situations, when the confidence intervals overlap or when the average time-series lies within the confidence intervals of another one, one cannot conclude. A more detailed analysis of Fig. 4 shows that the test group exhibits higher consumption during the low price period and lower consumption in the high price period with respect to the CBL. The lower consumption in the period 23:05 to 5:05 is induced by the smart controllers in the experiment shifting load to the lower price period that starts at 07:05. Smart controllers receive a day-ahead price forecast (as well as an hour-ahead price forecast every half hour) allowing them to schedule consumption in an optimal manner. The value of the relative real-time price with respect to recent and limited forecasted prices therefore contributes to visual estimation of whether a test group is price response or not. For example, in Fig. 4, the relative price is high in the period 23:05 to 5:05, so it is expected that a price-responsive cluster would have lower consumption than the CBL during this period.

C. Hypothesis Testing to Assess Price-responsiveness

A standard way to assess results in a clinical trial test is to employ hypothesis testing. The hypothesis obviously depends on the question, e.g., is the test group's consumption different than that of the CBL during a DR event? in this question it can be even be specified lower or higher instead of 'different'. Based on this hypothesis, a test is formulated and applied to the data. The method used to analyze the hypothesis test should be chosen according to the assumptions on the sample values' distribution. The aim of the EcoGrid EU DR program is to displace electric power consumption from periods with higher prices to periods with lower prices. Whether this goal is achieved or not can then be determined based on the economic value to the households, i.e., in relation to cost per unit of

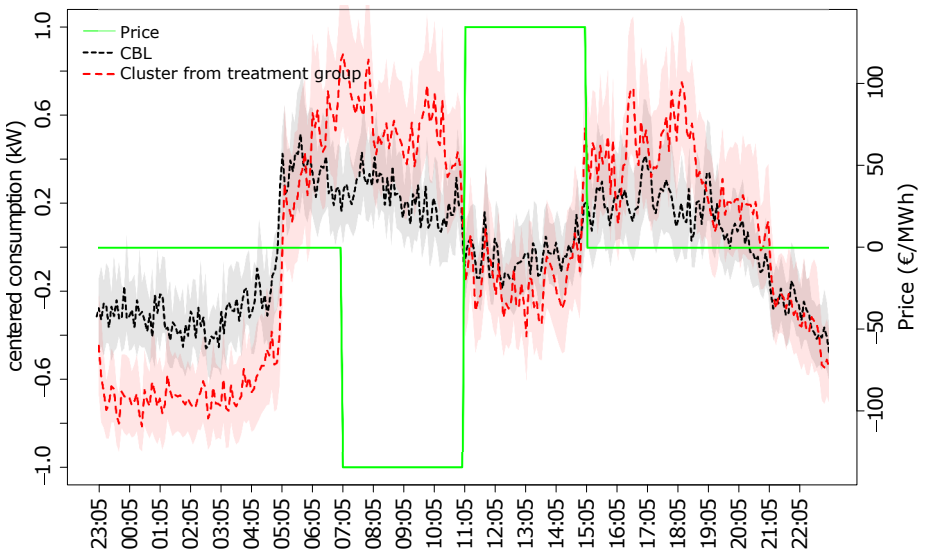

Fig. 4: The average time-series from the CBL and a cluster from the test group with their respective 95% confidence intervals generated from the bootstrap. The green line is the price.

electricity consumed. Consequently here, hypothesis testing may allow us to objectively state whether a test group is price responsive or not. We use a framework similar to that of conventional clinical trial tests, with a type I error threshold α of 0.05.

A hypothesis test can be formulated, since the average cost of a kWh of electricity consumed during a test-case by the test group should be lower than the cost for the CBL during the same period. The average unit cost $\bar{C}_i$, for a test case with T time steps, is calculated as

$$\bar{C}_i = \frac{\sum_{t=1}^{T} C_{ti} P_t}{\sum_{t=1}^{T} C_{ti}} \tag{8}$$

where C_{ti} is the consumption of electricity from household i at time t and P_t the price at time t. A simple observation of the average unit cost distributions tells us that the variances of the 2 samples are different and that they may have heavy tails. Therefore, standard parametric tests are excluded. The Mann-Whitney test (also known as the Wilcoxon rank sum test) is a convenient solution, since the number of households in each of the subgroups is large. A one-sided Mann-Whitney test is performed on the ranks. The hypotheses are the following,

$$\begin{aligned} H_0 &: \mu_{test} \geqslant \mu_{CBL} \\ H_1 &: \mu_{test} < \mu_{CBL} \end{aligned} \tag{9}$$

where μ corresponds to the sum of ranks, H_1 is the one-sided tailed alternative hypothesis and H_0 is the null hypothesis. The null hypothesis means that the activity of the price-responsive controllers is not significantly modifying the average unit cost, so that it could be considered lower than the control group average unit cost. If the H_0 is rejected, the alternative hypothesis is confirmed statistically.

The one-sided tailed alternative hypothesis is more restrictive than the two-sided tailed standard hypothesis test, as it specifies that the samples should not only be different, but that the test sample's mean should be lower than the control sample's mean. The Mann-Whitney test defines the statistic U with the following formula

$$\begin{aligned} U \quad = \quad & \min\Big(n_1 n_2 + \frac{n_1(n_1-1)}{2} - R_1, \\ & n_1 n_2 + \frac{n_2(n_2-1)}{2} - R_2\Big) \end{aligned} \tag{10}$$

where n_1, n_2 are the size of the 2 samples and R_1, R_2 are the sum of the ranks for these two samples respectively. U follows a normal distribution and we can calculate the p-value as

$$P(U \geqslant U_{1-\alpha} | \mu_{test} \geqslant \mu_{CBL}) \tag{11}$$

The P-value can be seen as the probability of obtaining a test statistic result at least as extreme or as close to the one that was actually observed, assuming that the null hypothesis is true. The test is considered significant when the p-value is lower than the type I error threshold α, which is the chance that we mistakenly reject the null hypothesis (that the samples' means are different). All the details related to statistical aspects can be found in [27].

IV. Results

A. Clustering Results

The cluster analysis aims to identify the price-responsive participants in the test group (possibly in the form of various subgroups) and to separate them from obviously non-responsive households. Emphasis is placed here on how many households are kept in the analysis from the original subgroups after computation of the HAC, as it influences the subsequent analysis.

The clusters are visually selected by comparing the averaged consumption time-series of each cluster to the averaged CBL consumption time-series during event with price variations (Fig. 3). If the averaged consumption time-series of a cluster seems to be flat (no activity, e.g., as for cluster 5 in Fig. 3), following the same pattern as the averaged CBL time-series

TABLE II: Number of households in various test cases: number in the test group (number deemed price-responsive after clustering) / number in the CBL.

Date	Manufacturer 1 Electric Heating	Manufacturer 1 Heat Pump	Manufacturer 2 Electric Heating
25/10/2013	68 (48) / 288	36 (24) / 197	88 (55) / 82
07/11/2013	65 (58) / 289	36 (33) / 197	88 (61) / 92
21/11/2013	67 (61) / 292	36 (36) / 200	87 (75) / 94
27/11/2013	66 (55) / 292	36 (34) / 201	89 (78) / 91
06/12/2013	—	—	115 (74) / 99
10/12/2013	—	—	103 (84) / 91
11/12/2013	—	—	100 (70) / 86
12/12/2013	—	—	106 (69) / 89
20/01/2014	—	—	230 (194) / 105
21/01/2014	—	—	223 (121) / 100
22/01/2014	—	—	230 (110) / 104
23/01/2014	—	—	229 (107) / 105
08/03/2014	30 (30) / 324	20 (17) / 236	237 (125) / 75
11/03/2014	38 (38) / 317	24 (18) / 229	232 (171) / 76
09/04/2014	101 (99) / 249	58 (43) / 188	249 (197) / 109
13/04/2014	38 (38) / 311	24 (22) / 222	269 (188) / 114

(e.g., as for cluster 2 in Fig. 3) or showing unexpected pattern, it will be excluded from the dataset used in the evaluation of the price responsiveness. When all the clusters are non price-responsive, only the aberrant ones will be removed.

Table II gives a summary of the clustering selection; the range of the selection from the original data goes from 52% to 100%. In other words, a maximum of a half (48%) of the smart controllers were in the test group, but did not visually appear to be price-responsive. The graphical representation of clusters is also useful for identifying different types of price-responsive behavior. For example, in Fig. 3, cluster 1 gathers the controllers which have been stimulated by the first price variation, while cluster 3 gathers the ones which have been stimulated by the second price variation and cluster 4 gathers the ones which have reacted to both stimuli. It also illustrate the differences of behavior between the manufacturers as the price-response strategies and constraints are implemented differently. Such information was not known beforehand, and brought more insight on how a population of controllers behave at the occasion of large price variations. However, this paper do not focus on this aspect, but it worth mentioning it as it is a good way to illustrate it.

B. Results of the Clinical Trial Test Approach

The chosen clusters are used to generate graphical overviews of each group during the different test-cases (Fig. 4). Table III summarizes the visual evaluation of the graphs displaying the averaged time-series associated with the 95% confidence intervals of the treatment and CBL groups for each manufacturer, equipment type and for different test-days. Results here should be interpreted as, for each experiment, whether it was possible to find one or more clusters that could be seen as price responsive, or not.

In the roll-out phase of the EcoGrid EU demonstration, controllers and other infrastructures were continually developed and improved, which explains the improvement of the DR as the heating period went on.

C. Results of the Hypothesis Testing

The main goal of the EcoGrid EU project is to push electricity consumption during periods of high prices to periods of low electricity prices. This means an economic evaluation can be done, by comparing the average unit cost of selected test groups to the CBL. In this case, hypothesis testing could be applied to each and every identified clusters, or only to those where visual assessment indicated that price response may be present. As for the visual assessment before, the test is applied to all clusters that were not discarded through the clustering analysis, for instance since deemed as outliers or clearly non-responsive.

TABLE III: The color of the cell return the results of the visual evaluation; gray is responsive, light gray is non-responsive. The figure is the p-value from the Mann-Whitney test. Significant test at $\alpha = 5\%$ are shown in bold and italic.

Date	Manufacturer 1 Electric Heating	Manufacturer 1 Heat Pump	Manufacturer 2 Electric Heating
25/10/2013	0.98	0.44	0.20
07/11/2013	0.39	***0.0013***	0.88
21/11/2013	0.95	0.20	0.09
27/11/2013	0.34	0.34	0.81
06/12/2013	—	—	0.13
10/12/2013	—	—	***0.00022***
11/12/2013	—	—	***0.0015***
12/12/2013	—	—	0.12
20/01/2014	—	—	0.99
21/01/2014	—	—	0.22
22/01/2014	—	—	0.21
23/01/2014	—	—	0.63
08/03/2014	0.54	0.59	***0.0068***
11/03/2014	0.86	0.80	0.28
09/04/2014	***0.0034***	***0.0096***	0.21
13/04/2014	0.96	0.12	***0.0014***

The Table III shows the Mann-Whitney test's results for the different test periods. A standard type I error threshold is chosen ($\alpha = 5\%$). The significant tests are shown in bold and italic. The comparison between the results from visual evaluation and the hypothesis testing in Table III exposes the difference between price-responsiveness which can be visually noticed but not statistically validated using the measure of unit cost, and the price-responsiveness that does have a significant economical impact on the average unit cost. The results show that towards the end of the roll-out of the EcoGrid EU project, it was possible to visually and rigorously find differences between CBL and test groups (manufacturer 1 electric heating, manufacturer 1 heat pump and manufacturer 2 electric heating), indicating a price-responsive behavior overall. Further steps in such an evaluation work would consist in quantifying and characterizing this price-responsiveness, while also assessing if this corresponds to the maximum response that could be provided by these groups of households.

V. Conclusions

The method presented in this paper shows how a systematic evaluation of DR can be done even with datasets that contain outliers, noise, and other undesirable effects. The clustering

can easily be generalized to other time series classification, although scalability to data with more observations remains an area for inquiry. We have successfully applied it to 2 weeks data with a resolution of 5 minutes, but further work should investigate clustering of time-series with more observations. Clustering based on the coefficients of an auto-regressive model of each subject may be viable.

The methodology established provides a springboard to further understand the different types of DR present in residential loads. User interaction with DER controllers is expected to have a large impact on the DR available, and the HAC used to separate useful households from those which do not appear extremely effective in this circumstance.

From a widespread power system perspective, being able to identify which customer segments exhibit a price response is important for grid operators looking to identify and invest in customers to participate in new DR schemes. Such clustering may also be a useful technique to decide additional financial reward for customers who perform best, in the form of a capacity payment, perhaps funded by the same public service obligations (PSOs) that support renewable generation.

Comparing treatment subgroups to the CBL graphically is also useful for presenting the differences in consumption to a broad audience in an intuitive manner. However, visual interpretation is not a statistically valid way of confirming a response. Therefore, the 2 sample Mann-Whitney test comparing the averaged unit cost of price-responsive and non price-responsive subgroups supplements the graphical approach well, as it allows us to validate or reject hypothesis for each test-case. This analysis answers one of the key points of the demonstration: cost can be reduced for some consumers. Obviously, a necessary further step is to characterize and quantify the responsiveness of this electric load. This has been the focus of our further research over a 8 month live experiment in the EcoGrid EU project, which kicked off after the first assessment results presented here allowed to verify the demand response potential in our electric load population.

ACKNOWLEDGEMENT

The authors would like to thank all their partners in the EcoGrid EU project for their contribution to the methodological and experimental work. Special thanks go to Maja Felicia Bendtsen (Østkraft A/S) and her team for their hard work on the field, Dieter Gantenbein and his colleagues at IBM and Martin Bo Sjøberg and Andreas Arendt at Siemens for providing equipment and expertise, and finally Niels Ejnar Helstrup Jensen, Stig Holm Sørensen and Niels Per Lund from Energinet.dk for help with the data and constant feedback on this work.

REFERENCES

[1] "European Council Conclusions on 2030 Climate and Energy Policy Framework," European Council, Tech. Rep. October, 2014.

[2] N. O'Connell, P. Pinson, H. Madsen, and M. O'Malley, "Benefits and challenges of electric demand response: A critical review," *Renewable & Sustainable Energy Reviews*, vol. 39, pp. 686–699, 2014.

[3] G. Strbac, "Demand side management: Benefits and challenges," *Energy Policy*, vol. 36, no. 12, pp. 4419–4426, dec 2008.

[4] J. Torriti, M. G. Hassan, and M. Leach, "Demand response experience in Europe: Policies, programmes and implementation," *Energy*, vol. 35, no. 4, pp. 1575–1583, Apr. 2010.

[5] J. L. Mathieu, D. S. Callaway, and S. Kiliccote, "Examining uncertainty in demand response baseline models and variability in automated responses to dynamic pricing," in *IEEE Conference on Decision and Control and European Control Conference*. IEEE, Dec. 2011, pp. 4332–4339.

[6] O. Corradi, H. Ochsenfeld, H. Madsen, and P. Pinson, "Controlling Electricity Consumption by Forecasting its Response to Varying Prices," *IEEE Transactions on Power Systems*, vol. 28, no. 1, pp. 421–429, 2012.

[7] S. B. Harvey, "The Harvard Medical School Guide to Men's Health," *Publishers Weekly*, vol. 249, no. 31, 2002.

[8] P. Bartholomew, W. Callender, C. Hindes, C. Grimm, K. Johnson, M. Straub, D. Williams, M. Williamson, D. Hayes, W. Johnson, B. Nix, J. Lynch, and S. Romer, "Demand response measurement & verification," AEIC website, 2009. [Online]. Available: http://aeic.org/wp-content/uploads/2013/07/AEIC-MV-Whitepaper-Rev-051613.pdf

[9] J. Kwac, J. Flora, and R. Rajagopal, "Household energy consumption segmentation using hourly data," *Smart Grid, IEEE Transactions on*, vol. 5, no. 1, pp. 420–430, 2014.

[10] S. Haben, C. Singleton, and P. Grindrod, "Analysis and clustering of residential customers energy behavioral demand using smart meter data," *Smart Grid, IEEE Transactions on*, vol. in press, 2015.

[11] M. Chaouch, "Clustering-based improvement of nonparametric functional time series forecasting: Application to intra-day household-level load curves," *Smart Grid, IEEE Transactions on*, vol. 5, no. 1, pp. 411–419, 2014.

[12] F. Quilumba, W.-J. Lee, H. Huang, D. Wang, and R. Szabados, "Using smart meter data to improve the accuracy of intraday load forecasting considering customer behavior similarities," *Smart Grid, IEEE Transactions on*, vol. 6, no. 2, pp. 911–918, March 2015.

[13] "EcoGrid EU Website." [Online]. Available: www.eu-ecogrid.net

[14] Y. Ding, S. Pineda, P. Nyeng, J. Østergaard, E. M. Larsen, and Q. Wu, "Real-Time Market Concept Architecture for EcoGrid EU - A Prototype for European Smart Grids," *IEEE Transactions on Smart Grid*, vol. 4, no. 4, pp. 2006–2016, 2013.

[15] N. E. Helstrup, P. Lund, M. F. Bendtsen, D. Gantenbein, and A. Arendt, "Deliverable 6.3 - System operation and monitoring: Large-scale smart grids demonstration of real time market-based integration of DER and DR," EcoGrid EU Internal Report, Tech. Rep., 2013.

[16] G. Chicco, R. Napoli, and F. Piglione, "Comparisons among clustering techniques for electricity customer classification," *IEEE Transactions on Power Systems*, vol. 21, pp. 933–940, 2006.

[17] R. Xu and D. C. Wunsch II, *Clustering*. Wiley-IEEE Press, 2008, no. August.

[18] L. Kaufman and P. Rousseeuw, "Finding groups in data: an introduction to cluster analysis," *Journal of the American Statistical Association*, vol. 86, no. 415, pp. 830–832, 1991.

[19] M. Zepeda-Mendoza and O. Resendis-Antonio, "Hierarchical Agglomerative Clustering," in *Encyclopedia of Systems Biology SE - 1371*, W. Dubitzky, O. Wolkenhauer, K.-H. Cho, and H. Yokota, Eds. Singer New York, 2013, pp. 886–887.

[20] B. Efron, "Bootstrap Methods for Standard Errors, Confidence Intervals, and Other Measures of Statistical Accuracy," *Statistical Science*, vol. 1, no. 1, pp. 54–75, 1986.

[21] R. Yaffee, "Introduction to time series analysis and forecasting with applications of SAS and SPSS," *International Journal of Forecasting*, vol. 17, no. 2, pp. 301–302, 2001.

[22] P. Mahalanobis, "On the generalized distance in statistics," *Proceedings of the National Institute of Sciences*, pp. 49–55, 1936.

[23] Z. Prekopcsák and D. Lemire, "Time series classification by class-specific Mahalanobis distance measures," *Advances in Data Analysis and Classification*, vol. 6, no. 3, pp. 185–200, jul 2012.

[24] O. Ledoit and M. Wolf, "Honey, I Shrunk the Sample Covariance Matrix," pp. 110–119, 2004.

[25] J. Schaefer and K. Strimmer, "A shrinkage approach to large-scale covariance matrix estimation and implications for functional genomics," *Statistical Applications In Genetics and Molecular Biology*, vol. 4, no. 1, 2005.

[26] J. P. Benzécri, *Analyse des données, Tome 1, La Taxinomie*, 1st ed. Dunod, 1976, [in french].

[27] R. R. Wilcox, *Applying contemporary statistical techniques*. Gulf Professional Publishing, 2003.

PAPER C

Demonstration of market-based real-time electricity pricing on a congested feeder

This paper was presented at the 12th International Conference on the European Energy Market.

Demonstration of Market-Based Real-Time Electricity Pricing on a Congested Feeder

Emil Mahler Larsen
Pierre Pinson
Guillaume Le Ray
Department of Electrical Engineering
Technical University of Denmark
Kongens Lyngby
Email: {emlar,ppin,gleray}@elektro.dtu.dk

Georgios Giannopoulos
Elia
Brussels, Belgium
Email: georgios.giannopoulos@elia.be

***Abstract*—Congestion management can delay grid reinforcements needed due to the growth of distributed technologies like photovoltaics and electric vehicles. This paper presents a method of congestion management for low voltage feeders using indirect control from the smart grid demonstration EcoGrid EU, where five minute electricity pricing is sent to demand. A method for forecasting demand and generating prices in a market framework is presented, and a novel mechanism to ensure prices are fair to customers who can and cannot participate is developed. The proposed market is currently being used to send prices to 1900 houses, with a virtual feeder of 28 houses receiving congestion pricing. Simulations are used to calculate the cost from using this congestion management method, while demonstration results indicate that congestion can be managed successfully.**

***Index Terms*—Demand response, real-time pricing, congestion management, demand forecasting, smart grid.**

NOMENCLATURE

$t \in T$	Index for time
$g \in G$	Index for conventional generation
$l \in L$	Index for demand
$s \in S$	Index for scenario
$q_{t,s}$	Probability of scenario
$c_{l,t,s}$	Demand
$c^{\mathrm{D}}_{l,t}$	Day-ahead demand forecast
$c^{\mathrm{shed}}_{l,t,s}$	Load shedding
λ^{D}_{t}	Day-ahead price for demand
$\lambda^{\mathrm{R}}_{t,l}$	Real-time price for demand
λ^{shed}	Price for load shedding
λ^{spil}	Price for wind spillage
$\alpha_{t,s}$	Price-elasticity parameter
$B_{t,s}$	System imbalance
$p^{\mathrm{D}}_{g,t}$	Conventional generation scheduled day-ahead
w^{D}_{t}	Wind power day-ahead forecast
$w^{\mathrm{spill}}_{t,s}$	Wind power spillage
$\lambda^{\uparrow}_{g,t}, \lambda^{\downarrow}_{g,t}$	Price for up/down regulation
$p^{\uparrow}_{g,t,s}, p^{\downarrow}_{g,t,s}$	Up/down regulation delivered
$P^{\uparrow}_{g,t}, P^{\downarrow}_{g,t}$	Up/down regulation bid into market
$r_{g,t}$	Generator ramp rate
$x_{g,t,s}, z_{g,t,s}$	Up/down regulation on/off
γ_t	Generation behavior

I. INTRODUCTION

Electric vehicles (EVs), photovoltaics (PVs) and other new distributed energy resources (DERs) will significantly increase the strain on low voltage feeders and potentially raise the peak load, causing over-loading and a need for greater capacity. Demand response (DR) is widely accepted as the key to reducing congestion at a distribution level and postponing costly investment in new infrastructure such as transformers and cables. Such DR can be activated by indirect control, e.g. an electricity price, or direct control, e.g. an on-off signal through a bilateral contract. There are benefits to both [1], with the former requiring less stringent communication requirements and the latter offering a more reliable response.

Congestion has been thoroughly investigated at medium and high voltage levels [2], [3], while the focus of smart charging EVs has been at low voltage levels [4]. Mechanisms for managing congestion include using distributed controllers in transformer stations that send a control signal onwards to demand [5]. Controlling household devices, such as heat-pumps, with direct [6] and indirect [7] control methods have also been proposed for solving local congestion. Control-by-price techniques have also been developed in [8] and [9], however a limitation of these works is that the price-response is unbounded.

In this paper, we perform congestion management with DR using a centralised market developed and tested in the EcoGrid EU project. EcoGrid EU is smart grid demonstration on the Danish island of Bornholm, where 1900 residential houses with a peak load of 5MW receive electricity prices every five minutes. 28 of these houses constitute our virtual feeder, which means they are not physically connected to the same cable, but their load is aggregated virtually. Houses are equipped with smart meters and a range of DERs with automated controllers that optimize consumption levels according to price forecasts and customer comfort. DR from these households is used to reduce congestion on a local level, and imbalances on a system level. The demonstration setup is shown in Fig. 1.

The EcoGrid EU market sees demand as a black box since the price-responsive controllers used in the demonstration

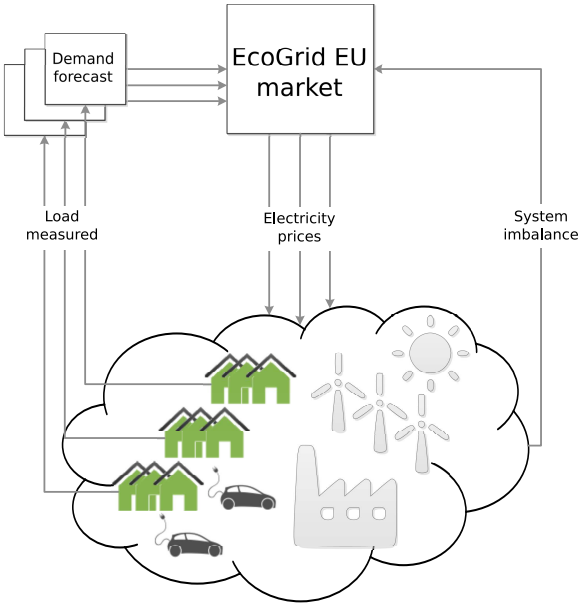

Fig. 1. Demonstration setup, with loads receiving different pricing based upon their feeder limitations, and feedback used to update the demand forecast

have proprietary designs from different manufacturers, which control a wide array of DERs. A data-driven forecasting method with novel bounded price-elasticity terms has been developed. This paper also investigates the question of how to reward customers fairly for providing DR, should policy makers legislate feeder-level congestion management. Paying a customer for shifting their consumption away from peak hours is potentially unfair when a customer on a different feeder is not offered that option. And if a majority of customers participate, then those who cannot may effectively pay a higher price than those who can participate at the feeder level. From the Distribution System Operator (DSO) perspective, knowing the value of congestion management in a market setting is also an area for inquiry when deciding if reinforcements should be chosen over DR programs.

In summary, our contribution lies in using a realistic model of demand with a method that is being validated in real-life, quantitative figures for the cost of congestion management via indirect control, and a market-based approach that makes efficient use of DR and is fair to customers who can and cannot participate in congestion management. The paper is structured with section two introducing the demand and market models used for simulation and in the experiment. Section three shows initial demonstration results taken from a virtual feeder and simulated costs with and without congestion management. Section four concludes.

II. Methodology

A. Model of the Demand

Demand is broken down into non-interacting parts comprised of autoregressive components that are a function of recent demand, a component that is dependent on the price, and a component that is only dependent on external variables using the notation from [8], [9]. An initial abstract split of the price and non-price responsive parts is considered

$$c_t = f\left(\tilde{c}_{t-1}, \tilde{z}_t\right) + g\left(\tilde{\lambda}_t, \tilde{z}_t\right) \tag{1}$$

with

$$\begin{aligned} \tilde{c}_{t-1} &= [c_{t-1}, \ldots, c_{t-n_c}]^\intercal \\ \tilde{\lambda}_t &= [\lambda_{t+u_\lambda}, \ldots, \lambda_{t-n_\lambda}]^\intercal \\ \tilde{z}_t &= [z_{t+u_z}, \ldots, z_{t-n_z}]^\intercal \end{aligned}$$

where n_c, n_λ and n_z are a finite number of lagged values of demand, c, price, λ , and external variables, z. For the price and external variables there are u_λ and u_z forecast values, which are used to capture the scheduling dynamics of DERs.

Price forecasts are converted to relative prices each time a new price forecast is made. When considering only the known future values, $1..u_z$ in the vector $\tilde{\lambda}_t$, the relative day-ahead price is first adjusted for the mean, $\bar{\lambda}_t$, and then normalised to a value between 0 and 1

$$\tilde{\lambda}_t^{\mathrm{D_r}} = \tilde{\lambda}_t^{\mathrm{D}} - \bar{\lambda}_t \tag{2}$$

$$\tilde{\lambda}_t^{\mathrm{D_n}} = \frac{\tilde{\lambda}_t^{\mathrm{D_r}} - \tilde{\lambda}_{t,min}^{\mathrm{D_r}}}{\tilde{\lambda}_{t,max}^{\mathrm{D_r}} - \tilde{\lambda}_{t,min}^{\mathrm{D_r}}} \tag{3}$$

Real-time prices are also converted to relative prices, but with respect to the absolute day-ahead price, i.e. $\tilde{\lambda}_t^r = \tilde{\lambda}_t - \tilde{\lambda}_t^{\mathrm{D}}$.

External variables, z, include weather data wind speed, solar irradiance, ambient temperature, Φ, as well as a base load term, y_t. The base load is a Fourier series that describes demand due to the time of day, day of the week, and day of the month [10]. The base load is given by

$$y_t = a_0 + \sum_{j=1}^{J} a_j \sin\left(\frac{2\pi k t}{j}\right) + b_j \cos\left(\frac{2\pi k t}{j}\right) \tag{4}$$

j must be suitably large to cover different seasonal variations (for example 288 when capturing trends of different hours of the day using five minute data) and k is increased until enough high-resolution detail is captured.

Additional terms are added to capture the interaction between the base load and temperature, $y_t \cdot \Phi_t$, and the price and temperature, $\tilde{\lambda}_t \cdot \Phi_t$, included in the array of variables $\tilde{\chi}_t$. This can be expressed in a general linear model form

$$c_t = \tilde{c}_{t-1}^\intercal \theta_c + \tilde{\lambda}_t^\intercal \theta_\lambda + \tilde{z}_t^\intercal \theta_z + \tilde{\chi}_t^\intercal \theta_\chi + \epsilon_t = x_t^\intercal \boldsymbol{\theta} + \epsilon_t \tag{5}$$

where ϵ_t is Gaussian noise with zero mean and finite variance and all prices are relative.

Variables c, λ, z and χ were populated with measurements from 2014 and the parameters $\boldsymbol{\theta}$ of the general linear model were found by minimizing the residual sum of squares while shrinking parameters using the Lasso penalisation [11], the objective of which is

$$\min \sum_{t=1}^{T} \left(c_t - \sum_{n=1}^{N} \theta_n x_{n,t}\right)^2 + \eta \sum_{n=1}^{N} |\theta_n| \tag{6}$$

η is the tuning parameter and is found using a 10-fold cross-validation routine, minimising the mean square error over all folds. The relationship between price and consumption has previously been observed to be non-linear [8], and this characteristic is taken advantage of to find some sensible boundaries for the price-response. A non-linear model containing a generalised logistic function that is centred around zero is defined

$$c_t^{\lambda} = \sum_{n=1}^{N_\lambda} -\frac{A_n}{2} + \frac{A_n}{1+e^{-\tau_n \lambda_n}} - \frac{B_n \Phi_t}{2} + \frac{B_n \Phi_t}{1+e^{-\rho_n \Phi_t \lambda_n}} \tag{7}$$

c_t^{λ} contains only price information with other linear components removed. Parameters in this model are found by minimising the sum of square errors using the Levenberg-Marquardt algorithm [12] with the linear parameters for price used as starting estimates for τ and ρ. The upper and lower bounds of the price response are

$$\Delta c_t^{\max\,/\,\min} = \pm \sum_{n}^{N_\lambda} \left(\frac{|A_n| + |B_n \Phi_t|}{2} \right) \tag{8}$$

To find the expected price-elasticity of the demand, the logistic function (7) is differentiated with respect to price for each price lag. The reciprocal of this result is taken and the mean of over all price lags is taken, i.e.

$$\alpha_t = \frac{1}{N_\lambda} \sum_{n}^{N_\lambda} \left(\frac{4}{A_n B_n + C_n D_n \Phi_t} \right) \tag{9}$$

Price elasticity and its bounds are found for different times of the day, as control algorithms have been observed to behave very differently - especially at night. The final demand model has been used to forecast consumption in real-time in the EcoGrid demonstration, with an online five-minute ahead mean absolute percentage error (MAPE) of 2% and a day-ahead MAPE of 7% for 1900 houses.

B. Market Structure

The EcoGrid EU demonstration uses a hardware in-the-loop process to generate prices. Generator bids are based on historical Nord Pool bid data, while demand and wind power injection data come from real-time forecasts from the Bornholm electricity network. The imbalance signal is derived from the day-ahead forecast error. Load is scaled to 50MW to represent the entire island of Bornholm. The day-ahead market is assumed to operate in a similar, deterministic manner, as today.

The objective of the market is to maximise social welfare (customer utility minus the cost of generation) while determining an optimal amount of balancing power from generation and DR. The output commits bids for conventional generation until the market is performed again, and creates real-time prices for demand. The imbalance caused by wind power production and demand must be remedied and maximum and minimum feeder limits must be respected. Whenever a DSO would like to reduce a load in their network, feeder limits are specified. In this study, a baseline market without congestion management is operated in parallel, and the difference in social welfare is the cost the DSO pays for reducing congestion with DR. Electricity network dynamics are ignored in this paper, as they are in the Nord Pool market, although the unit commitment models can be expanded to consider losses as in [13].

$$\max \sum_t \sum_s q_{t,s} \Bigg\{ \sum_l \lambda_t^{\mathrm{D}} \Delta c_{l,t,s} + \frac{1}{2} \alpha_{t,s} {\Delta c_{l,t,s}}^2 - \sum_g \beta_{g,t,s} - \lambda^{\mathrm{spil}} w_{t,s}^{\mathrm{spil}} - \sum_l \lambda^{\mathrm{shed}} c_{l,t,s}^{\mathrm{shed}} \Bigg\} \tag{10}$$

s.t.

$$\beta_{g,t,s} = \lambda_{g,t}^{\uparrow} p_{g,t,s}^{\uparrow} - \lambda_{g,t}^{\downarrow} p_{g,t,s}^{\downarrow} \qquad \forall g,t,s \tag{11}$$

$$p_{g,t,s} = \sum_g p_{g,t}^{\mathrm{D}} + p_{g,t,s}^{\uparrow} - p_{g,t,s}^{\downarrow} \qquad \forall g,t,s \tag{12}$$

$$c_{l,t,s} = c_{l,t}^{\mathrm{D}} - c_{l,t,s}^{\mathrm{shed}} + \Delta c_{l,t,s} \qquad \forall t,s \tag{13}$$

$$w_{t,s} = w_t^{\mathrm{D}} - w_{t,s}^{\mathrm{spill}} \qquad \forall t,s \tag{14}$$

$$\sum_l c_{l,t,s} = p_{g,t,s} + w_{t,s} - B_{t,s} \qquad \forall t,s \tag{15}$$

$$\Delta p_{g,t,s}^{\uparrow} = p_{g,t,s}^{\uparrow} - p_{g,t-1,s}^{\uparrow} \qquad \forall g,t,s \tag{16}$$

$$\Delta p_{g,t,s}^{\downarrow} = p_{g,t,s}^{\downarrow} - p_{g,t-1,s}^{\downarrow} \qquad \forall g,t,s \tag{17}$$

$$\Delta p_{g,t,s}^{\uparrow} = \Delta p_{g,t-1,s}^{\uparrow} \qquad \forall g,t,s,\gamma_t = 0 \tag{18}$$

$$\Delta p_{g,t,s}^{\downarrow} = \Delta p_{g,t-1,s}^{\downarrow} \qquad \forall g,t,s,\gamma_t = 0 \tag{19}$$

$$\Delta p_{g,t,s}^{\uparrow} = 0 \qquad \forall g,t,s,\gamma_t = 2 \tag{20}$$

$$\Delta p_{g,t,s}^{\downarrow} = 0 \qquad \forall g,t,s,\gamma_t = 2 \tag{21}$$

$$p_{g,t,s}^{\uparrow} \le x_{g,t,s} p_{g,t,s}^{\uparrow} \qquad \forall g,t,s \tag{22}$$

$$p_{g,t,s}^{\downarrow} \le z_{g,t,s} p_{g,t,s}^{\downarrow} \qquad \forall g,t,s \tag{23}$$

$$p_{g,t,s}^{\uparrow} \ge x_{g,t,s} \chi_g p_{g,t,s}^{\uparrow} \qquad \forall g,t,s,\gamma_t = 2 \tag{24}$$

$$p_{g,t,s}^{\downarrow} \ge z_{g,t,s} \chi_g p_{g,t,s}^{\downarrow} \qquad \forall g,t,s,\gamma_t = 2 \tag{25}$$

$$x_{g,t,s} = 0 \qquad \forall t,s,P_{g,t}^{\uparrow} = 0 \tag{26}$$

$$z_{g,t,s} = 0 \qquad \forall t,s,P_{g,t}^{\downarrow} = 0 \tag{27}$$

$$p_{g,t,s}^{\uparrow} \le d_{t,s} p_{g,t,s}^{\uparrow} \qquad \forall g,t,s \tag{28}$$

$$p_{g,t,s}^{\downarrow} \le \kappa_{t,s} p_{g,t,s}^{\downarrow} \qquad \forall g,t,s \tag{29}$$

$$d_{t,s} + \kappa_{t,s} \le 1 \qquad \forall g,t,s,\gamma_t = 2 \tag{30}$$

$$\Delta c_{l,t,s} \le \Delta c_{l,t}^{\max} \qquad \forall t,s \tag{31}$$

$$\Delta c_{l,t,s} \ge \Delta c_{l,t}^{\min} \qquad \forall t,s \tag{32}$$

$$\sum_t \Delta c_{l,t,s} + \sum_i \Delta c_{l,i} = 0 \qquad \forall l,s \tag{33}$$

$$c_{l,t}^{\min} \le c_{l,t,s} \le c_{l,t}^{\max} \qquad \forall t,s \tag{34}$$

For each decision variable in constraints (11) - (34) there exists a non-anticipativity constraint that ensures its outcome is identical across all scenarios in the first few time periods for which prices are fixed, for example $t = 1 \ldots 6$ if the market is run every half an hour. In later time periods, scenarios for

price-elasticity, α, follow a Gaussian distribution. Imbalance scenarios, B, are generated using a non-parametric method (bootstrapping), where historical outcomes are sampled with replacement. Reduction of scenario trees is then done using the Fast Forward method [14].

The regulating cost from conventional generation is defined in (11). The total power produced by each unit is stated in (12). The total demand and production from wind are defined in (13) and (14). Equation (15) is the balance constraint, also considering the imbalance from wind and inflexible demand, $B_{t,s}$. In the absence of any further constraints, and considering zero flexibility, the dual variable of (15) is the price sent to generation and demand. With these constraints and considering that the problem is quadratically constrained, the real-time price is

$$\lambda_{l,t,s} = \alpha_{t,s}\Delta c_{l,t} + \lambda^{\mathrm{D}}_{l,t} \tag{35}$$

Constraints (16) and (17) define generator ramp rates. Constraints (18) and (19) keep ramping constant when generation behavior dictates. Constraints (20) and (21) keep generation at a plateau when generation behaviour dictates. When used with the generator behavior of the Scandinavian regulating market, γ_t, constraints (16)-(21) result in a minimum on-time of 45 minutes and the ramping characteristics seen in Fig. 2. Constraints (22) and (23) limit maximum regulation. Constraints (24) and (25) limit minimum generation. In the Scandinavian regulating market, bids under 10MW must be activated in full, while bids above 10MW can be activated in part; the proportion of each bid to be activated is described by the parameter χ_g. Constraints (26) and (27) ensure that a generator is off when it bids zero into the market. Constraints (28) and (29) determine whether any up or down generation is active, and (30) prevents simultaneous up and down regulation. Constraints (31) and (32) enforce the price-elasticity limits. The fairness constraint is defined in (33), which ensures all loads have the same load shifting scheduled, considering all historical DR scheduled, $\Delta c_{l,i}$, and future DR, $\Delta c_{l,t}$. This constraint is only fair if loads are homogeneous, as they are in the EcoGrid EU project, and aims to send near-identical average prices to different loads every day. Constraints (34) specify the maximum and minimum feeder limits, which usually occur in the winter and summer respectively. EcoGrid EU participants exhibit the vast majority of their flexibility in the winter and, as such, this case study only considers the maximum feeder limit, which is set to the 5% below the unconstrained maximum daily peak load.

EcoGrid EU market clearing code in the GAMS language and without proprietary datasets is available in [15]. The main EcoGrid EU market is a mixed integer quadratically constrained program (MIQCP) solved using the CPLEX solver.

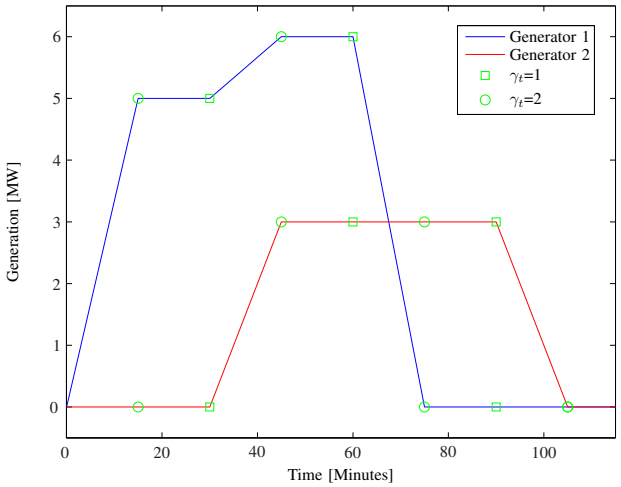

Fig. 2. Example of two generators acting within behaviour constraints

III. Results

A. Demonstration outcome

Preliminary demonstration results show that the system is broadly capable of keeping consumption under the feeder limit, as shown in Fig. 3. However, short-lived spikes in consumption do occur, which the forecasting tool is unable to predict, although overloading for a few minutes is unlikely to be problematic. This problem is exacerbated by the 20 minute delay in smart meter data being collected. In a full-scale roll-out, real time measurements (<5 minutes) would be needed at the congestion point in order to better avoid congestion. Additional problems with this test are that the load appears to exhibit some oscillating behaviour. Poor forecasting of the virtual feeder and not explicitly accounting for cross elasticity in the market are thought to be the main causes.

B. Simulated benefits

Simulations were done for one month to determine the scalability of the system and the costs associated with widespread congestion management. Fig. 4 shows an example day for a feeder with and without congestion management. Market

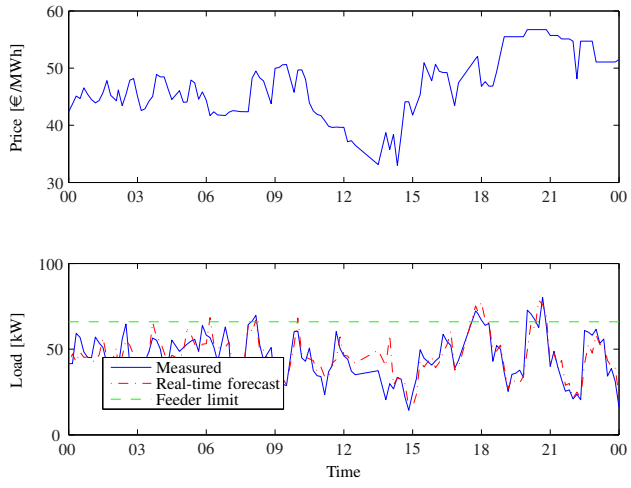

Fig. 3. Demonstration results from 28th March 2015 on the island of Bornholm for 28 houses performing congestion management

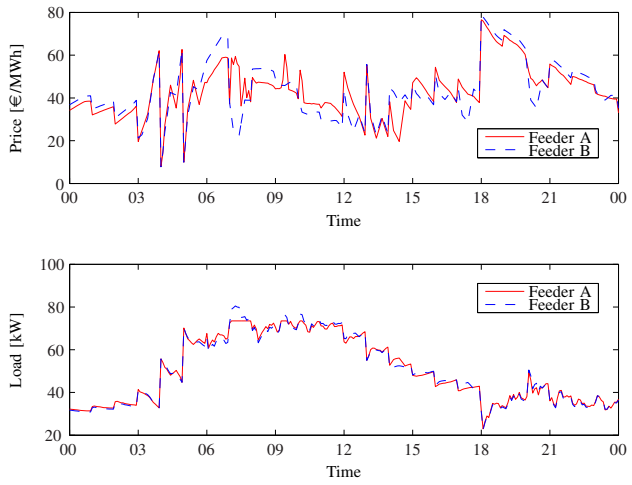

Fig. 4. Real-time price and load, where feeder A experiences peak load shaving and feeder B is unconstrained

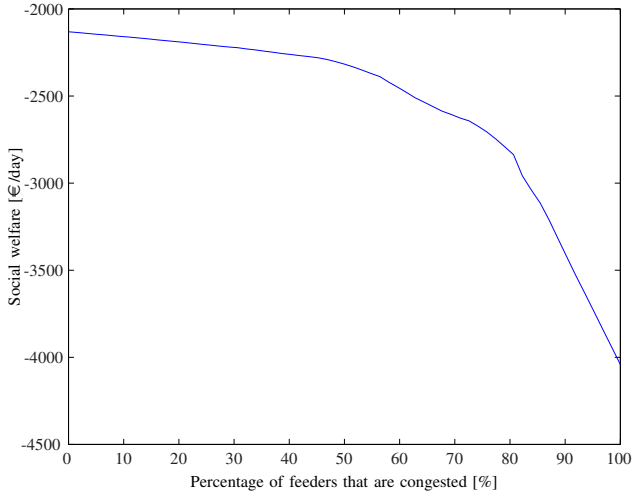

Fig. 5. Social welfare decreases as the number of congested feeders are acted upon

simulations show that average prices were successfully kept the same for different loads - with and without congestion management - to the nearest Euro Cent.

Fig. 5 shows the relationship between the number of congested loads and social welfare. The relationship is initially linear, but as many loads become congested, costs increase greatly, since additional generation must be activated to compensate. The initial linear relationship in this figure reveals that the average cost to the regulating market is about €3 per day per feeder, which is a cost that could then be passed onto DSOs willing to participate. If the EcoGrid EU demand reduces the need for faster moving reserves, for example primary frequency reserves, then the cost to DSOs may be higher, since this makes DR more valuable to other services.

IV. Conclusion

We have developed a centralised electricity market that is designed to replace the existing regulating market in Denmark and that determines a fair market price for all players affected by congestion management: transmission system operators (TSOs), DSOs and consumers. The trade-off between using DR for congestion management and system balancing is explicitly taken account of in the market model. The results are highly dependent on existing bidding strategies (e.g. the Nord Pool generation bid curve) and many assumptions may change if and when DR becomes a significant reality.

Acknowledgment

This work was supported by the EcoGrid EU project, which is funded by the E.U. Seventh Framework Programme under grant ENER/FP7/268199, and by Mogens Balslev's Foundation. We would like to thank all our partners in the EcoGrid EU consortium, especially IBM, Energinet.dk, Siemens and Østkraft whose help made this work possible. The authors would like to thank Henrik Bylling for scenario reduction advice. Finally, the authors are also grateful for weather forecast data from DMI and ECMWF, and wind power forecasts from ENFOR.

References

[1] K. Heussen, S. You, B. Biegel, L. H. Hansen, and K. B. Andersen, "Indirect control for demand side management - A conceptual introduction," *IEEE PES Innov. Smart Grid Technol. Conf. Eur.*, pp. 1–8, 2012.

[2] H. Glavitsch and F. Alvarado, "Management of multiple congested conditions in unbundled operation of a power system," *IEEE Trans. Power Syst.*, vol. 13, pp. 1013–1019, 1998.

[3] T. Krause and G. Andersson, "Evaluating congestion management schemes in liberalized electricity markets using an agent-based simulator," *2006 IEEE Power Eng. Soc. Gen. Meet.*, 2006.

[4] J. Hu, S. You, M. Lind, and J. Ø stergaard, "Coordinated charging of electric vehicles for congestion prevention in the distribution grid," *IEEE Trans. Smart Grid*, vol. 5, no. 2, pp. 703–711, 2014.

[5] F. Sossan, M. Marinelli, G. T. Costanzo, and H. Bindner, "Indirect control of DSRs for regulating power provision and solving local congestions," *IYCE 2013 - 4th Int. Youth Conf. Energy*, 2013.

[6] B. Biegel, P. Andersen, T. S. Pedersen, K. M. Nielsen, J. Stoustrup, and L. H. Hansen, "Smart grid dispatch strategy for ON/OFF demand-side devices," in *Control Conf. (ECC), 2013 Eur.*, 2013, pp. 2541–2548.

[7] Z. Csetvei, J. Ø stergaard, and P. Nyeng, "Controlling price-responsive heat pumps for overload elimination in distribution systems," *IEEE PES Innov. Smart Grid Technol. Conf. Eur.*, pp. 1–8, 2011.

[8] O. Corradi, H. Ochsenfeld, H. Madsen, and P. Pinson, "Controlling electricity consumption by forecasting its response to varying prices," *IEEE Trans. Power Syst.*, vol. 28, no. 1, pp. 421–429, 2012.

[9] G. Dorini, P. Pinson, and H. Madsen, "Chance-constrained optimization of demand response to price signals," *IEEE Trans. Smart Grid*, vol. 4, no. 4, pp. 2072–2080, 2012.

[10] S. A.-h. Soliman and A. M. Al-Kandari, *Electrical load forecasting: Modeling and model construction*. Elsevier, 2010.

[11] G. James, D. Witten, T. Hastie, and R. Tibshirani, *An introduction to statistical learning*. Springer, 2006, vol. 102.

[12] J. Nocedal and S. J. Wright, *Numerical optimization*. Springer, 2006.

[13] Y. Fu, M. Shahidehpour, and Z. Li, "Security-Constrained Unit Commitment With AC Constraints," *IEEE Trans. Power Syst.*, vol. 20, no. 2, pp. 1001–1013, May 2005.

[14] N. Growe-Kuska, H. Heitsch, and W. Romisch, "Scenario reduction and scenario tree construction for power management problems," *2003 IEEE Bol. Power Tech Conf. Proc.*, vol. 3, pp. 152–158, 2003.

[15] E. M. Larsen, "EcoGrid EU market clearing simulation code," 2014. [Online]. Available: https://github.com/emillarsen

PAPER D

The Cobweb effect in balancing markets with demand response

This paper has been submitted for publication in IEEE Transactions on Power Systems.

The Cobweb Effect in Balancing Markets with Demand Response

Emil M. Larsen, Pierre Pinson, Jianhui Wang, Yi Ding and Jacob Østergaard

***Abstract*—Integration of renewable energy sources like wind into the power system is a high priority in many countries, but it becomes increasingly difficult as renewables reach a significant share of generation. Demand response (DR) can potentially mitigate some of these difficulties. However, activating DR in existing electricity markets has been observed to be unstable, resulting in oscillations in supply and demand. This so-called Cobweb effect is presented here using a Scandinavian real-time market structure that is adapted in a novel way to consider cross-time elastic terms. A demand profile based on real measurements from the EcoGrid EU demonstration is used, where five-minute electricity pricing is sent to 1900 houses. Volatility is measured for 1900 houses in the experiment and through further simulation, which demonstrates increased volatility leads to lower social welfare. A key outcome of this research shows that increases in social welfare due to DR appear to be limited by the cost of volatility in existing market structures.**

***Index Terms*—Demand response (DR), Cobweb effect, real-time pricing, volatility, smart grid.**

NOMENCLATURE

$t \in T$	Index for time
$g \in G$	Index for conventional generation
$s \in S$	Index for scenario
$q_{t,s}$	Scenario probability
$c_{t,s}$	Real-time demand
α	Price-elasticity ratio
c_t^{D}	Day-ahead demand forecast
$c_{t,t',s}^{\lambda}$	Demand response with t' cross elasticities
$c_{t,s}^{\mathrm{shed}}$	Load shedding
λ_t^{D}	Day-ahead price
λ_t^{R}	Real-time price
λ^{shed}	Price for load shedding
λ^{spill}	Price for wind spillage
$B_{t,s}$	System imbalance
$p_{g,t}^{\mathrm{D}}$	Conventional generation scheduled day-ahead
w_t^{D}	Wind power day-ahead forecast
$w_{t,s}^{\mathrm{spill}}$	Wind power spillage
$\lambda_{g,t}^{\uparrow}, \lambda_{g,t}^{\downarrow}$	Price for up/down regulation
$p_{g,t,s}^{\uparrow}, p_{g,t,s}^{\downarrow}$	Up/down regulation delivered
$P_{g,t}^{\uparrow}, P_{g,t}^{\downarrow}$	Up/down regulation bid into market
$n_{g,t,s}, m_{g,t,s}$	Up/down regulation on/off

Manuscript submitted 03/02/2016. This work was partly supportly by the European Commission through the project EcoGrid EU (grant ENER/FP7/268199) and by Mogens Balslev's Foundation.

E. M. Larsen is at the Danish Energy Agency, Denmark (email: eml@danskenergi.dk). P. Pinson and J. Østergaard are with the Centre for Electric Power and Energy, Technical University of Denmark, Kgs. Lyngby, Denmark (email: {ppin,joe}@elektro.dtu.dk). J. Wang is at Argonne National Laboratory, USA (email: jianhui.wang@anl.gov). Y. Ding is at Zhejiang University, China (email: yiding@zju.edu.cn).

I. INTRODUCTION

DEMAND response (DR) is being strongly pursued because it increases the value of renewable energy sources (RES) when they are available, provides some additional capacity when renewables are not available, and balances the system when renewables do not behave as predicted [1]. In Denmark, the shift to RES meant that wind power met 43% of national electricity consumption in 2015, and is well on its way to hitting goals of 50% electricity consumption from wind power in 2020, and 100% of all energy consumption from renewable energy in 2050 [2].

There are many dynamic and static electricity price tariffs that can be used to activate DR, but two methods in particular have gained traction in recent years due to their fast activation characteristics that complement the uncertainty in RES generation. These are direct control, where utilities turn devices on and off remotely, and indirect control, where an incentive signal, e.g., an electricity price, is used to influence the load to change its consumption. Direct control is typically targeted at medium and large commercial and industrial loads and has the challenges of requiring reliable communication equipment, while indirect control is aimed at a large number of small-scale loads and has challenges of predictability [3]. Key benefits of indirect control include lower equipment costs and, when a price-based mechanism is used, there can be a clear value attributed to the resource. When traded in a power pool, DR has the additional benefit of improving liquidity and lowering the cost of supply, since it reduces the market power of price-maker generators. However, indirect control by means of true market-based pricing sent to supply and demand has long been associated with unstable behavior, as first identified in [4], where it was named the Cobweb effect due to the spider web-like back-and-forth oscillations that occur when a stable market equilibrium cannot be achieved.

The Cobweb effect has traditionally been studied in markets where demand for a commodity, for example apples, was higher or lower than supply had expected. The following season, apple growers then change their production level, but the market becomes over- or under-supplied and an overshoot causes demand to behave in a seemingly opposite fashion to what had been experienced the previous season. If every market participant has a perfect forecast of supply and demand, then the Cobweb effect should not happen, but uncertainty is usually present in markets. This is true in a modern power system and especially true for DR [5]. Electricity market clearing algorithms must also make assumptions about demand, including linearising non-linear behavior, in order to find a

feasible and timely solution in an optimization framework. This can result in power and prices being more volatile than is optimal, as seen in Fig. 1. Here, an imbalance that exists only at the first time step where supply and demand intersect, causes the market clearing price to oscillate outwards as the initial decision leads to a greater imbalance, via feedback, in subsequent steps.

In this paper, we investigate the Cobweb effect, which is discussed in more detail in section II, using the market structure and data collected from the EcoGrid EU project [6], which is DR demonstration on the Danish island of Bornholm. The EcoGrid EU experiment has 1900 residential households with a peak load of 5MW. Houses are equipped with smart meters and a range of distributed energy resources (DERs) with automated controllers that receive a new electricity price every five minutes and optimize consumption levels accordingly. DR from these customers is scheduled optimally with conventional generation in a market structure to meet the imbalance caused by wind power.

The contribution of this work lies in developing a real-time market that considers cross-time elasticity. We identify the different causes of volatility and investigate the impact the Cobweb effect has on social welfare, and how market re-commitment frequency changes volatility and social welfare. We believe the latter to be important as system operators move to shorter settlement periods.

The paper is structured with section II presenting existing knowledge of the Cobweb effect. Section III defines price- and cross-time elasticity and illustrates the corresponding demand model. Section IV presents the market structure. Section V presents results for social welfare and volatility from simulations and the real experiment. The final section concludes.

II. The Cobweb effect

Since initially investigated in 1938, the Cobweb effect was expanded to markets with non-linear supply and demand curves in [7], where it was also shown that the Cobweb effect happens with monotonic demand and supply curves, as is the case in electricity markets. In [8], the impact of demand expectation using auto-regressive methods on the Cobweb effect was identified. Traditional economics literature has been more focused on identifying the problem and improving the expectation of demand, including considering larger forecast horizons, leading to more stable market outcomes [9]. Solutions other than a better demand forecast have not been explored. Recent economics research on the Cobweb effect has moved to analyzing games between different players, the result of which is an equilibrium with the lowest forecast error on both the supply and demand side [10].

In the field of power system research, market-based volatility due to real-time pricing was first identified in [11], where it was noted that there is an upper limit on the market clearing time and the delay of the price signal beyond which the system becomes unstable. Here it was shown that delaying communication of the price sent to customers increased system stability greatly, while increasing the gate-closure time led to fragile system behavior. Cobweb-like volatility has been particularly problematic when using models from the New York ISO power system [12], however, the authors there used a mirror image of supply to represent demand in the absence of reliable information about its actual shape. In addition, authors there also assumed demand would only be non-linear with respect to time, but not conditional on past and future prices.

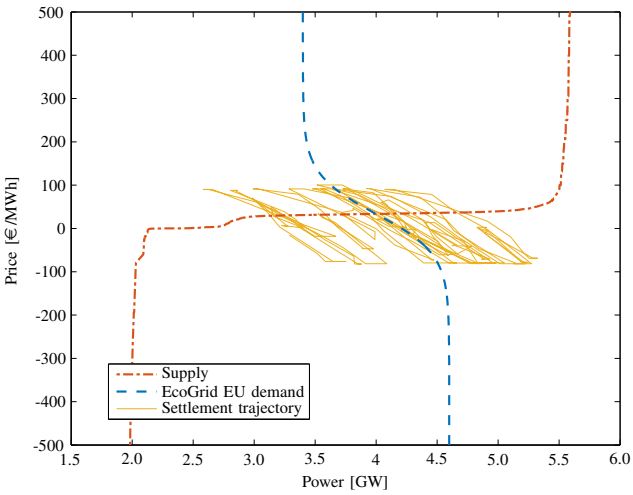

Fig. 1. The Cobweb effect in the EcoGrid EU market, where the settlement trajectory starts at the intersection of the initial supply (Nord Pool bid data) and demand (EcoGrid EU demand model) curves shown.

Recently, [13] identified the boundaries for volatility when closed-loop real-time pricing structures are used without an appropriate feedback law. No remedy was offered for the closed-loop instabilities simulated in this research, but it was noted that price volatility increases as the price-elasticity of consumers increases with respect to the price-elasticity of suppliers, indicating that volatility will vary from case to case. Real data was not used in [13], highlighted by a demand profile with eight peaks per day, rather than the archetypal one or two daily peaks. Consequently, there remains a lack of evidence about how much volatility will truly be observed in a power system with DR and real-time pricing, hence our curiosity as to whether the Cobweb effect is observable or significant in a realistic market setup.

III. Price and cross-time elasticity ratios

In this section, a definition of price and cross-time elasticity is given and the demand model is illustrated.

Price elasticity, also called self or own elasticity [14], describes how sensitive a load is to a change in price [15]. It is traditionally dimensionless and is often used to describe how consumption responds to a 1% change in price. For the purposes of operating a real-time market, however, we define price elasticity in absolute terms as a linear function of observed changes in load, ΔC, i.e.

$$\alpha_t^{DA} = \frac{\lambda_t^{DA}}{\Delta C_t^{DA}} \tag{1}$$

where λ_t^{DA} is day-ahead price. Real-time price elasticity is defined with respect to the day-ahead state, i.e.

$$\alpha_t = \frac{\lambda_t^{RT} - \lambda_t^{DA}}{\Delta C_t} \tag{2}$$

where λ_t^{RT} is the real-time price. α_t^{DA} and α_t are the ratios of price to change in consumption with units of €/MW^{2}h.

In addition to regular price elasticity, there also exists cross-time elasticity. This is the influence of past and future prices on the current demand, often occurring due to some overriding comfort boundaries that must be adhered to. When applied to electric heating, cross-time elasticity occurs because the heating device cannot stay on or off forever. It will have to stay within a comfortable temperature range and cross-time elasticities can describe how long the device can be perturbed for.

Conceptually, the impact of cross-time elasticity can be explained using the relationship

$$\Delta C_t = \sum_{t'=T_a}^{T_b} \frac{\lambda_{t'}}{\alpha_{t,t'}}, \qquad T_a \leq t \leq T_b \tag{3}$$

where $\lambda_{t'}$ can be a day-ahead price or the difference between the real-time and day-ahead prices, as in equation (2). To clarify the definition given in (3), first consider that we have a time-series of length T. We then place a sliding window around each time-step with the index t'. The sliding window starts at T_a and goes on to T_b and DR (ΔC_t) is a function of all the prices valid from T_a to T_b. This process describes the energy shifted from each slice of time, past and future, to the present time-step, t. In other words, the sum over the whole sliding window describes the energy shifted to the current time-step.

Fig. 2 encapsulates price and cross-time elasticity for the EcoGrid EU load, when given a step increase in price, in the form of a finite impulse response (FIR). The change at t_0 represents the self elasticity, while any differences between this consumption and previous and future changes represent cross-time elasticity. A full description of this model is described in [16], which also describes a congestion management experiment using the EcoGrid EU market framework. The model was based on consumption during the coldest six months of the year. DR peaks 15 minutes after the price change and subsequently fades away.

The elasticity matrix is derived from the FIR by laying it out in a matrix with the structure

$$\theta_{t,t'} = \begin{bmatrix} \theta_1 & \theta_0 & \theta_{-1} & \vdots \\ \theta_2 & \theta_1 & \theta_0 & \theta_{-1} \\ \theta_3 & \theta_2 & \theta_1 & \theta_0 \\ \vdots & \theta_3 & \theta_2 & \theta_1 \end{bmatrix} \tag{4}$$

Each column has the FIR according to external conditions such as ambient temperature, with the diagonal containing new time steps [17]. The element-wise reciprocal of $\theta_{t,t'}$ gives the elasticity matrix, $\alpha_{t,t'}$.

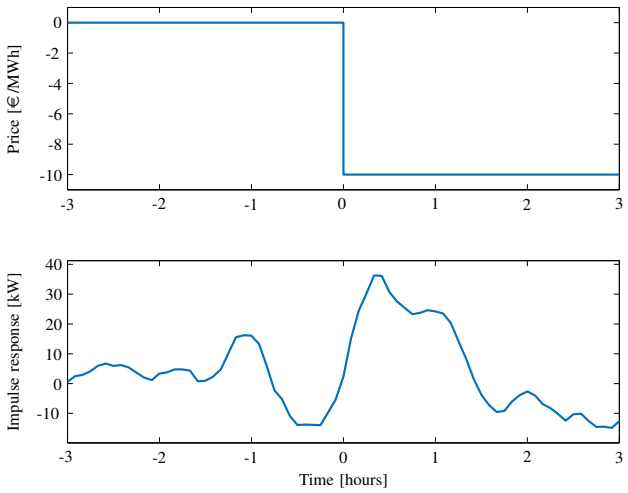

Fig. 2. Finite impulse response (FIR) of the EcoGrid EU demand in early 2014, peaking at 36kW when given a 10€/MWh price decrease at t_0.

IV. Market Structure

This section presents the market structure used experimentally and simulated for different cases. The EcoGrid EU demonstration has two hardware in-the-loop market steps, as shown in Fig. 3, which were used to generate five minute electricity pricing for 1900 houses in 2014 and 2015. Generator bids are based on historical Nord Pool bid data, as shown in Fig. 1, while inflexible demand and wind power injection comes from commercial real-time observations. The imbalance signal is derived from the day-ahead wind power forecast error, scaled by the Danish nominal capacity, which is around 5%.

The timeline for market operation is shown in Fig. 4. The day-ahead market price is given at 13:00 the day before operation. Real-time prices are then revealed one minute before each five minute settlement period they are valid for. In the experiment, an hour-ahead price forecast was sent to demand half past every hour. This forecast comes naturally from the market clearing, so long as the market clearing has a long enough forecast horizon. The forecast helps DERs schedule their consumption optimally, but the forecast itself is optional.

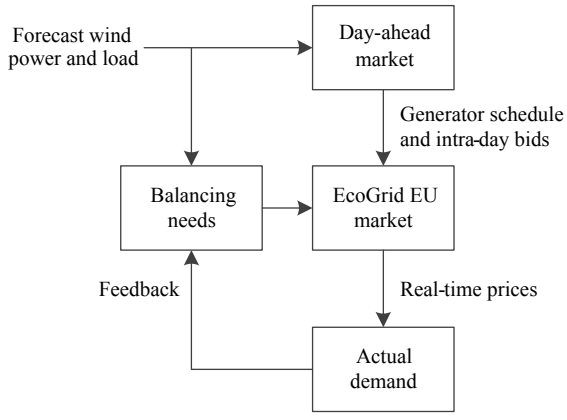

Fig. 3. Hardware-in-the-loop market structure of the EcoGrid EU demonstration.

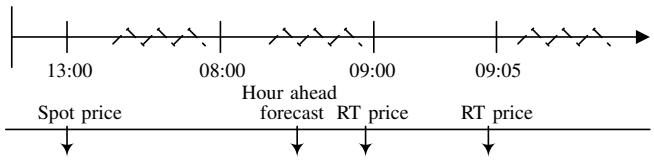

Fig. 4. Timing of EcoGrid EU real-time market.

Without the forecast, the elasticity matrix will become more reactive, with fewer terms before the diagonal values [17].

The first step is a day-ahead market that minimizes the cost of conventional generation, considering the day-ahead wind power production forecast, the known Nord Pool spot price, and the demand forecast including price-response to spot prices. If there is no imbalance, then the spot price is sent to consumers and demand. However, the day-ahead market is not the main area of focus, because it does not generate the day-ahead price and demand is a fixed input. This step is only needed to find reasonable and feasible starting points for generators participating in the real-time market. The overall problem reads

$$\min_{\Theta} \sum_{g,t} \lambda_{g,t} p^{\mathrm{D}}_{g,t} + \sum_{t} \lambda^{\mathrm{shed}} c^{\mathrm{shed}}_{t} - \sum_{t} \lambda^{\mathrm{spill}} w^{\mathrm{spill}}_{t} \tag{5a}$$

subject to

$$\sum_{g} p^{\mathrm{D}}_{g,t} + w^{\mathrm{D}}_{t} - w^{\mathrm{spill}}_{t} = c^{\mathrm{D}}_{t} - c^{\mathrm{shed}}_{t} \qquad \forall t \tag{5b}$$

$$p^{\mathrm{D}}_{g,t} \geq P^{\min}_{g}; \quad p^{\mathrm{D}}_{g,t} \leq P^{\max}_{g} \qquad \forall g,t \tag{5c}$$

$$p^{\mathrm{D}}_{g,t} - p^{\mathrm{D}}_{g,t-1} \leq r_{g,t}; \quad p^{\mathrm{D}}_{g,t-1} - p^{\mathrm{D}}_{g,t} \leq r_{g,t} \qquad \forall g,t \tag{5d}$$

where the set of decision variables, $\Theta = p^{\mathrm{D}}_{g,t}, c^{\mathrm{shed}}_{t}, w^{\mathrm{spill}}_{t}$, are generation, load shedding and wind spillage. These variables are balanced with day-ahead wind power and load forecasts in (5b). Wind power injection is a parameter that is treated as a negative load (minus wind spillage). Minimum and maximum generation is constrained in (5c), while up and down ramp rates are bound by the ramp rate parameter $r_{g,t}$ in (5d).

The second market step is the EcoGrid EU market, where social welfare is maximized with respect to the day-ahead market outcome. The market schedules an optimal amount of manual reserves and flexible demand, and is formulated as a stochastic optimization problem that commits bids for conventional generation and creates real-time prices (RTP) for demand until the market is cleared again. Unscheduled and scheduled generation from the first market step is used as the up and down regulation bids respectively in the real-time market, i.e. $p^{\uparrow}_{g,t,s} = P^{\max}_{g} - p^{\mathrm{D}}_{g,t}$ and $p^{\downarrow}_{g,t,s} = p^{\mathrm{D}}_{g,t} - P^{\min}_{g}$. This yields

$$\max_{\Theta} \sum_{t} \sum_{s} q_{t,s} \Bigg\{ \lambda^{DA}_{t} \sum_{t'} c^{\lambda}_{t,t',s} + \frac{1}{2} \sum_{t'} \alpha_{t,t',s} c^{\lambda}_{t,t',s} \sum_{t'} c^{\lambda}_{t,t',s} - \sum_{g} \beta_{g,t,s} - \lambda^{\mathrm{spill}} w^{\mathrm{spill}}_{t,s} - \lambda^{\mathrm{shed}} c^{\mathrm{shed}}_{t,s} \Bigg\} \tag{6a}$$

subject to

$$c^{\lambda}_{t,t',s} = c^{\lambda}_{t-1,t',s} \frac{\theta_{t,t',s}}{\theta_{t-1,t',s}} \qquad t \neq t', \theta_{t,t'} \neq 0 \tag{6b}$$

$$c^{\lambda}_{t,t',s} = 0 \qquad \forall t,t',s,\alpha_{t,t',s} = 0 \tag{6c}$$

$$\sum_{t'} c^{\lambda}_{t,t',s} = 0 \qquad \forall s, t > 2h \tag{6d}$$

$$c^{\lambda,\min}_{t'} \leq c^{\lambda}_{t,t',s} \leq c^{\lambda,\max}_{t'} \qquad \forall t,t',s \tag{6e}$$

$$c_{t,s} = c^{\mathrm{D}}_{t} - c^{\mathrm{shed}}_{t,s} + \sum_{t'} c^{\lambda}_{t,t',s} \qquad \forall t,s \tag{6f}$$

$$w_{t} = w^{\mathrm{D}}_{t} - w^{\mathrm{spill}}_{t,s} \qquad \forall t,s \tag{6g}$$

$$\beta_{g,t,s} = \lambda^{\uparrow}_{g,t} p^{\uparrow}_{g,t,s} - \lambda^{\downarrow}_{g,t} p^{\downarrow}_{g,t,s} \qquad \forall g,t,s \tag{6h}$$

$$p_{g,t,s} = \sum_{g} p^{\mathrm{D}}_{g,t,s} + p^{\uparrow}_{g,t,s} - p^{\downarrow}_{g,t,s} \qquad \forall g,t,s \tag{6i}$$

$$c_{t,s} = p_{g,t,s} + w_{t,s} - B_{t,s} - e_{t} \qquad \forall t,s \tag{6j}$$

$$\lambda^{R}_{t,s} = \sum_{t'} \alpha_{t,t',s} c^{\lambda}_{t,t',s} + \lambda^{D}_{t} \qquad \forall t,s \tag{6k}$$

$$\Delta p^{\uparrow}_{g,t,s} = p^{\uparrow}_{g,t,s} - p^{\uparrow}_{g,t-1,s} \qquad \forall g,t,s \tag{6l}$$

$$\Delta p^{\downarrow}_{g,t,s} = p^{\downarrow}_{g,t,s} - p^{\downarrow}_{g,t-1,s} \qquad \forall g,t,s \tag{6m}$$

$$\Delta p^{\uparrow}_{g,t,s} = \Delta p^{\uparrow}_{g,t-1,s} \qquad \forall g,t,s,\gamma_{t} = 0 \tag{6n}$$

$$\Delta p^{\downarrow}_{g,t,s} = \Delta p^{\downarrow}_{g,t-1,s} \qquad \forall g,t,s,\gamma_{t} = 0 \tag{6o}$$

$$\Delta p^{\uparrow}_{g,t,s} = 0; \quad \Delta p^{\downarrow}_{g,t,s} = 0 \qquad \forall g,t,s,\gamma_{t} = 2 \tag{6p}$$

$$p^{\uparrow}_{g,t,s} \leq n_{g,t,s} p^{\uparrow}_{g,t,s} \qquad \forall g,t,s \tag{6q}$$

$$p^{\downarrow}_{g,t,s} \leq m_{g,t,s} p^{\downarrow}_{g,t,s} \qquad \forall g,t,s \tag{6r}$$

$$p^{\uparrow}_{g,t,s} \geq n_{g,t,s} \chi_{g} p^{\uparrow}_{g,t,s} \qquad \forall g,t,s,\gamma_{t} = 2 \tag{6s}$$

$$p^{\downarrow}_{g,t,s} \geq m_{g,t,s} \chi_{g} p^{\downarrow}_{g,t,s} \qquad \forall g,t,s,\gamma_{t} = 2 \tag{6t}$$

$$n_{g,t,s} = 0; \quad m_{g,t,s} = 0 \qquad \forall t,s,P^{\uparrow}_{g,t} = 0 \tag{6u}$$

$$p^{\uparrow}_{g,t,s} \leq d_{t,s} p^{\uparrow}_{g,t,s}; \quad p^{\downarrow}_{g,t,s} \leq l_{t,s} p^{\downarrow}_{g,t,s} \qquad \forall g,t,s \tag{6v}$$

$$d_{t,s} + l_{t,s} \leq 1 \qquad \forall g,t,s,\gamma_{t} = 2 \tag{6w}$$

where the set of decision variables, $\Theta = \{c^{\lambda}_{t,t',s}, \beta_{g,t,s}, w^{\mathrm{spill}}_{t,s}, c^{\mathrm{shed}}_{t,s}, \lambda^{R}_{t,s}, c_{t,s}, p^{\uparrow}_{g,t,s}, p^{\downarrow}_{g,t,s}, n_{g,t,s}, m_{g,t,s}, d_{t,s}, l_{t,s}\}$, contains DR due to self and cross-time elasticities, generator cost, wind spillage, load shedding, real-time price, aggregated demand, up regulation, down regulation, on/off status of up regulation bid, on/off status of down regulating bid, on/off status of global up regulation, and on/off status of global down regulation for all $g \in G$, $t \in T$, $t' \in T$ and $s \in S$ respectively.

The objective function (6a) maximises social welfare, where the first term is customer utility and the last terms are cost of generation and slack variables.

When cross-time elasticity is ignored, then only the diagonal term in $\alpha_{t,t'}$ is non-zero, and is fixed to the average price and cross-time elasticity until the market is cleared again, i.e. if the market is run hourly, then the first 12 values of price elasticity are used to determine price elasticity. Clearing an electricity market considering cross-time elasticity is not needed in today's deregulated power systems because the loads that participate in existing DR schemes have a cross-time elasticity that is longer than the re-commitment time of

the system they participate in. For example, a factory that reduces its consumption for an hour to meet the terms of a DR contract will not compensate for this reduction in the following hour, since it will cause an imbalance and be penalised as a result. Instead, its cross-time elasticity depends on long term planning ranging from days to years, far slower than day-ahead and real-time markets recommit bids today. This is highlighted in [18], where the average rebound effect of an office building, a furniture store and a bakery was 15.5%. Small-scale DR, which indirect control leans towards, usually has time-constant of just a few minutes, which means the response does not last very long, and with a rebound effect of 42% as seen in Fig. 2. This time-constant is a similar order of magnitude to the re-commitment frequency in real-time markets today, which suggests that cross-time elasticities must be fully incorporated into the market to obtain an economically efficient and controllable outcome.

Methods for clearing day-ahead markets considering cross-time elasticities have previously been proposed in [14]. However, existing algorithms do not converge on a solution if the demand's self elasticity is smaller than its cross-time elasticity. This solution may work well in an hourly market, where the demand characteristics are likely to lead to a solution, but in a balancing market, the cross-time terms will often be larger than the self elastic terms. In addition, the previously proposed market structure requires the elasticity matrix to be symmetrical. In reality, demand does not prepare for an event in exactly the same way as it behaves after the event has happened. I.e. load shifting is not symmetrical and therefore not controllable when the wrong (symmetrical) elasticity matrix is used. Previous market structures with cross-time elasticities do not consider generation constraints, which necessitate additional constraints on the supply side to reach a controllable outcome. Constraints (6b)-(6d) are the most important in this respect. Constraint (6b) ties DR together in an auto regressive fashion, so that a full model of the FIR for price is included in the market formulation. Equation (6c) ensures that the resulting FIR is zero when price-elasticity is zero. Constraint (6d) sets DR to zero for twice the FIR length, h, so that market outcomes do not create infeasible starting points for subsequent re-commitments.

Constraint (6e) determines the flexible demand limits for each price lag. The total demand and production from wind are defined in (6f) and (6g). The regulating cost from conventional generation is defined in (6h). The total power produced by conventional generation is stated in (6i). Constraint (6j) is the balance constraint, also considering the imbalance from wind and inflexible demand, B_t, and the error term e_t, which describes undesirable feedback that is caused when DR does not behave as scheduled. It is the dual variable of this constraint that gives the real-time price, $\lambda^R_{t,s}$, which can also be found in constraint (6k).

Constraints (6l) - (6w) dictate generator behaviour like minimum on-times and ramping characteristics that are in-line with the Scandinavian balancing market today. Constraints (6l) and (6m) define generator ramp rates. Constraints (6n) and (6o) keep ramping constant for 15 minutes. Constraints (6p) ensure that a generator is at a fixed set-point for at least 15 minutes. When used with the generator behavior of $\gamma_t = \{1, 0, 0, 2, 0, 0, 1, 0, 0, 2, 0...\}$, (6l)-(6p) result in a minimum on-time of 45 minutes. Constraints (6q) and (6r) limit maximum regulation. Constraints (6s) and (6t) are minimum generation constraints. In the Scandinavian regulating market, bids under 10MW must be activated in full, while bids above 10MW can be activated in part; the proportion of each bid to be activated is described by the parameter χ_g. Constraints (6u) ensure that a generator is off when it does not bid into the market. Constraints (6v) determine whether any up or down generation is active, according to binary variables $d_{t,s}$ and $l_{t,s}$ respectively, and (6w) prevents simultaneous up and down regulation.

For each scenario-based decision variable there exists a non-anticipativity constraint that ensures its outcome is identical across all scenarios in the first few time periods for which prices are fixed, for example $t = 1 \dots 6$ if the market is cleared every half hour. Scenarios for imbalance, B, are generated using a non-parametric method. Bootstrapping is employed, where historical outcomes are sampled with replacement. Scenarios for price elasticity are normally distributed and scenario reduction is done using the Fast Forward method [19].

Any imbalance after the market cleared is penalised by a primary frequency reserve (PFR) energy cost, which is set to the highest and lowest electricity price observed in each hour ex-post (after delivery), as in Scandinavia today. All other prices in Nord Pool and EcoGrid EU are defined ex-ante (before delivery).

When only self-elasticity is considered, the market is formulated as a mixed integer quadratically constrained program (MIQCP) which is readily solved with CPLEX. When considering all cross-time elasticities that results in an asymmetrical elasticity matrix, the formulation becomes a mixed integer non-linear program (MINLP). Such problems are typically solved by decomposition into NLP and MIP subproblems. We do so by first relaxing the problem (i.e., no binary variables) and solving with CONOPT. Subsequently, DR ($c^{\lambda}_{t,t',s}$) is fixed, which removes all non-linearities, and bid commitment is finalised in the MIP subproblem using CPLEX. This approach led to solutions consistently being found in under 60 seconds.

V. Results

A. Quantifying Volatility

To measure volatility, we use a rainflow counting algorithm [20], which is traditionally used in material fatigue and battery ageing analysis. The rainflow counting algorithm is a simple but powerful tool and the result is intuitive; Whenever there is a change of sign in the signal of interest, a turning point is defined. The distance between turning points is measured and binned for similar distances to give the number of oscillations observed per day. In Fig. 5, trough half cycles are counted and the distance for each cycle is measured for a time-series of DR. The total number of full cycles (troughs plus peaks) in this example are 16, with an average amplitude of 80.6MW.

B. The cause of the Cobweb effect

The main cause for the Cobweb effect is uncertainty, but this can be further specified as structural uncertainty, that is

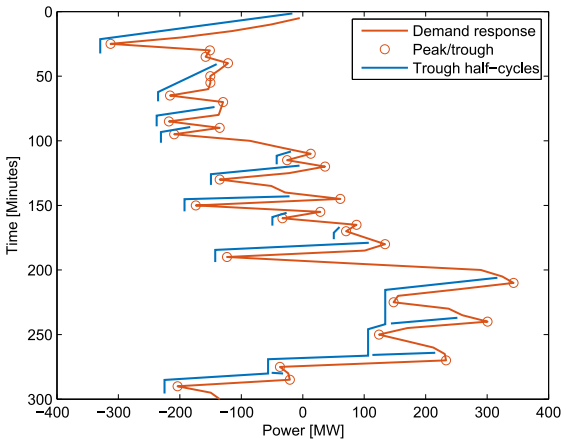

Fig. 5. Rainflow counter, where the broken blue lines are half-cycles used count the number and amplitude of oscillations.

the linearisation of demand characteristics to fit into a market structure, and aleatoric uncertainty, which is the intrinsic randomness in natural processes. Structural uncertainty in our system comes from the non-linear demand curve, assumed to be linear in the market, and ignoring cross-time elastic effects.

To understand which source of uncertainty causes the greatest volatility, we performed simulations for Denmark for one month for a range of different cases. The first case is one with no DR. The second case is an open loop system, where feedback is ignored by the market and left for faster moving reserves like PFR to remedy. An open loop cannot be operated in reality, because it requires no uncertainty in the source of an imbalance, but it is a useful benchmark since most academic electricity market studies are open loop. The next case is a closed loop system, where the market is run without cross-time elasticities, as in Scandinavia today, and feedback from an unexpected response creates a new imbalance in subsequent market re-commitments. In the fourth and fifth cases (Closed NL and CE), feedback from non-linear and cross-time elastic behaviour (based on demand models in [16]) is remedied by the market, one at a time, while the other is left as an open loop imbalance. This allows us to identify which is the bigger cause of the Cobweb effect. The sixth case (Closed M) simulates a full closed loop but with a modified market, where the full cross-time elastic effects are optimised for in the market. Finally, demonstration results are included. The demonstration cannot be directly compared to simulated cases because it uses a local imbalance signal derived from an island, and is a pseudo-closed loop where delayed meter data causes imbalance-feedback with a 15 minute delay.

Fig. 6 shows a simulation day with outcomes of market clearing price, demand and regulating power activated respectively. In a closed-loop system, oscillating behaviour is seen in both regulating power and demand. In an open loop system, similar volatility as the closed loop system can be seen in the first few hours of the system price. Increased volatility is therefore not a problem in itself from a market perspective - DR increases volatility of the demand even when expectation of demand is perfect, and this is to be cherished if DR is to help balance volatile renewable energy production. However, increased activation of regulating power is a clear indicator of the Cobweb effect in action.

Table I summarises the number of cycles counted by the rainflow counting algorithm for different cases. There is an increase in demand cycles across all cases with DR, which occurs naturally as the demand becomes dynamic. There is a reduction in supply cycles for all DR cases, which should be interpreted as fewer regulating bids being committed, which in turn means that DR has achieved its goal of reducing reliance on conventional power generation. The closed loop experiences the most volatile pricing, with the most price cycles.

Table II shows the cycle amplitude summed per day. For supply and demand, this describes the total amount of balancing power activated, and for prices, this represents the sum of price changes. Higher demand cycle amplitudes in all DR cases suggests load shifting is occurring. Price amplitudes are lowest in the open loop and the Closed NL case, suggesting they behave in a similar manner and that feedback from a non-linear demand curve is insignificant for volatility. In the basic closed loop setup and the Closed CE case, price amplitude is quadruple the open loop case. Price amplitudes paint a similar picture, with the greatest volatility in the cases with feedback from cross-time elasticity, and less volatility in the non-linear feedback case. The modified case should be directly compared

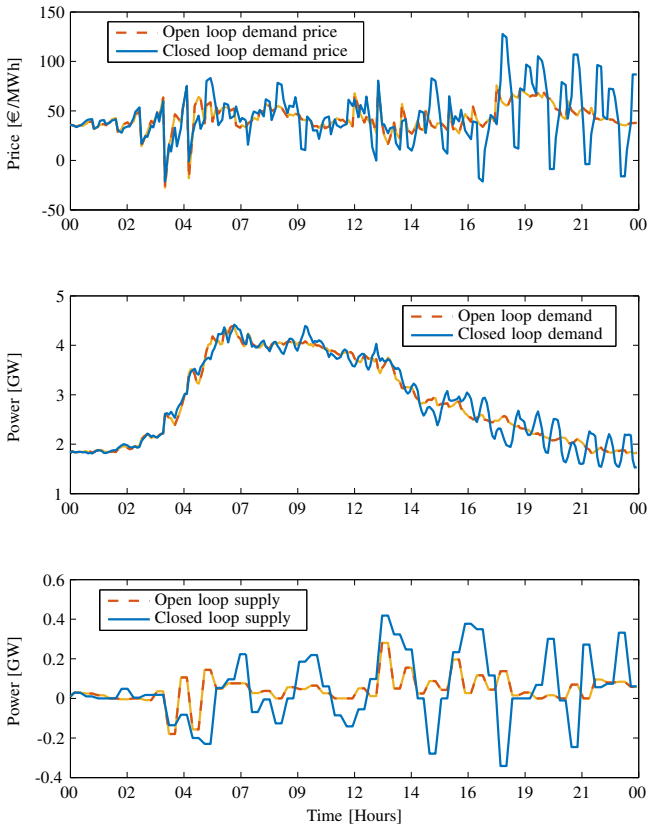

Fig. 6. Electricity prices, demand and supply for an open- and closed-loop simulation day.

TABLE I
AVERAGE CYCLES PER DAY

	Price [Cycles]	Demand [Cycles]	Supply [Cycles]
No DR	0	62.9	20.4
Open	56.8	58.6	15.9
Closed	38.9	39.6	18.1
Closed NL	56.1	56.1	15.9
Closed CE	39.4	36.7	16.9
Closed M	88.6	75.0	17.1
Demonstration	73.3	65.9	24.5

TABLE II
AVERAGE SUM OF CYCLE AMPLITUDES PER DAY

	Price [€/MWh]	Demand [GWh]	Supply [GWh]
No DR	0	1.9	1.4
Open	482.8	4.3	1.1
Closed	2013.8	16.1	4.7
Closed NL	507.7	4.7	1.2
Closed CE	2122.0	15.6	4.2
Closed M	1690.3	5.2	2.3
Demonstration	475.2	3.8	3.6

to the closed loop case, where it exhibits half the supply volatility and a reduction of 46% in supply price. Despite this, it exhibits higher supply amplitudes (but at a lower price) than the zero-DR case, suggesting the Cobweb effect is still present here, but the market is able to exploit lower generation costs in spite of volatility.

C. Demand response penetration

To see if the Cobweb effect increases cost, cases were simulated for different levels of DR penetration. DR penetration was scaled from 0% to 100%, as shown in Fig. 7. The upper limit assumes that all of Denmark behaves like an EcoGrid EU load and represents a DR peak response about twice that of DR in the Nord Pool day-ahead market today, albeit with significantly more activations due to a lower price-elasticity characteristic (i.e. DR is cheaper to activate). DR penetration beyond 30% results in a reduction in social welfare in the closed-loop system, as the cost of volatility outweighs the benefit of DR. The case where feedback stems from cross-time elastic effects (Closed CE) results in equally low social welfare, while the case where only non-linear effects are feedback has a very similar result to the open loop case. As with the rainflow counting results, this confirms that cross-time elasticity is a bigger cause of the Cobweb effect than our approximation of a non-linear demand curve. Finally, the modified market, which is a full closed loop, successfully increases social welfare for all levels of DR penetration. At low levels of DR penetration, social welfare gains are very small compared to the other cases because the modified market treats DR far more rigidly with fewer activations when it knows that a rebound will occur after 90 minutes. Lower DR activations means that costly conventional generator bids are activated instead, when leaving residual imbalances to faster moving reserves might have been more cost efficient.

Fig. 7 shows that DR has the potential to significantly increase social welfare in a real-time market, equivalent to €3.5 per flexible house per day, but only when cross-time elasticity is explicitly optimized for in the market. However, this result should be moderated by the fact that revenue here is significantly smaller than in the day-ahead market. In addition, this result is only applicable to the winter months when DR from heating in Denmark is expected to be active, so the year-round gain will be lower. The results are also highly dependent on assumptions about the supply curve, which may change as DR schemes grow.

D. Market re-commitment frequency

System dynamics change as system operators move to shorter settlement periods, shorter gate-closure times, and more regular unit re-commitments to reduce the impact of RES uncertainty. We investigated re-commitment frequency by increasing how often the market was cleared from 15 minutes to 150 minutes in 15 minute intervals. The settlement period remains five minutes throughout (i.e. prices and set-points are valid for five minutes at a time), but new decisions are only taken every time the market is cleared. The theoretical benefit of using a higher re-commitment frequency is that newer forecasts with less uncertainty can be used, leading to lower costs and therefore higher social welfare. Fig. 8 shows the outcome of changing unit commitment frequency on generation volatility and social welfare. The cross-time elastic market exhibits similar behaviour for all timings, while the closed loop market actually exhibits lower volatility and higher social welfare for longer re-commitment intervals, which is the opposite to what would traditionally be expected. Volatility here translates to more generator bids being activated for more frequent re-commitments. The local peak in volatility at 45 minutes suggests also that the market clearing frequency

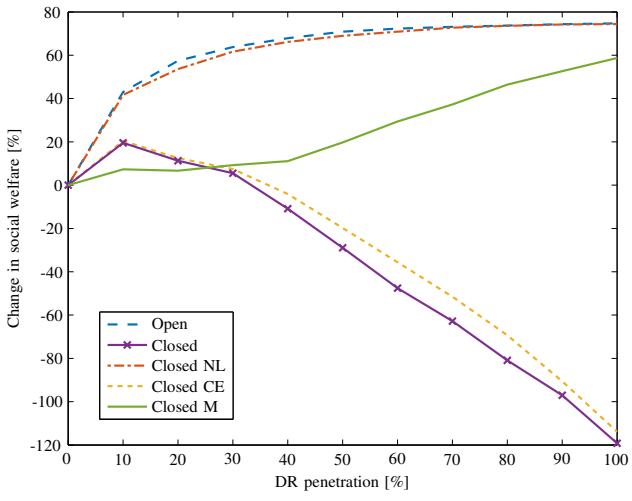

Fig. 7. Social welfare as a function of DR penetration. There is a reduction in social welfare as DR reaches significant proportions in closed-loop cases that do not account for a cross-time elastic response.

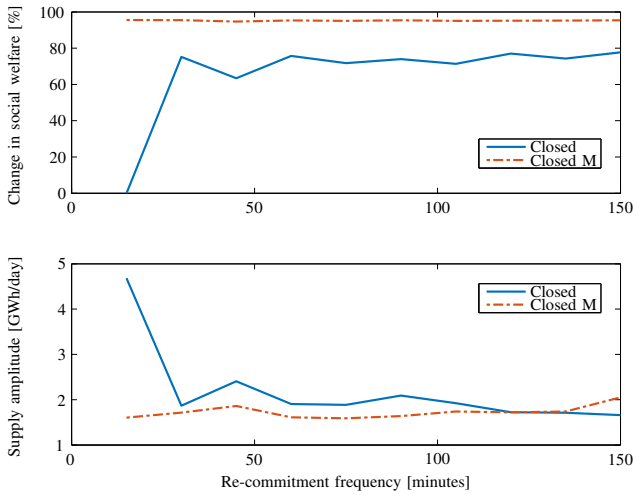

Fig. 8. Social welfare increases and volatility decreases as the re-commitment frequency is reduced in the standard closed-loop case.

is resonating with the minimum-on time for generation, and highlights additional market design challenges.

VI. Conclusion

We have provided evidence that the Cobweb effect impacts balancing markets, provoking costly oscillations on the supply side. Simulations, broadly in line with empirical results from the EcoGrid EU's experiment with 1900 households, show that the Cobweb effect causes three times more generator bids to be activated than in a market with no DR, leading to higher costs and lower social welfare. We observed that a non-linear demand curve does cause the Cobweb effect, but not enough to reduce social welfare. Aleatoric uncertainty appears to have no discernible impact on the Cobweb effect, contrary to previous studies. This means that the natural uncertainty from stochastic generation such as wind and solar power do not provoke the Cobweb effect. However, ignoring cross-time elasticities in a market does lead to significant volatility and reduced social welfare. To mitigate this, we have directly incorporated cross-time elasticity into the market clearing algorithm. Such a solution may appear obvious, yet new, DR-focussed market designs that ignore cross-time elasticity continue to appear in the literature [21]. Reducing re-commitment frequency appears to be another option for reducing the Cobweb effect.

The question remains how well existing markets can control fast-moving, non-linear DR. Our market and demand models are unlikely to capture all sources of volatility, and our measure for social welfare does not count all the costs that stem from it. Voltage and frequency instability could result from a seemingly small amount of volatility, and future research should determine how much volatility is acceptable.

Future research should also investigate uplift payments [22] for markets considering cross-time elasticities, since no method has currently been shown to ensure prices that support all market outcomes.

Acknowledgment

The authors thank Henrik Bylling for scenario reduction advice. We are grateful for the support of all EcoGrid EU's partners. We also thank DMI and ECMWF for weather forecasts, and Nord Pool and ENFOR for market data and power system forecasts respectively.

References

[1] Ea Energianalyse, "The future requirements for flexibility in the energy system," 2012.
[2] "Energistatistik 2011," Danish Energy Agency, Tech. Rep., 2011.
[3] K. Heussen, S. You, B. Biegel, L. H. Hansen, and K. B. Andersen, "Indirect control for demand side management - A conceptual introduction," *IEEE PES Innovative Smart Grid Technologies Conference Europe*, pp. 1–8, 2012.
[4] M. Ezekiel, "The cobweb theorem," *The Quarterly Journal of Economics*, vol. 52, no. 2, pp. 255–280, 1938.
[5] J. L. Mathieu, D. S. Callaway, and S. Kiliccote, "Examining uncertainty in demand response baseline models and variability in automated responses to dynamic pricing," in *IEEE Conference on Decision and Control and European Control Conference*, dec 2011, pp. 4332–4339.
[6] Y. Ding, S. Pineda, P. Nyeng, J. Østergaard, E. M. Larsen, and Q. Wu, "Real-time market concept architecture for EcoGrid EU - A prototype for European smart grids," *IEEE Transactions on Smart Grid*, vol. 4, no. 4, pp. 2006–2016, 2013.
[7] C. H. Hommes, "Dynamics of the cobweb model with adaptive expectations and nonlinear supply and demand," *Journal of Economic Behavior & Organization*, vol. 24, no. 3, pp. 315–335, 1994.
[8] ——, "On the consistency of backward-looking expectations: The case of the cobweb," *Journal of Economic Behavior & Organization*, vol. 33, no. 3, pp. 333–362, 1998.
[9] D. Dufresne and F. Vázquez-Abad, "Cobweb theorems with production lags and price forecasting," *Economics Discussion Paper*, no. 2012-17, 2012.
[10] J. Sonnemans, C. Hommes, J. Tuinstra, and H. Velden, "The instability of a heterogeneous cobweb economy: A strategy experiment on expectation formation," *Journal of Economic Behavior & Organization*, vol. 54, no. 4, pp. 453–481, 2004.
[11] J. Nutaro and V. Protopopescu, "The impact of market clearing time and price signal delay on the stability of electric power markets," *IEEE Transactions on Power Systems*, vol. 24, no. 3, pp. 1337–1345, 2009.
[12] R. Masiello, J. Harrison, and R. Mukerji, "Market dynamics of integrating demand response into wholesale energy markets," *The Electricity Journal*, vol. 26, no. 6, pp. 8–19, 2013.
[13] M. Roozbehani, M. A. Dahleh, and S. K. Mitter, "Volatility of power grids under real-time pricing," *IEEE Transactions on Power Systems*, vol. 27, no. 4, pp. 1926–1940, 2012.
[14] C. D. Jonghe, B. F. Hobbs, and R. Belmans, "Optimal generation mix with short-term demand response and wind penetration," *IEEE Transactions on Power Systems*, vol. 27, no. 2, pp. 830–839, 2012.
[15] M. G. Lijesen, "The real-time price elasticity of electricity," *Energy Economics*, vol. 29, no. 2, pp. 249–258, mar 2007.
[16] E. M. Larsen and P. Pinson, "Demonstration of market-based real-time electricity pricing on a congested feeder," in *12th International Conference on the European Energy Market*, 2015.
[17] A. K. David and Y. Z. Li, "Effect of inter-temporal factors on the real time pricing of electricity," *IEEE Transactions on Power Systems*, vol. 8, no. 1, pp. 44–52, 1993.
[18] J. L. Mathieu, P. N. Price, S. Kiliccote, and M. A. Piette, "Quantifying changes in building electricity use, with application to demand response," *IEEE Transactions on Smart Grid*, vol. 2, no. 3, pp. 507–518, 2011.
[19] N. Growe-Kuska, H. Heitsch, and W. Romisch, "Scenario reduction and scenario tree construction for power management problems," *2003 IEEE Bologna Power Tech Conference Proceedings*, vol. 3, pp. 152–158, 2003.
[20] S. Downing and D. Socie, "Simple rainflow counting algorithms," *International Journal of Fatigue*, no. January, pp. 31–40, 1982.
[21] C. Ruiz, A. J. Conejo, and S. a. Gabriel, "Pricing non-convexities in an electricity pool," *IEEE Transactions on Power Systems*, vol. 27, no. 3, pp. 1334–1342, 2012.
[22] P. Andrianesis, G. Liberopoulos, G. Kozanidis, and A. D. Papalexopoulos, "Recovery mechanisms in day-ahead electricity markets with non-convexities - Part I: Design and evaluation methodology," *IEEE Transactions on Power Systems*, vol. 28, no. 2, pp. 960–968, 2013.

{2.7182818284}